Reviews and syntheses: Physical and biogeochemical processes associated with upwelling in the Indian Ocean

Puthenveettil Narayana Menon Vinayachandran[1*], Yukio Masumoto[2,3], Michael J. Roberts[4], Jenny A. Huggett[5,6], Issufo Halo[5,7], Abhisek Chatterjee[8], Prakash Amol[9], Garuda V. M. Gupta[10], Arvind Singh[11], Arnab Mukherjee[12], Satya Prakash[8], Lynnath E. Beckley[13], Eric Jorden Raes[14], Raleigh Hood[15]

[1]Centre for Atmospheric and Oceanic Sciences, Indian Institute of Science, Bengaluru, 560012, India

[2]Graduate School of Science, University of Tokyo, Tokyo, Japan

[3]Application Laboratory, Japan Agency for Marine-Earth Science and Technology, Kanagawa, 236-0001, Japan

[4] Nelson Mandela University, Port Elizabeth, South Africa & National Oceanography Centre, Southampton, United Kingdom

[5]Oceans and Coasts Research, Department of Forestry, Fisheries and the Environment, Private Bag X4390, Cape Town 8000, South Africa

[6]Department of Biological Sciences and Marine Research Institute, University of Cape Town, Private Bag X3, Rondebosch, 7701, Cape Town, South Africa

[7]Department of Conservation and Marine Sciences, Cape Peninsula University of Technology, PO Box 652, Cape Town 8000, South Africa

[8]Indian National Centre for Indian Ocean Services, Ministry of Earth Sciences, Hyderabad, 500090India

[9]CSIR-National Institute of Oceanography, Regional Centre, Visakhapatnam, 530017, India

[10]Centre for Marine Living Resources and Ecology, Ministry of Earth Sciences, Kochi, 682 508India

[11]Physical Research Laboratory, Ahmedabad, 380009, India

[12] National Centre for Polar and Ocean Research, Ministry of Earth Sciences, Goa, India

[13] Environmental and Conservation Sciences, Murdoch University, Perth, Western Australia 6150, Australia

[14] Ocean Frontier Institute and Dept. of Oceanography, Dalhousie University, Halifax, B3H 4R2 Nova Scotia, Canada

[15] University of Maryland Center for Environmental Science, Cambridge, MD, USA

Correspondence to: P. N. Vinayachandran (vinay@iisc.ac.in)

Abstract. The Indian Ocean presents two distinct climate regimes. The North Indian Ocean is dominated by the monsoons, whereas the seasonal reversal is less pronounced in the south. The prevailing wind pattern produces upwelling along different parts of the coast in both hemispheres during different times of the year. Additionally, dynamical processes and eddies either cause or enhance upwelling. This paper reviews the phenomena of upwelling along the coast of the Indian Ocean extending from the tip of South Africa to the southern tip of the west coast of Australia. Observed features, underlying mechanisms, and the impact of upwelling on the ecosystem are presented.

In the Agulhas Current region, cyclonic eddies associated with Natal pulses drive slope upwelling and enhance chlorophyll concentrations along the continental margin. The Durban break-away eddy spun-up by the Agulhas upwells cold nutrient-rich water. Additionally, topographically induced upwelling occurs along the inshore edges of the Agulhas Current. Wind-driven coastal upwelling occurs along the south coast of Africa and augments the dynamical upwelling in the Agulhas Current. Upwelling hotspots along the Mozambique coast are present in the northern and southern sectors of the channel, and are ascribed to dynamical effects of ocean circulation in addition to wind forcing. Interaction of mesoscale eddies with the western boundary, dipole eddy pair interactions, and passage of cyclonic eddies cause upwelling. Upwelling along the southern coast of Madagascar is caused by Ekman wind-driven mechanism and by eddy generation, and is inhibited by the Southwest Madagascar Coastal Current. Seasonal upwelling along the East African coast is primarily driven by the Northeast monsoon winds and enhanced by topographically induced shelf-breaking and shear instability between the East African Coastal Current and the island chains. The Somali coast presents a strong case for the classical Ekman type of upwelling; such upwelling can be inhibited by the arrival of deeper thermocline signals generated in the offshore region by wind stress curl. Upwelling is nearly uniform along the coast of Arabia, caused by the alongshore component of the summer monsoon winds and modulated by the arrival of Rossby waves generated in the offshore region by cyclonic wind stress curl. Along the west coast of India, upwelling is driven by coastally trapped waves together with the alongshore component of the southwesterlies. Along the southern tip of India and Sri Lanka, the strong Ekman transport dives upwelling. Upwelling along the east coast of India is weak and occurs during summer, caused by alongshore winds. In addition, mesoscale eddies lead to upwelling, but the arrival of river water plumes inhibits upwelling along this coast. Southeasterly winds drive upwelling along the coast of Sumatra and Java during summer, with Kelvin wave propagation originating from the Equatorial Indian Ocean affecting the magnitude and extent of the upwelling. Both ENSO and IOD events cause large variability of upwelling here. Along the west coast of Australia, which is characterized by the anomalous Leeuwin Current, southerly winds can cause sporadic upwelling, which is prominent along the southwest, central, and Gascoyne coasts during summer. Open ocean upwelling in the southern tropical Indian Ocean and within the Sri Lanka Dome are driven primarily by the wind stress curl but are also impacted by Rossby wave propagations.

Upwelling is a key driver enhancing biological productivity in all sectors of the coast, as indicated by enhanced sea surface chlorophyll concentrations. Additional knowledge at varying levels has been gained through in situ observations and model simulations. In the Mozambique Channel, upwelling simulates new production, and circulation redistributes the production generated by upwelling and mesoscale eddies, leading to observations of higher ecosystem impacts along the edges of eddies. Similarly, along the southern Madagascar coast, biological connectivity is influenced by the transport of phytoplankton from upwelling zones. Along the coast of Kenya, both productivity rates and zooplankton biomass are higher during the upwelling season. Along the Somali coast, accumulation of upwelled nutrients in the northern part of the coast leads to spatial heterogeneity in productivity. In contrast, productivity is more uniform along the coasts of Yemen and Oman. Upwelling along the west coast of India has several biogeochemical implications, including oxygen depletion, denitrification, and high production of CH4 and dimethyl sulfide. Although weak, wind-driven upwelling leads to significant enhancement of phytoplankton in the northwest Bay of Bengal during the summer monsoon. Along the Sumatra and Java coasts, upwelling affects the phytoplankton composition and assemblages. Dissimilarities in copepod assemblages occur during the upwelling periods along the west coast of Australia. Phytoplankton abundance characterizes inshore edges of the slope during upwelling season, and upwelling eddies are associated with krill abundance.

The review identifies the northern coast of the Arabian Sea and eastern coasts of the Bay of Bengal as the least observed sectors. Additionally, sustained long-term observations with high temporal and spatial resolutions along with high-resolution modelling efforts are recommended for a deeper understanding of upwelling, its variability, and its impact on the ecosystem.

1. Introduction

Tangential winds that blow parallel to the coast result in the transport of water away from the coast (Ekman, 1905). The water that is transported from near the coast must be replaced by water from below, usually from a depth range of 100 - 300m. This upward motion of water from below is termed as (coastal) upwelling (Sverdrup, 1937). While the dynamics of the system primarily concerns the upward flow, the change in properties of water near the surface is what concerns most for the ecosystem and biogeochemistry. The water that upwells comes from below the Ekman layer, and therefore cooler, denser, and rich in nutrients. The transport away from the coast is governed by Ekman dynamics, and owing to the higher density of the upwelled water near the coast, a current is established parallel to the coast. The existence of a physical boundary, the coast, is a necessary condition for the upwelling to take place. Across the equator, the Coriolis force that changes its sign creates a dynamical boundary that supports upwelling. Thus, easterlies drive poleward Ekman transport on both sides of the equator causing equatorial upwelling. Upwelling is possible in the open ocean as well, even in the absence of a physical or dynamic boundary when the surface winds possess strong positive vorticity. Cyclonic wind stress curl leads to divergence within the surface layer leading to upward vertical velocity known as Ekman suction, which is often represented by a 'thermocline dome'. Upwelling has great significance in ocean science owing to its enormous potential to (1) cool the sea surface by several degrees and (2) increase the productivity of near-surface water by several orders of magnitudes (Messie et al., 2009; Messie and Chavez, 2015), compared to regions unaffected by upwelling.

Much of our present understanding of upwelling is derived from studies on eastern boundary current upwelling systems (EBUS). California, Iberian, Canary, Humboldt, and Benguela are the well-known EBUS in the world oceans (Kampf and Chapman, 2016). These classical eastern boundary upwelling systems are driven by winds blowing towards the equator, and effected by the offshore Ekman transport. The alongshore winds acting on a stratified ocean generates a coastal parallel jet and coastally trapped waves affect circulations and the regional extent of circulations (Allen, 1973, Suginohara, 1982). Mesoscale eddies and filaments associated with upwelling systems affect both dynamical structure and transport of properties and materials in the upwelling regions (Capet et al., 2008). Owing to the alignment of the irregular coastline with respect to the winds, the intensity of upwelling may vary along a given coastline and, consequently, there are regions known as upwelling nodes or centres where the intensity of upwelling is discernibly stronger. In the Indian Ocean, the upwelling is seasonal and strongest upwelling regions are located along the western boundary. Nevertheless, even for these upwelling systems, the dynamics that have been demonstrated to be in effect in EBUS holds good.

The upwelling process connects the upper wind-driven part of the ocean with the relatively quiescent sub-surface regimes. Upwelling brings cold, nutrient-rich bottom waters to the surface layer, which significantly supports primary production and hence the higher food web. This connection is vital for cycling tracers and nutrients and invigorating marine life across all states of the food chain. Water upwelled along EBUS harbour some of the world's largest marine ecosystems (Carr, et

al., 2003, Chavez and Toggweiler, 1995, Messié et al., 2009. Hutchings et al., 2009, Montecino and Lange, 2009, Checkley and Barth, 2009, Arístegui et al., 2009). Globally, the upwelling systems occupy less than 2% of the total oceanic area, but they alone contribute to ~20% of the total fish catch (Pauly and Christensen, 1995). Upwelling links the ocean interior with the surface where the ocean and atmosphere interact, exchanging heat, water, and gases, and serves as the source for major biogeochemical and ecological transformations. Though the impact of upwelling is most pronounced regionally, its impact could affect basin-scale circulation and regional climate.

The Indian Ocean is different from the Atlantic and Pacific due to its unique geographical setting marked by the northern land boundary located in the tropics itself. The vast landmass situated to the north of the ocean gives rise to the region's monsoon climate, which is characterized by seasonally reversing winds and copious rainfall during summer. The monsoon winds (**Figure 1A**) are southwesterly during May-September and northeasterly during December-February. The transition from one Monsoon to the other occurs during the spring and autumn months of March - April and October - November, respectively (Schott and McCreary, 2001). Therefore, the most striking characteristic of the upwelling in the Indian Ocean, particularly concerning other typical Eastern boundary upwelling systems, is its seasonality which has been highlighted by reviews in the past. A review of the coastal currents in the Indian Ocean was carried out by Shetye and Gouveia (1998). Schott and McCreary (2001) provide a comprehensive review of the monsoon circulation in the Indian Ocean, and an update of this review has been given in Schott et al. (2009). Shankar et al. (2002) has presented a detailed description of the monsoon currents and a synthesis of their dynamics. More recently, Hood et al. (2015) have reviewed the boundary currents in the Indian Ocean and their impact on biogeochemistry. Indian Ocean science has witnessed a surge in activities in the last decade. Several multidisciplinary research programs that cut across institutional and national boundaries have been deployed towards developing new data sets and testing hitherto unknown hypotheses. Concurrently, numerical models have evolved into higher levels of sophistication, resolution, accuracy, and complexity. Motivated by the rapid progress that the Indian Ocean has witnessed in the last few years, this paper aims to synthesize the knowledge that has accumulated in recent times focussing on upwelling regions that have not received enough attention in past reviews. It is expected that the review will assist in developing future programs in the Indian Ocean coastal oceanography such as those outlined in the UN Decade of the Oceans.

The alignment of the coastline with respect to the winds offers favourable conditions for upwelling along several parts of the Indian Ocean boundaries **(Figure 1B**). The southwesterlies are favourable for upwelling along the western boundary of the North Indian Ocean, particularly along the coast of Somalia and Oman. As they approach the west coast of India, the southwesterlies turn towards the equator and blow nearly parallel to the west coast of India, owing to the presence of the Sahyadri (Western Ghats) mountain ranges (Kurian and Vinayachandran, 2007). The summer monsoon winds are also favourable for upwelling along the southern coast of Sri Lanka and along the east coast of India. Persistent wind stress curl in the Southern Tropical Indian Ocean (STIO) leads to a very shallow thermocline (Xie et al., 2002) and makes it one of the

strongest open ocean upwelling regions. In the southern hemisphere, upwelling has been observed in the Agulhas Current region, Mozambique channel, in the region of the East African Coastal Current, and along the coast of Java and Australia. In the section that follows, upwelling in each of the above regions is described.

2. Coastal Upwelling Systems

In this section, each of the coastal upwelling systems in the Indian Ocean are described in detail. We first present an overview using historic portrayal followed by recent observations; these sections render characteristics of the upwelling and its impact on physical parameters. A review of the present status of modelling these upwelling systems is presented next, along with mechanisms that drive upwelling. The impact of upwelling on the marine ecosystem is discussed next, including those on the fisheries. Progress made during the IIOE-2 (2015–2010) era is paid particular attention, major outstanding issues are listed, and plausible approaches are suggested.

2.1 Agulhas Current

2.1.1. Background

The warm, fast-flowing Agulhas Current is the western-most outflow of the Indian Ocean. In the form of a 1000 km-long western boundary current along the south-eastern side of the African continent, it transports an average of 84 Sv of upper IO water into the south Atlantic and Subtropical Convergence (STC; Lutjeharms, 2006; Beal et al., 2015). It is considered the largest of the WBCs. As such, the Agulhas Current plays a critical role in the planets global circulation of thermocline water and the MOC (Rahmstorf, 2003; Donners and Drijfhout, 2004; Biastoch et al., 2008; Beal et al., 2011).

Agulhas Current originates from the Mozambique Channel, the East Madagascar Current, and the southern Indian Ocean subtropical gyre (**Figure 2; satellite pic**) carrying water masses from the Arabian Sea, Red Sea, and the equatorial Indian Ocean on the shoreward side, while offshore waters comprise Atlantic Ocean, Southern Ocean, and southeast Indian Ocean (Lutjeharms 2006; Beal et al., 2006). This convergence occurs in the vicinity of the Delagoa Bight in southern part of Mozambique. With a volume transport that can at times reach 160 Sv, it is one of the most powerful WBCs. Typically the narrow core (~200 km wide) has a velocity of ~2 ms^{-1} with maximum reaching 3.5 m s^{-1} (Lutjeharms, 2006; Beal et al., 2015). The core closely follows the steep slope of the African continent once south of the Delagoa Bight at 27°S. The very narrow shelf (~3 km) off northern KwaZulu-Natal (also known as Maputoland) ensures that the warm subtropical surface waters reach the coast and consequently extend the subtropical IO fauna and flora towards the poles (Turpie et al., 2000; Griffiths et al., 2010). South of Cape St Lucia the coastline retracts northwards away from the shelf edge for some 120 km

forming the KZN Bight (**Figure 2**). Mid-bight the Agulhas Current is some 40 km from the coast following the undeviating continental edge/slope. The small KZN Bight which has a shelf edge depth of around 100 m and mid shelf depth of 50 m, offers the only refuge from the strong Agulhas Current flow in the upper half of its trajectory.

Further downstream, more or less mid-length, the core again moves away from the coast as the continental shelf gradually widens at 27°E, near Port Alfred (**Figure 2**) to become the Agulhas Bank — an area of great importance for spawning and the early life cycle of many of South Africa's commercially fisheries (Hutchings et al., 2002). The Agulhas Bank is the most expansive shelf on the African continent and has a shelf edge at 200 m depth with typical mid shelf depths around 120-150 m. The eastern part of the bank up to 22°E is commonly influenced by plumes of warm water from current meanders which extend northward (Lutjeharms and Connel, 1989; Krug et al., 2017). The Agulhas Bank has some of the most intense thermoclines found world-wide (Swart and Largier, 1987). At the southern tip of the Agulhas Bank the jet-like Agulhas Current becomes unstable with several possible trajectories (Lutjeharms, 2006). Ordinarily the core retroflects south then eastwards forming the Agulhas Return Current (ARC) which flows along to the north of the Subtropical Convergence (STC) — a divide between the IO and colder Southern Ocean. A temporary northward displacement of the Return Current around the Agulhas Plateau (**Figure 2**) at times causes a fusion (occlusion) of the ARC with the Agulhas Current resulting in the formation of warm Agulhas Rings which propagate westwards into the south Atlantic Ocean — a critical contribution to the MOC (Biastoch et al., 2008; Beal et al., 2011). Occasionally the end of the Agulhas Current turns northwards and follows the steep slope of the Western Agulhas Bank.

Surface temperatures of the Agulhas Current range between 22 and 30°C in the northern reaches reflecting seasonal oscillations but these decrease with southward latitude along the current's length in both seasons (Lutjeharms, 2006). Being of subtropical origins, the surface waters of the Agulhas Current are oligotrophic, but at depth reflect nutrient concentrations typical of the SEC. As with all WBCs, isopycnals slope upwards across the current towards the shelf slope moving nutrient-rich, cooler water to shallower depths (Lutjeharms et al., 2000; **Figure 3**).

Notwithstanding the current's planetary importance, it also is a major driver of local processes that in particular underpin the shelf ecosystems along the east and southern shelf region of South Africa. This is underscored in the composite image shown in **Figure 4** where several important productivity features are highlighted by enhanced surface chlorophyll levels along the current's boundary. Some are bathymetrically fixed — others transient. All are underpinned by some form of upwelling of cooler, nutrient-rich water.

2.1.2. Mechanisms

2.1.2.1 Transient meanders and cyclonic eddies (core upwelling)

A range of transient meanders and associated cyclonic eddies on the inshore boundary of the Agulhas Current commonly occur promoting shelf edge upwelling which does not usually break the surface. The most well-known is the Natal pulse which is observed on average 1.6 times a year, but this appearance ranges anywhere between 0 and 6 events a year (Lutjeharms and Roberts, 1988; Ruijter et al., 1999; Brydon et al., 2005; Rouault and Penven, 2011; Beal et al., 2015; Leber and Beal, 2015). These large solitary meander events do not have a discernible seasonal cycle butt display considerable interannual variability (Krug & Tournadre, 2012). Natal pulses are of the order of 100 km in diameter, and originate in the upper reaches of the current usually due to the interaction of the core flow with adjacent anticyclonic eddies (Tsugawa and Hasumi, 2010). Natal pulses propagate down the east coast of South Africa at approximately 10-20 km/day and grow in size (amplitude) (upstream ~30 km, downstream ~200 km) (Lutjeharms et al., 2003), extending the full depth of the Agulhas Current, i.e. ~2000 m (Lutjeharms et al, 2001, 2003; Elipot and Beal (2015); Pivan et al., 2016). The passage of a Natal pulse is often followed by the spawning of an Agulhas ring which moves off into the south Atlantic (Van Leeuwen et al., 2000; Lutjeharms 2006; Elipot and Beal, 2015).

Natal pulses drive slope upwelling with an order of magnitude of 50–100 m per day (Bryden et al., 2005; Pivan et al., 2016), and given their slow propagation, are associated with relatively long residence times. Their cold cyclonic cores temporarily move deeper water onto the narrow continental slope along the Transkei shelf and are coincident with enhanced surface chlorophyll (**Figure 5**), their influence on the coastal waters is perhaps greatest between Port Alfred and Algoa Bay on the far eastern Agulhas Bank where they facilitate cross-shelf exchange (Jackson et al., 2012: Krug et al., 2014; Pivan et al., 2016). Goschen et al., (2015) observed the dynamics of six Natal pulses using *in situ* moorings, and found slope upwelling-induced cold bottom water events (10–12°C) to extend over the entire shelf reaching the inshore areas of Algoa Bay. These lasted 1–3 weeks during the passing of the pulse, but the cold water on the shelf could linger a further 3 weeks. During upwelling, the isotherms ascended at an average rate of 1.8m/day as the cold bottom layer increased in thickness to 40–60 m, although upwelled water did not break the surface in all cases. Cold water remained in the area for a further 2–3 weeks.

Using a combination of two ocean models (INALT01 and AGU HYCOM) Malan et al. (2018) showed that large meander events in the Agulhas Current drive strong shear with the shelf waters on the meander leading and trailing edges. This induces areas of strong negative vorticity which promotes upwelling events in the bottom boundary layer, resulting in a significant decrease in subsurface temperatures at 100 m at the shelf edge. This is particularly prevalent along the slope of

the eastern Agulhas Bank. They used a tracer experiment to directly observe the uplift of water from 400 m beneath the surface of the Agulhas Current (**Figure 6**), on the leading edge of a large meander.

Another common recurring cold-core cyclonic eddy is the Durban break-away eddy (Lutjeharms and Connell, 1989; Guastella and Roberts 2016). This is a semi-permanent feature of smaller proportions than the Natal pulse (~ 60 km). It is considered to be lee-trapped during its early development as a result of a submerged bight off Durban in the 100 m depth contour configuration. It is hypothesized that the cyclone is spun-up by the strong south-westward flowing Agulhas Current offshore of the regressed shelf edge near Durban. Analysis of ADCP data and satellite imagery show the eddy to be present off Durban approximately 55% of the time with an average lifespan of 8.6 days. After spin-up the eddy breaks loose from its lee position and propagates downstream on the inshore boundary of the Agulhas Current (**Figure 2**). The eddy is highly variable in occurrence, strength and downstream propagation speeds. There is no detectable seasonal cycle in the eddy occurrence, with the Natal pulse causing more variability than any seasonal signal. Moorings and ship data confirm upward doming of the thermal structure in the eddy core associated with cooler water and nutrients being moved higher in the water column, stimulating primary production. Gaustella and Roberts (2016) also noted a second mechanism of upwelling by this feature, viz. divergent upwelling in the northern limb of the eddy (where the cyclonic radial flow separates from the shelf). Moreover, satellite-tracked surface drifters released in the eddy demonstrated the potential for nutrient-rich eddy water to be transported northwards along the inshore regions of the KwaZulu-Natal (KZN) Bight, thus contributing to the functioning of the bight ecosystem (see **Figure 6)**, as well as southwards along the KZN and Transkei coasts – both by the eddy migrating downstream and by eddy water being recirculated into the inshore boundary of the Agulhas Current itself.

2.1.2.2. Dynamic boundary upwelling

Another form of upwelling also occurs at two bathymetric points along the inshore boundary of the Agulhas Current. Historically referred to as dynamic or divergent upwelling, surface upwelling expressions (isotherm outcropping) occur west of Cape Lucia (near Richards Bay) where the very narrow Maputoland shelf (3 km) widens to become the KZN Bight, and near Port Alfred (27°E) further downstream where the Transkei shelf widens into the Agulhas Bank (**Figure 2**). Both Lutjeharms et al. (2000) and Meyer et al. (2002) showed that low water temperatures of <19 °C, high salinities (c. 35.30) and nitrate levels (c. 15 μmol kg^{-1}) indicated upwelling in the northern KZN Bight with an epicentre between Cape St Lucia and Richards Bay **(Figure 6**). This is the prime source of upwelled water and nutrients for the KZN Bight. This upwelling is responsible for elevated chlorophyll levels commonly observed in the northern part of the Bight (c. 1.5 mg m^{-3}, cf. c. 0.5 mg m^{-3}. More recent work by Roberts and Nieuwenhuys (2016) showed upwelling events to last 5–10 days with temperatures commonly dropping by 7°C. The earlier studies (Lutjeharms et al., 2000; Meyer et al., 2002) suggested this upwelling was topographically and dynamically driven by the juxtaposition of the Cape St Lucia offset and the Agulhas Current (a solitary mechanism). However Roberts and Nieuwenhuys (2016) showed almost all major and minor cold-water

intrusions on the shelf coincided with upwelling-favourable north-easterly winds that simultaneously force a south-westerly coastal current. Analysis of in situ mooring data indicates the strongest upwelling events here are driven by a coupled mechanism of Ekman bottom veering on the continental slope and upwelling-favourable wind.

Some 150 km south of Durban, the coastline again undergoes a small northward retraction from the shelf edge — which begins the slowly southward expanding Transkie shelf (at Port St Johns; see **Figure 2**). The shelf north of here is very narrow as is the case north of the KZN Bight. South of Durban (and the Durban Eddy), the Agulhas Current flows close to the coast. But at Port St Johns the Current begin to move offshore following the smooth continental slope. Roberts et al., (2010), using S–ADCP data and satellite SST demonstrated the existence of cyclonic flow in the Port St Johns–Waterfall Bluff coastal inset, with a northward coastal current similarly ranging in velocity between 20 and 60 cm s^{-1}. CTD data indicated that this was associated with shelf-edge upwelling, with surface temperatures 2–4 °C cooler than the adjacent core temperature (24–26 °C) of the Agulhas Current (**Figure 7**). Vertical profiles of the S–ADCP data showed that the counter current, about 7 km wide, extends down the slope to at least 600 m, where it appeared to link with the deep Agulhas Undercurrent at 800 m. It is not known how often this feature exists. Satellite images at times show enhanced surface chlorophyll on the narrow shelf here, but often this is overtaken by passing turbulent features on the inshore boundary of the current.

Surface upwelling near Port Alfred occurs on a much grander scale than the KZN Bight or Port St Johns, at times stretching from East London (29°E) to Port Elizabeth (80-300 km in length **Figure 4**), and is considered the most important upwelling on the south-east coast of South African. Lutjeharms et al. (2000) using cruise data showed the upwelled water to originate from a depth of 200-300 m in the Agulhas Current resulting in water of 8-11°C moving up onto the continental shelf which has an edge break at 100 m depth. This colder, nutrient-rich water is derived from the upper to middle levels of South Indian Central Water and forms a thermocline which at times breaks the surface here resulting in extensive chlorophyll blooms that propagate westwards well onto the Eastern Agulhas Bank (e.g. **Figure 4**). Lutjeharms et al. (2000) suggested that topographically induced changes in the structure of the Agulhas Current underpins the mechanism for this 'dynamic' upwelling. Intermittent outcropping of upwelled water occurs more than 40% of the time and changes the surface temperatures dramatically (Lutjeharms et al., 2000). Moreover, Lutjeharms (2006) suggested that the cold, nutrient-rich bottom layer on the eastern Agulhas Bank has its origins from upwelling in the Port Alfred region underpinning the intense thermoclines found here (Swart and Largier, 1987). However,

Leber et al. (2017) found that meanders act in combination with upwelling-favorable winds to force the strongest cold events, while upwelling-favorable winds alone, possibly primed by Ekman veering, force weaker cold events. This is not unlike the situation near Cape St Lucia, where the frontal curvature of warm Agulhas Current meanders link with the atmosphere to drive local wind stress curl anomalies that reinforce upwelling. [see below]

2.1.2.3. Wind-driven coastal upwelling

Surface coastal upwelling is also found along the south coast of South Africa (i.e. eastern and central Agulhas Bank) some far removed from the Agulhas Current which is some 200 km away off Mossel Bay. This coastal upwelling is driven by the easterly winds which tend to dominant during the austral summer months (Walker, 1986). It has been shown that the dynamic upwelling near Port Alfred is also augmented with easterly wind driven coastal upwelling (Leber et al. 2017).

While upwelling is found on the westward sides of prominent capes that reach out into deeper water, the epicenter occurs further along the 100 km Tsitsikamma Coast (**Figure 4**) where the coastal bathymetry is steep (Roberts and van den Berg, 2005). A 100 km-long, thin offshore extension of this upwelling is commonly observed in satellite data during the summer months. This banana-shaped feature, known as the 'cold ridge', is associated with high levels of chlorophyll (**Figure 4**). Roberts (2005) suggested that the cold ridge is an upwelling filament drawn out by the shelf circulation, however, this hypothesis is still under investigation.

2.1.3. Productivity and ecosystem impacts

Satellite composite (**Figure 4)** of near-surface chlorophyll (chl-*a*) highlights the main drivers of productivity on the south and east coast of South Africa — the former being warm-temperate and the latter warm ecoregions. On the Agulhas Bank, the combination of wind-driven coastal upwelling and the cold ridge filament, are clearly dominant. Underlying these, and not mentioned above, is also a deep chlorophyll maximum that overlay the subsurface thermocline. This very intense thermocline (change of 10°C over 10 m) results from an insolation-warmed top layer and a bottom layer of cold, nutrient rich, Central Indian Ocean Water. Added to this productivity is that seen on the eastern extremity of the Agulhas Bank near Port Alfred (**Figure 4**). As indicated in 2.1.2.2, this productivity is not seasonally linked, but rather is divergent-driven by the Agulhas Current. The blooms are advected westwards onto the widening Agulhas Bank. Together these make the Agulhas Bank a productive region that supports the early life stages (nursery grounds; see Hutchings et al., 2002) of many of South Africa's commercial fish species — e.g. clupeoids (Roel et al., 1994), chokka squid (Augustyn et al., 1994), and sparids such as shad, geelbeck, and white steenbras (Govender and Radebe, 2000; Griffiths and Hecht, 1995; Bennett, 1993).

Unlike the Agulhas Bank, the east coast has a very narrow shelf that is strongly influenced by the fast, warm, Agulhas Current. The warm waters encourage a diverse number of temperate species, often seasonally abundant. These support a diverse range of trawler, longline, commercial and recreational ski boat, charter boat, shore angling, small-scale, artisanal and subsistence fisheries. Pelagic game fish include king mackerel, tuna, bonito and dorado, with a fair number of sailfish and black, blue and striped Marlin. There are numerous shark species in these waters too. Line fish include species such as

shad, blacktail, stumpnose, karanteen, pompano, stonebream in the ocean with grunter, kob and perch in the numerous estuaries. Along the rocky and sandy shore — crabs, mussels, red bait, oysters, winkles, octopus, and lobsters are harvested. The well-known annual sardine run is a major world-wide phenomenon that also supports a small-scale, seasonal beach seine fishery. Many species use the Agulhas Bank, KZN Bight and the estuaries as spawning and nursery grounds — some even combinations of these.

On the east coast shelf, the only refuge from the Agulhas Current is the 100-km long KZN Bight which is important (Hutchings et al., (2002) for local recruitment of species such as the commercial sparid (*Chrysoblephus puniceus*), otherwise known as slinger, and KZN sardines. This importance is underscored by the considerable productivity that occurs in the Bight due to divergent upwelling near Cape St Lucia (**Figure 4**), coastal wind-driven upwelling in the bight, and the Durban eddy (Roberts et al., 2016; Guastella and Roberts, 2016, Roberts and Nuiwenhuis, 2016). What is not understood yet, is the value of the eddy-driven productivity ecosystems, as highlighted in 2.1.2.1, to the east coast. This productivity is along the southern KZN–Transkei shelf which is very exposed to the current, and apart from estuaries, has no obvious refuge for spawning and recruitment. This is the topic of a new research project called CYCLOPS, which hypothesizes east coast larvae are retained in the productively rich eddy cores.

2.2 The Mozambique Channel

2.2.1 Background

Oceanographic sampling within the Mozambique Channel was limited before the first International Indian Ocean Expedition (IIOE; 1959-1965), with merely six voyages and fewer than 100 stations recorded between 1913 and 1952 (Jorge da Silva et al., 1981). The Commandant Robert Giraud conducted extensive sampling throughout the Mozambique Channel during October and November 1957 as part of the International Geophysical Year (Menaché, 1963), but few of the 65 stations were located close to the coast. It seems likely that prior to the IIOE, coastal upwelling processes in this region were unknown, as the Somali upwelling system was the only upwelling area in the western Indian Ocean to be investigated during the expedition.

The first hydrographic data used to report on upwelling phenomena in the Mozambique Channel, as inferred from sloping isotherms and isohalines in the upper 500 m of the water column, were collected onboard RV *Dr. Fridtjof Nansen*, which surveyed the entire coast of Mozambique four times between August 1977 and June 1978 (IMR 1977a; IMR 1978a, b, c). Saetre and de Paula e Silva (1979) concluded that, during the NE monsoon (Nov-April), wind-induced upwelling occurs in a narrow strip of the ocean along the northern Mozambique coast between 11 and 16°S. Although they did not observe any associated low temperatures or high nutrient concentrations in the surface waters, they observed cyclonic eddies off Angoche

in September and November 1977 and further south off Inhambane and along a transect off ~27°S during the September 1977 and January-March 1978 surveys. A special effort to investigate the upwelling in the northern section of the channel was subsequently undertaken onboard the RV *Alexander von Humboldt* in February and March 1980 to determine whether the upwelling was due mainly to wind or current effects (Nehring, 1984). Hydrographic sampling was conducted along nine transects normal to the coast between Cabo Delgado and Angoche. During this survey, dynamic topography revealed a cyclonic eddy in the Angoche region, with high NO3- and chlorophyll concentrations associated with the core of the eddy (Nehring, 1984; Nehring et al. 1987).

More detailed hydrographic surveys within the Delagoa Bight by the RV *Dr. Fridtjof Nansen* in October 1980 (Brinca et al., 1981) and RV *Ernst Haeckel* in January 1982 (Lutjeharms and Jorge da Silva, 1988) provided further information on upwelling and circulation in this southernmost part of the Mozambique coast. Lutjeharms and Jorge da Silva (1988) used data from all these cruises, in conjunction with satellite remote sensing SST imagery from AVHRR for the period spanning 1975 to 1985, to study the region in detail. Their results suggested that there is an area in the Delagoa Bight, the Inharrime terrace, where upwelling enhances biological productivity over the continental shelf. A later study by Kyewalyanga et al. (2007) using satellite ocean color products and a biological model corroborated this finding. Lutjeharms and Jorge da Silva (1988) also suggested that a cyclonic lee eddy present in the Delagoa Bight during the 1980 and 1982 cruises was topographically driven and a relatively consistent feature. Between 2004 and 2006, a series of four cruises on the RV *Algoa* was undertaken to investigate the persistence of this lee eddy, as well as the influence of passing eddies on upwelling in the Bight, as part of the African Coelacanth Ecosystem Project (ACEP), with hydrographic and biological sampling conducted along a series of shore-normal transects within the Bight (Lamont et al., 2010). The lee eddy was documented only once during these cruises, leading Lamont et al. (2010) to suggest that the Delagoa Bight eddy is more transient than previously thought.

The RV *Dr. Fridtjof Nansen* returned to the region almost three decades later in 2007 for a comprehensive ecosystem survey of the entire Mozambique coast (Johnsen et al., 2007), and again in 2009 to survey the Angoche upwelling area during the Agulhas and Somali Large Marine Ecosystem (ASCLME) program (Olsen et al., 2009). These efforts complemented several hydrographic surveys within the Mozambique Channel between 2002 and 2010, driven largely by a French–South African partnership through the multidisciplinary MESOBIO (Influence of mesoscale dynamics on biological productivity at multiple trophic levels in the Mozambique Channel) research programme (Ternon et al., 2014), which focused on the mesoscale eddies. Detailed information about the Angoche and Delagoa Bight upwelling events, based on hydrographic data collected during MESOBIO, has been documented by Malauene et al. (2014), Roberts et al. (2014), and Lamont et al. (2014).

2.2.2. Mechanisms

The northern part of the Mozambique Channel is influenced by the monsoonal wind system, with wind stress predominantly from the north to north-east during austral summer and the south to southeast during austral winter (Saetre and Jorge da Silva, 1982; Schott et al., 2009). The influence of the monsoon winds in the Mozambique Channel is halted at about 20°S (Tomczak and Godfrey, 1994; Schott et al., 2009). South of this latitude, the winds are southeasterly (known as the trade winds) almost all year round and are unfavourable for Ekman upwelling along the Mozambican coast.

The monthly mean wind stress (vectors) and wind stress curl (shading) within the Mozambique Channel and around Madagascar are shown for different seasons in **Figure 8.** January (**Figure 8a**) represents typical austral summer conditions, corresponding to the boreal northeast Monsoon (NEM) regime. April (fall; **Figure 8b**) represents the period of the transition from the NEM towards the austral southeast Monsoon (SEM), shown for July, corresponding to the austral winter season (**Figure 8c**). October (**Figure 8d**) represents the reversal of the Monsoon from the SEM to the NEM. In the southern hemisphere, negative and positive wind stress curl correspond to Ekman suction and pumping, respectively. Ekman suction in general leads to the emergence of upward vertical velocities within the water column, resulting in upwelling (blue areas), whereas Ekman pumping leads downward vertical velocities, leading to downwelling events (red areas). The strongest upwelling is predicted around Madagascar, especially during July and October.

With over 30 cruises in the Mozambique Channel since the late 1970s, there is now a clear picture of where upwelling hotspots are located along the Mozambique coast. In the northern sector, upwelling develops at Angoche, off the coast of Nampula between 15ºS and 18ºS, around the narrows of the Channel (**Figures 9 and 10**). Upwelling in the southern sector of the Mozambique Channel is more variable with regards to location, but several hotspot regions are evident, such as on the Sofala Bank, at Ponta Zavora, around Inhambane, and at the Delagoa Bight, directly offshore from the Mozambican capital Maputo. Upwelling within the Mozambique Channel, both in the northern and southern sectors, can be ascribed to two dynamic forcing mechanisms, one linked to the local characteristics of the oceanic circulation, and the other linked to the atmospheric wind forcing that transfers its momentum into the ocean's interior (Nehring et al., 1987; Quartly and Srokosz, 2004; Malauene et al., 2014; Roberts et al., 2014).

The drivers of upwelling at Angoche in the northern Mozambique Channel were recently investigated by Malauene et al. (2014), who inferred dominance of both wind-stress and oceanic mesoscale current instabilities. Data from an in situ underwater temperature recorder (UTR) deployed near Angoche between 2002 and 2007, combined with satellite data, revealed intermittent "cool water" events between August and March, which coincides with the period of the northeast monsoon winds. During this period, the alongshore winds in the northern Mozambique Channel are southward oriented and upwelling favorable; hence they induce surface divergence in the upper water column, thereby establishing the onset of

434 wind-driven Ekman coastal upwelling (Malauene et al., 2014). This seasonal wind-driven coastal upwelling results in
435 elevated chlorophyll-a signatures over an area between 15 and 18°S (**Figure 10**; Malauene et al., 2014).

436 The other contribution to upwelling at Angoche has been attributed to the dynamics of anticyclonic-cyclonic eddy pair
437 interaction with the continental shelf (Malauene et al., 2014), due to the southward passage of large anticyclonic eddies and
438 rings along the western boundary of the Channel (**Figure 9**; de Ruijter et al., 2002; Ridderinkhof and de Ruiter, 2003; Halo
439 et al., 2014). The interaction of mesoscale eddies with the continental slope on the western side of the Mozambique Channel
440 has been shown to cause upwelling of cooler, nutrient-rich water, resulting in elevated phytoplankton biomass in the shelf
441 regions, as described further below (Lamont et al., 2014; Roberts et al., 2014). Malauene et al. (2014) suggested that the
442 cool surface, elevated chlorophyll-a waters off Angoche are primed and formed by favourable wind-driven Ekman-type
443 coastal upwelling during August and March, but may be further enhanced in chlorophyll-a by anticyclonic/cyclonic eddy
444 pairs interacting with the shelf.

445 The interaction between mesoscale eddies and the Mozambican western boundary is intense and a frequent occurrence. This
446 interaction also causes lateral divergence of the flow-field and has been regarded as an important driver of the observed
447 upwelling events through slope current topographic-driven upwelling occurring predominantly at Ponta Zavora and Sofala
448 Bank (Roberts et al., 2014; Lamont et al., 2014). Roberts et al. (2014) used in situ observations of ocean currents measured
449 by a ship-borne Acoustic Doppler Current Profiler (S-ADCP) and hydrographic data from Conductivity Temperature Depth
450 (CTD) casts to investigate the interaction of a dipole eddy (with the cyclone to the south of the anticyclone, tracked using
451 altimetry maps of sea level anomalies) with the western continental slope of the southern Mozambique Channel, near
452 Inhambane. They observed strong (>100 cm s^{-1}) southward currents over the slope adjacent to the anticyclone, with
453 horizontal divergence over the shelf at the southern edge of the anticyclone, and intense slope upwelling between the dipole
454 and the shelf. Nutrient and chlorophyll concentrations were enhanced in the near-surface waters over the shelf, although
455 there was no evidence of upwelling at the surface. Data from a nearby UTR confirmed prolonged bouts of slope upwelling
456 over several weeks until the dipole had moved further south. Combined altimetry and UTR data also slowed that both
457 cyclonic and anticyclonic independent eddies (not part of a dipole) along the Mozambique continental shelf may induce
458 slope upwelling, with divergence north of the contact zone in the case of cyclonic eddies (Roberts et al., 2014). Cyclonic
459 eddies are usually associated with vertical suction in the eddy's interior, favouring upwelling of nutrient-rich deep waters
460 (i.e., new production) into the euphotic zone, particularly during the spin-up phase (Robinson, 1983; Tew-Kai and Marsac,
461 2009).

462 The southernmost upwelling region in the Mozambique Channel is the Delagoa Bight, centered around 26ºS and 34ºE
463 (Lutjeharms and Da Silva, 1988; Lamont et al., 2010). The region is one of the largest coastal indentations in the southwest
464 Indian Ocean, and the second richest area in terms of shrimp fisheries in the country, after the Sofala Bank. The oceanic
465 circulation in the Bight is dominated by a semi-permanent cyclonic lee eddy (Lutjeharms and Da Silva, 1988; Cossa et al.,

2016), which is topographically trapped and appears to occur about 25% of the time, with no clear seasonal signal (Cossa et al., 2016). The formation of the lee eddy in the Bight has been linked to the characteristics of the flow-field offshore, especially the Mozambique Channel rings. In particular, the passage of cyclonic eddies off the Inhambane region influences the water masses of the Delagoa Bight through upwelling onto the shelf, resulting in enhanced productivity (Quartly and Srokosz, 2004; Kyewalyanga et al., 2007; Lamont et al., 2010; Lamont et al., 2014). Kyewalyanga et al. (2007) recorded high chlorophyll a and primary production values in the northern part of the Delagoa Bight (**Figure 10**), where pelagic fish, mostly round herring (*Etrumeus teres*) have previously been recorded (Brinca et al., 1981).

2.2.3 Productivity and ecosystem impacts

In addition to stimulating primary production along the continental shelf of Mozambique, often in areas associated with higher biomass or pelagic fish or shrimps, the mesoscale eddies play an important role in ecosystem dynamics in the Mozambique Channel (MC) through the stimulation of new primary production via upwelling in cyclonic eddies, as well as the broad distribution of both coastal upwelling-generated and eddy-generated production. Using isotopic tracers, Kolasinski et al. (2012) showed that the new production is circulated throughout the mixed layer, while some cyclonic production may also be exported horizontally into the frontal region. Strong currents at the perimeters of these eddies result in the entrainment and offshore advection of this high biomass, dominated by siliceous diatoms, into the frontal regions (Kolasinski et al., 2012). Huggett (2014) found mesozooplankton populations were significantly enriched within the cyclonic eddies and divergence areas, with a higher abundance of copepod and euphausiid nauplii observed in the cyclonic eddies compared to the anticyclonic eddies. This suggests that the divergence areas are constantly "fed" by production from within the cyclonic eddies. This concentration of coastal production combined with the import of cyclonic production into the boundary region might explain why it is often the boundaries of eddies that are targeted by consumers in the MC. Sabarros et al. (2009) documented large aggregations of micronekton (small forage organisms including crustaceans, squid, and fish) mainly in areas where the local horizontal gradient of sea level anomalies is strong, i.e. at the periphery of eddies, and foraging frigatebirds tend to avoid the centre of cold-core (cyclonic) eddies, preferring the eddy edges (Weimerskirch et al., 2004). Mesoscale eddies are also thought to provide better conditions for tuna aggregations throughout the water column, not just at the surface, and high species diversity among longline catches (tunas and swordfish) in the MC suggests the eddies may function as biodiversity hotspots (Tew-Kai & Marsac, 2010). Through upwelling in the core of cyclonic eddies and offshore entrainment of shelf production in the inter-eddy frontal zones, mesoscale eddies are a major source and distributor of production and organic matter in an otherwise oligotrophic system, and a key driver in supporting the high biomass and diversity of pelagic consumers observed in this region.

2.3 Madagascar

2.3.1 Background

The island of Madagascar received little attention both before and during the IIOE. The transect made by RV *Atlantis II* in 1963, departing from Maputo at the Delagoa Bight, simply crossed the southern Madagascar coast as a pathway to Reunion and Mauritius Islands (Miller and Risebrough, 1963). No wonder not even the name Madagascar is mentioned in their description (Wallen, 1964; Fye, 1965). If a potential upwelling zone off southern Madagascar upwelling had been known of then, surely a drive to investigate it during the IIOE would have been easily motivated.

Even since the IIOE, relatively few large-scale hydrographic surveys have been conducted along the coastline of Madagascar, which at ~48000 km is the longest in Africa. The first extensive oceanographic survey over the southern continental shelf of Madagascar to provide evidence of upwelling was conducted in June 1983 onboard the RV *Dr. Fridtjof Nansen* (IMR, 1983a; Lutjeharms 2006). In the south, inshore surface temperatures in the vicinity of Cap Sainte Marie, and Taolagnaro (Fort Dauphin) at the southeastern corner of the shelf, were about 2ºC lower than farther offshore, with salinities indicating upwelled Subtropical Surface Water originating from depths of about 200 m. Just over a quarter of a century later, the first circumnavigation of this large island was achieved through two ecosystem surveys in 2008 and 2009 by the RV *Dr. Fridtjof Nansen* during the ASCLME programme. Between 24 August and 1 October 2008, the *Nansen* completed 115 CTD stations in total along 11 transects extending far offshore along the south and east coasts of Madagascar, ending at the northern tip (Krakstad et al., 2008). Evidence was found of upwelled Subtropical Surface Water at the southeastern corner of the shelf (25°S), while relatively fresher and cooler water inshore at 16°S and 14°S was suggestive of upwelling along the northeast coast (Krakstad et al., 2008). One year later, from 25 August to 3 October 2009, the Nansen revisited the western sector of the south coast and continued sampling along the southwestern and north-western coasts, ending once more at Antsiranana (Diego Suárez) in the north, completing 10 transects and 182 hydrographic stations (Alvheim et al. 2009). Once again, hydrographic sampling provided evidence of coastal upwelling on the southern coast (26°S), as well as at two locations on the west coast, near Cap Sainte André (16°S) and Nosy Be Island (13°S), with salinity maxima indicating upwelling of Subtropical Surface Water in the south and Equatorial Surface Water in the northern region (Pripp et al., 2014).

2.3.2 Mechanisms

Seasonal maps of wind stress curl indicate both strong upwelling and downwelling events around Madagascar are likely during austral winter (July, **Figure 8c**) through to late spring (October, **Figure 8d**). In July, the strongest upwelling is predicted to the northwest of Madagascar, around the Comoros basin. During this period, the winds are from the southeast. In October, the strongest upwelling is predicted all around the south, southeast, and southwest coasts of Madagascar. During

this period, the winds are northeasterly along the southeastern coast, and southeasterly along the southwestern coast of the Island, thus becoming upwelling favourable.

Since the first observation of upwelling off southern Madagascar, there has been considerable interest amongst the scientific oceanographic community, both locally and internationally, to confirm this upwelling and understand the physical mechanisms of its formation, frequency, characteristics, and spatial extension and temporal variability (Lutjeharms and Machu, 2000; DiMarco et al., 2000; Machu et al., 2002; Ho et al., 2004; Srokosz and Quartly, 2013; Ramanantsoa et al., 2018a,b; Collins, 2020). Lutjeharms and Machu (2000) used a snapshot composed satellite SST imagery from Advanced High-Resolution Radiometer (AVHRR) sensor onboard of NOAA satellite, with a spatial resolution of 1°x1° longitude and latitude, in conjunction with chlorophyll-a concentrations retrieved by SeaWiFS satellite, and Scatterometer wind field data from Quickscat satellite, to inspect the mechanisms of formation of this upwelling. Their finding suggested that this upwelling was caused by current instabilities at the inshore edge of the South East Madagascar Current, as no correlation was found with the local winds (Lutjeharms and Machu, 2000). In a parallel study using SST and wind field data from the same sources, DiMarco et al. (2000) concluded that upwelling over the southern continental shelf and along the southeastern continental slope, which extended over an area of 2° longitude by 1° latitude (nearly 24,642 km^2) during February and March (North-East Monsoon), was driven by both wind forcing and current interactions with the continental shelf and slope. However, the paucity of in situ wind and current data prevented them from quantifying the relative contribution of each process.

Machu and colleagues revisited the topic soon thereafter, and surveyed the southern and southeastern continental shelf of Madagascar on board the Dutch RV *Pelagia*, during the second phase of the Agulhas Current Source Experiment (ACSEX-2) project in March 2001. Hydrographic measurements conducted along three transects provided the first dedicated and comprehensive hydrographic evidence of the upwelling cell inshore of the East Madagascar Current (EMC). The combination of this dataset and satellite imagery led the authors to conclude that the southeastern Madagascar upwelling occurs through a combination of favourable wind stress in the area, enabling an Ekman wind-driven mechanism, and the dynamics of a cyclonic eddy generated inshore of the current, favoured by the concave-shaped bathymetry as the shelf widens (Machu et al., 2002).

An attempt to study the long-term inter-annual variability of the upwelling events to the south and off southeastern Madagascar and their interaction with the EMC was conducted by Ho et al. (2004). Their analysis of monthly SeaWiFs chlorophyll-a imagery spanning from September 1997 to November 2001 revealed that the upwelling was generally enhanced in austral winter and austral summer each year. They also concluded that the southern and southeastern upwelling boundary cells interact, based on the movement and deformation of the boundary between them, with a mechanism that can be explained by the shear wave propagation theory (Ho et al., 2004).

More recently, Ramanantsoa et al. (2018a) investigated the temporal and spatial variability of the coastal upwelling south of Madagascar. Using a suite of satellite remote sensing data, in-situ observations, and numerical model simulations, they provide new insight on the structure, variability, and drivers of this upwelling. Their results suggest that the southern and southeastern upwelling cells already indicated in former studies (**Figure 9**; Ho et al., 2004), which they termed core 2 and core 1 respectively, are characterized by distinct seasonal variability, have different intensities and water mass origins, and are formed by different physical mechanisms (Ramanantsoa et al., 2018a). The core in the southeastern sector is attributed to dynamical upwelling in response to the detachment of the EMC from the continental slope, reinforced by favorable winds. The southern core, situated to the west of the southern tip of Madagascar (Cap Ste Marie), is primarily attributed to Ekman-driven upwelling by favourable winds, whilst being inhibited by the recently described warm poleward current along the eastern boundary of the Mozambique Channel, the Southwest Madagascar Coastal Current, or SMACC (Ramanantsoa et al., 2018b).

During the *Nansen* survey in 2009, Pripp et al. (2014) observed upwelling off Cap Ste Andre and Nosy Be along the northwest coast, with elevated sea surface salinities indicative of upwelled Equatorial Surface Water. They suggested this upwelling was most likely current-driven due to strong northeastward bottom currents associated with passing anticyclonic eddies, which would have resulted in onshore bottom Ekman transport.

2.3.3. Productivity and ecosystem impacts

As with other upwelling regions, the upwelling areas on the Madagascar shelf are associated with elevated biological productivity (**Figure 10**). During the 2009 survey, Pripp et al. (2014) found all upwelling cells to be associated with relatively high surface chlorophyll and satellite-derived net primary production (NPP), as well as higher acoustic estimates of pelagic fish, elevated pelagic and demersal trawl catches, and greater whale sightings. Ockhuis et al. (2017) found the highest neuston biovolume on the Madagascan shelf to be associated with relatively cool water (<22 °C) in the core upwelling areas, and Ramanantsoa et al. (2018a) describe the coastal upwelling area south of Madagascar as a hotspot of marine biological productivity. As has been observed for the Mozambique coast, the interaction of eddies with the continental shelf can lead to the export of this shelf-based, upwelling-derived production into the open ocean. A young cyclonic eddy that formed off southern Madagascar in 2013 was observed to entrain chlorophyll-rich shelf water around its perimeter (Barlow et al., 2017), with the associated entrapment of plankton having implications for the dispersal and recruitment of larval stages and biological connectivity between regions (Braby, 2014; Noyon et al., 2019).

The southeast core of current-driven upwelling has been proposed (Longhurst 2001; Lévy et al., 2007; Raj et al., 2010; Srokosz & Quartly, 2013) to be the main driver of the South-East Madagascar Bloom, an extensive phytoplankton/cyanobacteria bloom that has been shown by satellite imagery to occur to the southeast of Madagascar during

late austral summer). However, analysis of a 19-year time series of ocean color satellite data by Dilmahamod et al. (2019) laid this as well as other theories to rest. Bloom occurrence was associated with La Niña conditions when upwelling intensity south of Madagascar was reduced due to a stronger than average Southeast Madagascar Current detaching from the coast. The resultant feeding of low-salinity water into the Madagascar Basin and enhanced stratification, along with ample light, are suggested as ideal conditions for a nitrogen-fixing cyanobacterial bloom onset (Dilmahamod et al., 2019).

2.4 East African Coastal Current system

2.4.1. Background

The equatorward-flowing East African Coastal Current (EACC) is present along the coasts of Tanzania and Kenya between 11ºS and 3ºS (**Figure 11, 12a-b**). Transporting about 19.9 Sv, as estimated by Swallow et al. (1991), the EACC draws much of its water from the westward-flowing South Equatorial Current. Even though it experiences the impact of the seasonally reversing winds, the northeast monsoon in austral summer (NEM, November to March) and southwest monsoon in austral winter (SW M, April to October, but note the prevailing winds are from the southeast in the southern hemisphere, see **Figure 8**, and regional papers refer to the southeast monsoon, or SEM) the EACC is northward-oriented all year round. This is in contrast to the Somali Current located in its downstream bounds, which reverses its southward – northward orientation in synchrony with the reversal of the monsoons (Wyrtki, 1973; Schott, 1983; Tomczak and Godfrey, 1994). Downwelling is prevalent throughout the year, particularly during the SWM when the coastal current is strongest, but irregular upwelling has been observed near the northern Kenyan coast during the NEM when the EACC moves away from the coast in the region of the confluence with the southward-flowing Somali Current (Heip et al., 1995; Jacobs et al., 2020).

Although upwelling off the East African coast was first documented by Newell (1959), later confirmed by Iversen et al. (1984), Bakun et al. (1998), and Roberts et al. (2008), it is only recently that the importance of these coastal upwelling cells have been given deserved consideration through various regional research initiatives, such as the Productivity of the East African Coastal Current (PEACC) project, the Sustainable Oceans, Livelihoods and food Security Through Increased Capacity in Ecosystem research in the Western Indian Ocean (SOLSTICE-WIO) programme (www.solstice-wio.org), and the Western Indian Ocean Upwelling Research Initiative (WIOURI) flagship programme of the IIOE-2, due to their potential to sustain food security to local coastal communities (Roberts, 2015). The dynamics of the overlying atmospheric wind forcing (Varela et al., 2015) and the progression of the EACC through the chain of small scale islands (from south to north - Mafia, Zanzibar and Pemba) along the coast of Tanzania (Roberts et al., 2008), combined with the varying local bottom topography characterized by the presence of shallow banks along the coast of Kenya, have been identified as potential drivers of upwelling events in the region (Roberts et al., 2008; Roberts 2015; Jacobs et al., 2020).

2.4.2 Mechanisms

The southern continental shelf off Kenya is very narrow (0-3 km wide), but in the northern sector the shelf widens to approximately 45 km due to the presence of the North Kenya Banks (NKBs; Nguli 1995; Jacobs et al. 2020). Upwelling events along the Kenyan coast are thought to be driven primarily by the northeast monsoonal winds that favor Ekman-driven coastal upwelling and increased productivity during November - April (Heip et al., 1995; Varela et al., 2015). However, recent findings based on outputs from a high-resolution global biogeochemical model and satellite remote sensing observations along the Kenyan coast suggest that, during the NEM, the Ekman wind-driven coastal upwelling is further enhanced in the NKBs by a secondary dynamical process, topographically induced shelf-break upwelling, (Jacobs et al., 2020). This shelf-break upwelling showed high levels of spatial and intensity variability at interannual timescales, related to the confluence position between the EACC and the Somali Current (**Figure 11a**). The model indicated that shelf-edge upwelling and productivity were enhanced over the NKBs when the confluence was located further south.

Along the coast of Tanzania, both the NEM winds and shear instabilities between the EACC and the chain of islands along the coast have been attributed as responsible physical mechanisms driving upwelling in the region, as suggested by a modeling study by Halo et al. (2020). Roberts (2015) suggested elevated chlorophyll-a concentrations in the lee (downstream) of Zanzibar Island, in particular, and to a lesser extent off Pemba Island, measured during a survey in 2007, were a consequence of localized upwelling induced by an island wake (Roberts, 2015). A ROMS model constructed by Zavala-Garay et al. (2015) also shows cool temperatures in the Zanzibar Channel during the NEM, potentially caused by wind-induced upwelling north of Zanzibar Channel, followed by advection into the Zanzibar Channel. A small but intense upwelling cell also develops around Tanga, between Pemba Island and the Tanzanian coast. This small upwelling cell has been observed in both monsoons (**Figure 11**), suggesting it is a regular occurrence (Halo et al., 2020).

2.4.3 Productivity and ecosystem impacts

The modeling study by Jacobs et al. (2020) found that upwelling of cold, nutrient-rich water along the Kenyan coast during the NEM results in elevated chlorophyll, primary production, and phytoplankton biomass (**Figure 12c, e**). This was particularly enhanced over the NKBs and likely to contribute to higher fishery potential in this area, which has been traditionally low along the Kenyan coast. Interannual variability in wind strength during the NEM is likely to be an important factor controlling upwelling intensity and subsequent phytoplankton production in the region (Painter, 2020). However, a recent study by Varela et al. (2015) documented a long-term decline in coastal upwelling off Kenya during the NEM for 1982-2010, which suggests that upwelling-related productivity may decline in the long-term if this trend continues. In contrast, analysis of weather station data for the period 1977-2006 generally showed long-term increases in winds along the coast of Tanzania, although the trends in mean and maximum wind speed varied with latitude and season (Mahongo et al.,

2012). Long-term trends were stronger during the SWM than during the NEM, with increased wind speeds for Tanga and Zanzibar in the north, but a decline in maximum wind speed for Mtwara in the south, and constant maximum wind speeds for Dar es Salaam. A coastal upwelling index (CUI) based on SST output from a coupled biophysical climatological model by Halo et al. (2020) showed a moderate and steady linear increase in upwelling for Tanga over a 23-year period (1990-2013), in line with the regional increase in wind speed observed by Mahongo et al. (2012).

The limited biogeochemical data for the EACC region were recently reviewed by Painter (2020), who noted that the warm surface waters are permanently N-limited, with low NO3-:PO43-, conditions that favor the nitrogen-fixing cyanobacterium *Trichodesmium*. *Trichodesmium* colonies are generally more abundant during the NEM off both Kenya and Tanzania (Kromkamp et al., 1997; Lugomela et al., 2002), but this is unlikely to be related to upwelled nutrients, and more likely due to wind-borne aeolian dust and land-based nutrient input during the rains, as well as the warmer, more stable conditions that prevail during the NEM compared to the SWM. Sampling in Kenyan waters aboard RV *Tyro* in 1992, Kromkamp et al. (1997) measured higher rates of primary production during the NEM than during the SWM, with maximum rates of 6 g C m^{-2} d^{-1}. Zooplankton biomass was also higher during the NEM, with maximum values of 18.6 mg C m^{-3} (Mwaluma, 1995).

2.5 Coast of Somalia

2.5.1 Background

Coastal currents off Somalia exhibit a strong seasonal cycle forced primarily by the seasonally reversing monsoon winds. During winter, alongshore currents are equatorward, during summer these are poleward and exhibit one of the strongest coastal upwelling in North Indian Ocean. In early May, as the Intertropical-Convergence-Zone moves north of the equator, the northward East African Coastal Current crosses the equator and extends till about 3-4°N along the Somali coast and then recirculates to form the Southern Gyre (SG) (Duing et al., 1980). A portion of SG meanders eastward and the rest flows southward to cross the equator offshore (Chatterjee et al., 2013). During this process, a cold upwelling wedge forms along its western and northern front. As the monsoon progresses, currents north of the SG turn very complex. By June, the southwesterly winds (Findlater Jet; Findlater, 1969) strengthen along the coast resulting in a strong alongshore current all along the Somali coast extending up to a depth of 1000 m and the offshore Ekman transport induced by strong alongshore winds cause a strong upwelling off the coast of Somalia. By July/August, currents along the Somali coast strengthen rapidly to reach up to 250-300 cm/s with transport reaching up to 37 Sv (Fischer et al., 1996; Beal and Donohue, 2013) and thus forms the strongest boundary current of the north Indian Ocean. In the process, another gyre forms towards the offshore side of the northern part of the Somali coast between ~5-9°N, known as Great Whirl (GW) (Leetmaa et al., 1982). This time, a

second cold-wedge forms along the northern flank of the GW north of ~9°N, where SST falls below 20°C. The summer monsoon upwelling off the coast of Somalia also drives one of the most productive zones of the north Indian Ocean. As the southwesterly alongshore winds strengthen, Ekman transport pushes the coastal surface water offshore, leading to cold subsurface water to upwell and then advect away offshore by the strong SG and GW fronts. This upwelled water brings a bounteous amount of nutrients to the euphotic zone (more than 15 μM), which results in enhanced phytoplankton concentration in the upper surface layer (Smith and Codispoti, 1980; Hitchcock and Olson, 1992; McCreary et al., 1996a, Wiggert et al., 2005).

2.5.2 Mechanisms

The first modern description of hydrography and circulation across the Somali coast was provided during cruise based observations between August-September of 1964 (Warren, 1966; Swallow and Bruce, 1966) under the first International Indian Ocean Expedition (IIOE); a series of cross-shore hydrographic sections were carried out between 3°S-12°N. They observed upwelled cold surface temperature (reaching up to 12.8°C) north of 7°N, and these cold waters spread offshore as cold tongues along the northern flank of the GW reaching up to 55°E. Later, an extensive survey of the Somali basin and the western Indian Ocean was carried out in the summer of 1979 using a multi-ship observation campaign known as the Indian Ocean Experiment (INDEX) under the framework of the Indian Ocean Panel of SCOR. Based on samples collected during INDEX, two separate zones of upwelling were identified: one in the south at ~3-4°N associated with SG and the another in the northern part of the coast north at ~9°N linked to the fronts associated to GW with a minimum SST of ~ 17°C (Leetmaa et al., 1982, Quadfasel and Schott, 1982). By the late 90s' the availability of the remotely sensed satellite observations provided an opportunity to observe long term SST variability along this coast and is being used widely for understanding the seasonal variability and climatic trend of coastal upwelling of this region (Goes et al., 2005; Wiggert et al., 2005; Prakash and Ramesh, 2007; Beal and Donohue, 2013).

Strong currents and double gyres off the Somali coast have attracted modelling studies to understand the mechanisms of the observed phenomena in the 1970s to late 1990s. The pioneering works by Lighthill (1969) and Cox (1979) were the first modeling studies on the strong Somali currents during the summer monsoon. Lighthill (1969) showed that as the westward propagating planetary waves excited by the offshore negative wind stress curl reflect along the continental boundary off Somalia, they generate short-wavelength Rossby waves that superpose to form the boundary currents. Thereafter, several papers studied the various aspects of this current system and mainly focused on the dynamical mechanisms of the alongshore currents, the generation and decay of the two gyre circulations off the Somalia coast, the impact of the slanted boundary in the propagation of these gyres (Anderson and Moore, 1979; Cox, 1979; McCreary and Kundu; 1988; Luther and O'Brien, 1989; McCreary et al., 1993) and the impact of internal instabilities (Wirth et al., 2002; Jochum and Murtugudde, 2005;

Chatterjee et al., 2013). In a recent study using a coupled ocean general circulation model, Chatterjee et al. (2019) showed that the upwelling off Somalia is limited to the early phase of the summer monsoon when the low-level Findlater Jet sets in across the Arabian Sea (Figure 13). As the Monsoon progresses, Ekman pumping induced by offshore negative wind stress curl deepens the thermocline in the interior Arabian Sea. Subsequently, these downwelling signals propagate westward to interfere with the upwelling signals off Somalia. As a response, the thermocline along the major part of the Somalia coast (~60%) deepens by about 40-60 m, particularly in the central part of the Somali coast. Moreover, strong alongshore winds and weaker stratification allow more mixing in the bottom of the mixed layer, which further deepens the thermocline and cools the surface mixed layer. As a result, during the peak summer months, upwelling becomes limited primarily to the eddy dominated frontal flows in the northern and to some extent in the southern part of the coast.

2.5.3 Productivity and ecosystem impacts

Observations collected during INDEX experiment indicate that the surface NO_3^- concentration along the cold wedge of the GW front can reach up to ~15-20 µmole/liter in the summer monsoon (Smith and Codispoti, 1980). This enhanced nutrients level increases productivity significantly to more than 300 g C m-2 yr-1 (Heileman and Scott, 2008). It was also observed that, in the middle part of the coast between ~5-8°N, the surface concentration of the NO_3^- is relatively much lower, with maximum concentration reaching up to 1.8 µmole/liter even during the peak monsoon (July/August) (Smith and Codispoti, 1980). Due to the large concentration of nutrients in the upper euphotic zone, primarily in the northern part, the phytoplankton communities are mostly dominated by large phytoplankton (diatoms) in the upwelled waters of the western Arabian Sea during the summer monsoon (Brown et al., 1999; Shalapyonok et al., 2001; Wiggert et al., 2005). Veldhuis et al. (1997) also reported strong upwelling with surface temperature no more than 20°C and dominance of diatoms between 7-11°N along the Somali coast in July 1992.

There are relatively much less modeling studies on the observed intense productivity in response to the upwelling. McCreary et al. (1996a) demonstrated the first reasonable simulation of the annual variability of the surface chlorophyll bloom of the Arabian Sea based on a simple 2½ layer model coupled with an NPZD biological module. He showed that the phytoplankton blooms in the northern and central Arabian Sea during summer monsoon is primarily driven by the lateral advection of upwelled nutrients off the Somalia and Oman coasts and local entrainment. However, it was noted that the model underestimates the lateral advection as it does not resolve the mesoscale features like filaments that transport nutrients offshore in the real ocean. Later, Kawamiya (2001) studied extensively the role of this offshore advected nutrients from the coastal upwelling region in the open ocean of the Arabian Sea and concluded that Somali upwelling is the primary source of nutrient supply into the southcentral Arabian Sea and the Oman upwelling water supplies nutrient in the northern Arabian Sea.

Despite the large abundance of nutrients in the upwelling wedges off Somalia, the concentration of chlorophyll does not grow exponentially. Smith and Codispoti (1980) suggest that the zooplankton grazing is the primary factor that limits the phytoplankton from growing exponentially. A few studies suggest that the swift Somali Current spreads these upwelled nutrients over a large part of the interior Arabian Sea and thus enhances the productivity offshore (Keen et al., 1997; Hitchcock et al., 2000; Prasanna Kumar et al., 2001; Kawamiya, 2001). Coupled physical-biogeochemical models were also used to identify the most limiting factors that suppress the exponential growth of the phytoplankton in this region. McCreary et al. (1996a) showed that nutrients and not the zooplankton grazing primarily limit phytoplankton growth in the upwelling region. However, as they used a very simple 4 component NPZD model, it was not clear, which are the limiting nutrients that control the phytoplankton growth. On the other hand, studies with the help of more complex models, in the last couple of decades, suggest that phytoplankton growth in this region are prone to iron limitation (Wiggert et al., 2006; Wiggert and Murtugudde, 2007) and also likely to be silicate stressed (Kone′ et al., 2009; Resplandy et al., 2011). This is in agreement with the conclusions based on observations of the upwelled water off the Oman coast which suggested that dissolved iron is one of the stressed micro-nutrient in this region and thus makes it an iron-limited High Nutrient Low Chlorophyll (HNLC) zone during the summer monsoon (Naqvi et al., 2010). Recently, Lakshmi et al. (2020) studied various limiting factors and distribution of phytoplankton along the coast of Somalia using a high-resolution physical-biogeochemical coupled model (**Figure 13**). They showed that high values of chlorophyll concentration are limited to the northern flank of the GW north of 9°N and exhibit moderate or low concentration in the south. The strong boundary currents advect the upwelled nutrients from the southern region to the northern part of the coast and thereby accumulate the advected nutrients. In contrast, the deepening of the thermocline and horizontal advection keep chlorophyll concentration low to the south of 9°N. They further noted that dissolved iron concentration (~1.2-1.8 nM) and the NO_3:Fe ratio (<15000) do not indicate iron-deficient conditions throughout the coast but suggests NO_3 limited growth of phytoplankton communities south of 9°N.

2.6 Coast of Arabia

2.6.1 Background

Unlike the Somali coast, upwelling along Arabia (the coast of Yemen and Oman) is more uniform and exhibits classical upwelling dynamics primarily driven by southwesterly alongshore winds during the summer monsoon. In the 1990s' the repeated multiple alongshore/cross-shore ship-based transacts under the US Joint Global Ocean Flux Study (US JGOFS), and the availability of the satellite observations of SLA, SST, and Chl-a led to a significant advancement in the understanding of the coastal current system and its associated upwelling dynamics of this region. A detailed review based on these

observations is presented in Schott and McCreary (2001) and Hood et al. (2017). Here we briefly highlight some of these results and review recent advances in our understanding of this upwelling system.

The first estimate of the intensity of upwelling along this coast was given by Smith and Bottero (1977) using hydrographic observations and winds observed during 1963 under the first IIOE campaign. They estimated a vertical velocity of the order of 2×10^{-5} m/s with an upwelling transport of ~8 Sv through the 50 m depth along the 1000 km long coastline and from the coast to 400 km offshore. Observations from the JGOFS cruises suggest that the upwelling signature on SST persists to about 120 km offshore, whereas in the subsurface, upsloping of thermocline can be evident to about 260 km (Shi et al., 2000). They find that, during the summer of 1995, the lowest SST recorded is 21ºC close to the southern part of the Oman coast in late August to early September, which upwelled from a depth approximately 100-150 m. However, note that the coolest temperature is observed on the shelf of Oman, where SST starts to fall immediately with the onset of alongshore winds and falls below 20˚C in early July.

2.6.2 Mechanisms

The alongshore wind off the coast of Arabia is much weaker than that off the Somali coast but significant enough to cause coastal upwelling as early as May (Kindle et al., 2002), much before the development of southwest Monsoon. The upwelling strengthens as the magnitude of the alongshore winds become stronger with the progression of the summer monsoon. During the late summer (August/September), SST close to the coast decreases by about 5˚C from the ambient offshore temperature to fall below 23˚C (Shi et al., 2000). SST gradually increases away from the coast indicating that the upwelling predominantly happens near the coast than offshore, where positive wind stress curl favors open ocean upwelling. McCreary et al. (1996a) further noted that in the open ocean, offshore of the coast of Oman, their model-simulated vertical velocity at the bottom of the mixed layer remains very small despite a large upwelling favorable Ekman pumping velocity. This negligible vertical velocity is attributed to the state of Sverdrup balance via the radiation of Rossby waves. Therefore, they advocated that the open ocean cooling off Oman and the associated biological response is primarily driven by advection of cold nutrient-rich upwelled water from Oman coast and the wind-driven mixing entrainment at the bottom of the mixed layer, which deepens the thermocline offshore.

During this season, owing to the offshore Ekman transport driven by the alongshore winds, sea level also drops by more than 30 cm along the coast. This is the time, owing to the crosshore sea level gradient, a northeastward coastal current, Oman Coastal Current (OCC; Shi et al., 2000) develops which persists throughout the summer monsoon (Cutler and Swallow, 1984). Interestingly, the maximum strength of the alongshore winds does not coincide with the minimum SST and sea level: while the alongshore wind reaches its peak in mid-June, the SST and sea level attain their minimum about one and a half month later by the end of August or early September (Manghnani et al., 1998; Vic et al., 2017). The reason for

this delay is not very clear. However, Vic et al. (2017) indicated that remotely forced Rossby waves generated due to offshore Ekman pumping by the upwelling favorable wind stress curl (Smith and Bottero, 1977) north of the Findlater Jet (Findlater, 1969) axis drive this delay by modulating coastal stratification of the Arabian peninsula.

2.6.3 Productivity and ecosystem impacts

This intense upwelling all along the coast of Yemen and Oman in the western Arabian Sea also drives one of the strongest primary productivity of this region. These waters are enriched with macronutrients (the near-surface NO_3^- recorded up to 15-20 μM (Smith and Codispoti, 1980; Morrison et al., 1998), which triggers large phytoplankton blooms; these upwelled waters transport quickly to the offshore due to strong Ekman flow and advection induced by strong offshore flows as filaments along the coast of Oman (McCreary et al., 1996a; Wiggert et al., 2005). This leads to the extent of upwelling induced fertilization and the high phytoplankton bloom to a distance exceeding ~1000 km offshore (Naqvi et al., 2003, 2006). This intense phytoplankton bloom close to the coast causes high primary productivity at a rate of more than 2.5 $gCm^{-2}day^{-1}$ (Marra et al., 1998; Morrison et al., 1998). Notably, unlike the Somali coast, here chlorophyll concentration is found to be more uniform all along the coast. Further, observations during summer monsoon indicate that the shelf off Oman is net autotrophic (Sarma, 2004) and exhibit moderately low surface pH (<7.9) (Takahashi et al., 2014).

Observations of the coastally upwelled water off Oman during US JGOFS indicates iron stress with N:Fe ratio ranging between 20,000-30,000 during the early phase of the summer monsoon. Later, this Fe limitation was also confirmed based on in-situ observations off the Oman shelf by Moffett et al. (2007) and Naqvi et al. (2010). Naqvi et al. (2010) further argued that this iron limitation fueled a shift in the phytoplankton communities from diatoms to smaller phytoplankton species which favours vertical export to the offshore deep ocean via lateral advection by the offshore currents (McCreary et al. 2013). In contrast, Rixen et al. (2006), based on sediment transport observations, suggests intense grazing in the silicon-rich near-shore upwelled water limits the diatom bloom off Oman coast. Further, modelling studies based on coupled physical-biogeochemical ocean models, suggests that iron (Wiggert et al., 2006 and Wiggert and Murtugudde, 2007) and silicate (Końe et al., 2009) are the most limiting nutrients that inhibit the growth of diatoms off the coast of Arabia.

The Indian Ocean, particularly the western Arabian Sea, is experiencing rapid warming over the last few decades. An estimate of the upper 300m water column of the western Arabian Sea (Oman region) show warming of ~1.5°C from 1960 to 2008; it lost dissolved oxygen by ~1 ml L^{-1} (at 100m) and became near anoxic with oxycline shoaled at ~19 m per decade during this period (Piontkovski and Al-Oufi, 2015). While it was hypothesized that the upper ocean warming reduces ocean mixing and biological production in the western Arabian Sea (Roxy et al., 2016), it was quickly refuted as a northward shift in monsoon low-level jet can orient the wind angle to the Oman coast in such a way that the net upwelling increases and so the primary production (Praveen et al., 2016). Moreover, the loss of snow cover over the Himalayan-Tibetan plateau owing

to global warming causing a shift from diatom dominated phytoplankton community to the *Noctiluca scintillans* in the northwestern Arabian Sea via weakening of convective mixing during winter monsoon (Goes et al., 2020).

Most of our understanding about the coastal upwelling off Oman is based on observations and modeling studies carried out in 90s' and early 2000. Unfortunately, the lack of observations and concerted modeling effort resulted in sluggish progress of our understanding in the last couple of decades for this region. The dynamical reasons for the development of offshore eddies and their impact on the coastal upwelling, coastal currents, SST, air-sea interactions, and finally, over the biology is still not clear. Thus, considering the importance of this region in regional physical and ecological processes and, most importantly its influence on the Indian Monsoon, a focused effort is needed from the scientific community for a complete understanding of oceanic processes of this coastal upwelling system.

2.7 West Coast of India

The signatures of upwelling along the west coast of India begin to appear during March, peak during June, and weaken by September. The upwelling is more intense along the southwest coast of India than that along the northwest coast. For the remaining months, the sea level anomaly is positive, and the thermocline is deeper, indicating conditions unfavorable for upwelling. A major consequence of west coast upwelling is the formation of anoxia that has a significant impact on the benthic ecosystem on the continental shelf (Banse 1959, Naqvi, 1991). Although the upwelling along the west coast of India is weaker than that along the coast of Somalia, the region accounts for 70% of the Arabian Sea fish production (Luis and Kawamura 2004).

2.7.1 Background

The earliest temperature observations along the west coast were collected by trading vessels along major shipping routes that were compiled into several atlases generated by different countries (Anonymous 1944, 1952). Though there were inconsistencies among the atlases, they showed the presence of cold water off the southwest coast of India from June to October (Sewel,1929; Banse, 1959). It was difficult to attribute this decrease in temperature to upwelling as the SST could also be controlled by other factors like atmospheric fluxes, horizontal advection, or mixing. Sewel (1992) showed that SST increased during April-May when the boreal summer is at its peak and dropped during June-July when the monsoon picks up. After the Monsoon, the temperature picked up again and dropped during the boreal winter when the winds were cooler. Sewell (1929) linked the double oscillation of SST to air temperature change.

The first evidence for upwelling along the west coast of India was presented by Sastry and Myrland (1959); they showed that the isotherms tilted upwards all along the southwest coast of India. Both Sastry and Myrland (1959) and Banse (1959)

858 argued that the upwelling along the southwest coast of India is not completely driven by monsoon winds because the fall in
859 SST occurred in April-May, which is a month before the onset of the summer monsoon. They hypothesized that the
860 prevailing current-system caused the upward tilting of isotherms. The reversal in the West India Coastal Current (WICC)
861 appeared to coincide with the beginning of upwelling at the southern tip of India. Banse (1959) suggested that after the onset
862 of Monsoon, the winds could intermittently push the cold water to the surface. Banse (1959) further noted that the poorly
863 aerated bottom water on the shelf during the summer monsoon was linked to upwelling that takes place along the coast.

864 Hydrographic sections in the decades that followed showed that the upwelling signatures extended all along the west coast
865 of India and Pakistan (Banse 1968; Sarma, 1968; Ramamirtham and Rao, 1973) and revealed that upwelling sets in earlier
866 in the south and progresses slowly towards the north (Sharma, 1968, Longhurst and Wooster, 1990). Due to the boisterous
867 nature of monsoon winds, upwelling along the west coast of India was still considered to be driven by alongshore winds
868 (Ramamirtham and Rao, 1973). The role of wind in driving the upwelling was disputed again by Sharma (1978), using the
869 available wind data from the atlases that showed that the wind was onshore and poleward and not favorable for upwelling
870 during the summer monsoon. Notwithstanding, recent wind data sets show that the alongshore winds are not poleward but
871 equatorward (but weak) during the summer monsoon.

872 Johannessen et al. (1981) used an extensive data set (consisting of 1500 Nansen casts collected from 1971-1975) and
873 confirmed the upwelling features highlighted in previous studies. The seasonal upwelling was found to repeat every year,
874 albeit with a certain amount of variability. Upwelling signatures were not evident in salinity but in temperature and oxygen
875 data. The upwelling process also increased phytoplankton and zooplankton production. However, no such correlation was
876 evident for the higher trophic level of the food chain. The calculated rate of upwelling was around 1.5 m/day, which was
877 consistent with the earlier observations.

878 The "wind-driven upwelling" hypothesis was again invoked in the mid-eighties. Shetye et al. (1985) found that offshore
879 Ekman transport, though weak, peaked during the summer monsoon. Using ship-based observations, Shetye et al. (1990)
880 confirmed that the upwelling intensity weakened from south to north. The width of the surface current, which is related to
881 the upwelling, extended about 150 km from the coast. The signatures of upwelling were evident only in the top 100 m below
882 which there were signatures of downwelling, indicative of an undercurrent. They refuted the "current-induced upwelling"
883 hypothesis using regression analysis between Ekman transport and temperature gradient.

884 Numerical models have provided considerable insight into the seasonal cycle of north Indian Ocean circulation (McCreary
885 et al., 1993; Shankar et al., 1996; McCreary et al., 1996b; Vinayachandran et al., 1996; Shankar and Shetye 1997). Using
886 linear wave theory, McCreary et al. (1993) proposed that the upwelling along the west coast of India was primarily driven
887 by coastal-trapped waves generated by remote winds from the Bay of Bengal (see section 2.7.3 for details). The wind-
888 driven upwelling was weaker than that caused by the propagation of these waves. The dominance of these waves suggests

that upwelling indices based on Ekman theory (Pankajakshan et al., 1997; Bakun et al., 1998) do not provide a complete picture of coastal upwelling along the west coast of India. The weak alongshore winds, however, would still contribute to upwelling and cannot be neglected (Shankar et al., 2002; Suresh et al., 2013). Unlike the west coast of India, the southern tip of India is unique in the sense that the Findlater jet is parallel to the coast and causes strong Ekman Transport (Bakun et al., 1998; Smitha et al. 2008). The wind-induced coastal upwelling index here was almost five times that along the southwest coast of India and the strong upwelling near the southern tip could generate coastal-trapped waves that could propagate along the west coast of India (Bakun et al., 1998).

2.7.2 Observations

The double oscillation (Sewell (1929) is evident in the SST climatology (**Figure 14a, 15a**). The temperature peaks during April and is highest along the southwest coast of India. The area surrounding the southwest coast of India, where the temperature remains above 30^{o}C, is often referred to as the Arabian Sea mini warm pool, and this region plays an essential role in the onset of the summer monsoon (Vinayachandran and Shetye, 1991;Rao and Sivakumar, 1999; Shenoi et al., 2005; Kurian and Vinayachandran, 2007; Vinayachandran et al., 2007). The increase in temperature is attributed to air-sea fluxes and is independent of the SST changes observed during the winter monsoon. The temperature begins to drop after April and is the lowest during July and August. The drop in temperature starts in the south and progresses northwards within a month. The progression of SST towards the north, also observed in hydrography data (Sarma, 1968 and Longhurst and Wooster, 1990), could be linked to the poleward propagation of coastal Kelvin waves. A typical first or second baroclinic mode Kelvin wave would cover the entire west coast of India within 7-21 days (these waves are sometimes too fast to be detected by a satellite over a small domain).

Along the southwest coast of India, the isotherms tilt upwards by April (**Figure 14b-c**). By June, the cooler water starts touching the surface, and the upwelling intensifies by July and August. The isotherms start lowering by September-October, and surface waters become warmer. In the north, the surface layers are cooler during April, and the downwelling of isotherms persists till June. The isotherms begin to rise by July-August, but they are very weak compared to the southwest coast of India. Unlike the SST, the depth of 26^{o}C isotherm shows an annual cycle; it decreases during summer and increases during winter. The lag associated with poleward propagation of the Kelvin wave is also evident in the isotherm depth (See Figure 7 in Shah et al., 2015 and Figure 6 in Shankar et al., 2019). The larger width of the upwelling region in the south is also indicative of Rossby waves, whose westward phase speed decreases with latitude. The westward drift of chlorophyll along with Rossby waves is evident in the satellite data but is not as prominent as seen during the winter monsoon (Amol, 2018; Amol et al., 2020).

Since wind is the primary driving factor for upwelling around the world, it is essential to look at its behavior along the west coast of India. Although the monsoon winds are strong (**Figure 15d,e**), they mainly blow perpendicular to the coast. The alongshore component of the wind is weak and equatorward all round the year. The winds peak during July along the entire west coast and this increase in the magnitude of the alongshore wind intensifies the upwelling during the summer monsoon. It is only at the southern tip of India that the alongshore winds reverse with the season. Upwelling indices show that it is weaker along the west coast of India, compared to Somalia, Oman, Tanzania, and south Madagascar but is equivalent to that in Mozambique and west Madagascar (Bakun et al., 1998). As the alongshore winds are weak compared to the cross-shore, there is also an ambiguity in the direction of the wind reported by previous authors (Sarma, 1978; Shetye et al., 1985;Shah et al., 2015). For example, Shah et al., (2015) showed that the alongshore winds were equatorward during the summer monsoon, but only south of 17^{o}N. The difference here lies in the angle of rotation applied to compute the alongshore component of wind. Shah et al. (2015) used coastline angle, which is almost parallel to the longitude in the north. The wind vectors in **Figure 15** are pointing northeast, which would lead to a poleward wind when rotated based on coastline angle. The slope angle, which is used to compute the alongshore wind in **Figure 15**, is different from the coastline angle because of the widening of the continental shelf north of 15^{o}N (see 1000 m contour in **Figure 15a**).

Unlike the unidirectional alongshore wind, WICC and the sea level anomaly show a strong seasonal cycle (**Figure 15,f**). The current (sea level anomaly) is equatorward (low) during summer and poleward (high) during winter. The reversal in current follows the drop in sea level, and the flow is poleward in March, much before the monsoon onset. The early reversal of current is evident in direct current measurements (Amol et al., 2014; Chaudhuri et al., 2020). Unlike the sea level, the currents, particularly along the southwest coast of India, have a significantly larger intraseasonal component (Vialard et al., 2009a; Amol et al., 2014; Chaudhuri et al., 2020). The current could flow in either direction during a particular time of a year, and the frequent intraseasonal bursts would further make it difficult to predict its direction. Still, it was the early reversal of current during March that prompted Banse (1959) to discard wind as the driving factor for upwelling.

In response to the raising of the isotherms, chlorophyll also increases from April onwards (**Figure 15c**). The chlorophyll concentration is highest along the southwest coast of India and peaks during July-August. During this time, the wind, the sea level, and the SST are at their minimum as well. The increase in chlorophyll concentration is weakest along the central west coast of India and only extends over a few months. In the north, the chlorophyll is high all around the year because of the winter convective mixing that follows the upwelling in the summer.

2.7.3 Mechanisms

McCreary et al. (1993) used a series of reduced-gravity model experiments to show that the upwelling along the west coast was driven by remote forcing. They concluded that winds in the Bay of Bengal and the equator caused upwelling along the

west coast of India. The local winds, however, enhanced upwelling, but their contribution was weaker than that by remote winds. They noted that the driving mechanism for upwelling was the generation of coastal Kelvin waves by winds along the western boundary of the Bay of Bengal. These winds generated upwelling Kelvin waves that propagated equatorward (with the coast on the right) along the east coast of India, turned around Sri Lanka, and propagated poleward along the west coast of India. The poleward propagation explained why the upwelling is delayed in the north. Shankar and Shetye (1997) further highlighted the mechanism for the early onset of upwelling using an analytical model. They showed that the upwelling along the west coast of India and the Lakshadweep low formed in the southeastern Arabian Sea resulted from poleward propagation of Kelvin waves and westward radiation of Rossby waves, which supported the results shown by McCreary et al. (1993). The model upwelling in a 5-6 km resolution coastal model that was nested into large-scale model Haugen et al. (2002) began during April and persisted till October, and was most intense along the southwest coast of India. Satellite chlorophyll data and a physical model Lévy et al. (2007) show that the onset of summer blooms in the southeastern Arabian Sea occurred during March and was primarily driven by upwelling. Koné et al. (2013) showed high values of NO3- that were associated with vertical advection in this region.

Differences in the strength of upwelling between north and south could affect the nature of fisheries along the coast of India (Shankar et al., 2019). In the south, stronger upwelling permits the growth of larger phytoplankton owing to a greater supply of nutrients, whereas in the north, phytoplankton tends to be smaller in size owing to weaker upwelling. The large phytoplankton is directly fed by planktivorous fishes that are not common in the north.

In summary, model simulations show that the upwelling is primarily driven by poleward propagation of coastal Kelvin waves. The linear wave theory explains the early onset of upwelling and the progression of upwelling from south to north. The alongshore winds also favor upwelling and could contribute significantly to its variability along the coast. A detailed analysis using observations and numerical models would be required to delineate the relative contribution of the wind and large-scale waves during the peak of the summer monsoon.

2.7.4 Productivity and ecosystem impacts

Unlike most parts of the world ocean, the biophysical provinces of the Indian Ocean vary seasonally (Rixen et al., 2020; Lévy et al., 2007). This is because during both monsoons, the underlying mechanisms for nutrient intrusion that support elevated primary productivity are different during summer and winter. During summer, there is strong coastal upwelling, while cooler and dry air from the northern Indian subcontinent drives convective mixing in the eastern Arabian Sea during winter (Madhupratap et al., 1996).

A fascinating feature of the ecosystem along the west coast of India is the seasonal occurrence of two phytoplankton blooms of different phyla. First, here are winter-mixing driven blooms of *Noctiluca scintillans* (hereafter *Noctiluca*), a

mixotrophic dinoflagellate that occur during winter in the northern Arabian Sea (Prakash et al., 2008; Gomes et al., 2008; Rixen et al., 2020). Second, during March-May, there are massive cyanobacterial blooms of *Trichodesmium* (N_2 fixers) in the central – eastern Arabian Sea (Capone et al., 1998; Gandhi et al., 2011; Kumar et al., 2017).

The occurrence of *Noctiluca* blooms was first discovered in the early part of this century and seemed to have displaced the previously occurring diatom blooms in this region (Gomes et al., 2008; Sarma et al., 2018). These blooms create a biogeochemical divide – making the northern Arabian Sea more productive than its southern part (Prakash et al., 2008). These massive outbreaks of *Noctiluca* blooms were reported to be fueled by an unprecedented influx of oxygen-deficient waters into the euphotic zone (Gomes et al., 2014). Prakash et al. (2017) refuted this claim and proved that they are naturally driven by changes in nutrient stoichiometry (Lotliker et al., 2018; Sarma et al., 2018).

Once nutrients supply driven by the winter mixing is consumed and the ocean begins to stratify, *Trichodesmium* blooms start to appear by early spring in the central Arabian Sea (Capone et al., 1998; Mulholland and Capone, 2009). These become so massive in the eastern Arabian Sea that they fix up to 34 mmol N m^{-2} d^{-1}, which is the highest reported rate of N_2 fixation ever among the world oceans (Gandhi et al., 2011; Kumar et al., 2017). In fact, when similar conditions prevail during fall intermonsoon immediately after the summer monsoon upwelling, the N_2 fixation rate makes a surplus contribution to the nitrogen-nutrients to fuel primary production in the eastern Arabian Sea (Singh et al., 2019).

N_2 fixers are associated with excess phosphate (compared to NO_3^- if normalized as per the Redfield Ratio) concentration (Deutsch et al., 2007). Summer upwelling of oxygen-deficient waters along the shelf break is the major process regulating the biogeochemistry on the west coast (Gupta et al., 2016). Summer upwelling, which drives high primary production, is followed by the occurrence of denitrification (a nitrogen loss process) at subsurface layers in the eastern Arabian Sea which would make these layers phosphate-rich. Hence, in this cycling, the upwelling would intrude phosphate-rich water to the sea surface (Sudheesh et al., 2016). The notion is that once parts of upwelled nutrients are utilized by autotrophs in the sunlit layers, it will create a niche for N_2 fixers. However, recent studies suggest that N_2 fixers can also occur in eutrophic conditions (Landolfi et al., 2015).

The progression of upwelling over the eastern Arabian Sea is slow, and the upwelled waters sustain for about 9 months over the shelf (Gupta et al., 2016); i.e., a wider shelf over the eastern Arabian Sea allows the upwelled waters to persist long enough till its little oxygen content is completely utilized and seasonally cover the entire shelf (area ~200,000 km^2), making it the largest shallow water oxygen-deficient zone in the world (Naqvi et al., 2000). The intensely oxygen-depleted environment favors the development of diverse microbial populations that utilize anaerobic pathways to derive energy, mediating elemental transformations that are of immense geochemical significance (Wright et al., 2012). Denitrification is one of the classical examples for this kind, which makes the eastern Arabian Sea upwelling system one of the 'hot spots' of N_2O production in the world ocean with N_2O saturations up to 8250% (Naqvi et al., 2005). Moreover, these upwelling

regions are also characterized by a high production of other climate-relevant trace gases such as CH_4 and dimethyl sulfide (Naqvi et al., 2010; Shenoy et al., 2012). Further, spring *Trichodesmium* blooms seem to be responsible for the emission of volatile organic compounds, such as isoprene – a precursor of ozone formation in the troposphere, in the eastern Arabian Sea (Tripathi et al., 2020a,b). The upwelling biogeochemistry of this seasonal oxygen-deficient zone also significantly impacts the cycling of several other micronutrients, like manganese, iron, etc. (Breitburg et al., 2018).

The variability in magnitude and intensity of upwelling and the characteristics of upwelled waters play a major role in shaping biogeochemistry of the eastern Arabian Sea shelf that designates it as a 'Hotspot' for greenhouse gas production during the summer monsoon. The upwelled waters are hypoxic in the south and suboxic in the central-eastern Arabian Sea (Gupta et al., 2016, Sudheesh et al., 2016), as the latter are sourced from the core oxygen minimum zone (OMZ with <10 µM of oxygewen) and former from outside of it (Gupta et al., 2021). Such spatial variation in degree of deoxygenation of upwelled waters is regulated by the intra-seasonal shift of cold-core eddy from south to central regions, which result in upliftment of oxycline from outside core OMZ in the south to within core OMZ in the centre (Gupta et al., 2021). This change in oxygen regime in upwelling source waters from hypoxia to suboxia combines with strong thermohaline circulation leading to high oxygen demand over the central shelf, relative to the south (Gupta et al., 2021), making the central shelf extremely oxygen-depleted and sulphidic with H_2S levels goes up to ~15 µM in the nearshore waters (Naqvi et al., 2006, 2009). While the hypoxic upwelling over the southern shelf restricts the denitrification to sediment, the anoxic/sulphidic conditions over the central shelf extend its occurrence to the water column as well (Sudheesh et al., 2016). Being limited with very few studies on carbon dynamics over both east and west coasts, the temporal evolution of coastal acidification is still not clear, although Kanuri et al. (2017) reported pCO_2 up to 630 µatm along the southeastern Arabian Sea shelf and even levels exceeding 1000 µatm are common during peak upwelling (Sudheesh, 2018). Refuting the charges levied by huge productions of CO_2 and N_2O, massive methane loss through anaerobic oxidation by sulphate in the nearshore waters of the eastern Arabian Sea during late summer monsoon upwelling (Sudheesh et al., 2020) is a great relief to the environment as the potential greenhouse effect is naturally diluted by converting methane to CO_2 (the latter is almost 300 times less potential compared to former).

On comparable lines of intensification of oxygen deficiency in the western Arabian Sea (Piontkovski and Al-Oufi, 2015), eastern Arabian Sea shelf was also earlier reported with such intensification (Naqvi et al., 2000, 2006), but the comparison of monthly studies for one year in 2012 with similar data set from July 1958 to January 1960 (Banse, 1959) revealed remarkably little change in oxygen concentrations (Gupta et al., 2016; **Figure 16**) with inter-annual variations between the years supported by global climatic events such as IOD, ENSO, etc., as these warm years impact upwelling intensity and prevents the anoxia formation on the shelf (Parvathy et al., 2017).

The productivity of the western Arabian Sea has earlier been shown to increase over the years (Goes et al., 2005) due to the warming of the Eurasian landmass, but such a trend was not discernible over the eastern Arabian Sea (Prakash and Ramesh,

2007) as neither wind speeds nor SSTs could show any significant change. Although no information available on such recent trends, the dissolved oxygen concentrations of recent years were comparable with that of five decades ago over the southwest coast of India (Gupta et al., 2016) despite the period gaining significant developmental activities on the hinterland co-occurred with a steep rise in Arabian Sea warming. In the absence of climatology data, the maintained dissolved oxygen levels can be considered as a proxy to show the sustained upwelling intensity and biogeochemistry of this region. Further, the upwelling intensity and consequent biological production over its eastern part are several-fold less than the western region. Yet, the famous and thickest Arabian Sea OMZ is closer towards the eastern side, underlying the importance of circulation in OMZ formation and source water characteristics for upwelling induced primary production. Though the upwelling over both east and west coasts is progressed from south to north during the summer monsoon, the coast of Somalia is pronounced with significant gradients in biological production – several folds high in the north during the advanced phase of summer monsoon when nutrients from local upwelling as well as advected from south support enhanced growth of phytoplankton (Lakshmi et al., 2020). In contrast, the productivity of eastern upwelling is higher in the south due to relatively intense upwelling compared to its north (Gupta et al., 2016; Shankar et al., 2019). Though upwelling over the west coast is much intense, it never experienced strong oxygen-depleted conditions, unlike its east coast. The strong biological pump (Ekman transport) operating from the west coast transports organic matter too far off distances beyond the central Arabian Sea and pushes the OMZ towards the east (Naqvi et al., 2003, 2006). Being closer, these OMZ waters feed the eastern Arabian Sea upwelling and develop hypoxic/anoxic conditions there (Gupta et al., 2016; Sudheesh et al., 2016). The upper 300m water column of the western Arabian Sea (Oman region) has witnessed warming by ~1.5 °C from 1960 to 2008; it lost dissolved oxygen by ~1 ml L^{-1} (at 100m) and became near anoxic with oxycline shoaled at ~19 m per decade during this period (Piontkovski and Al-Oufi, 2015). While it was hypothesized that the upper ocean warming reduces ocean mixing and biological production in the western Arabian Sea (Roxy et al., 2016), it was quickly refuted as a northward shift in monsoon low-level jet can orient the wind angle to the Oman coast in such a way that the net upwelling increases and so the primary production (Praveen et al., 2016). In the scenarios of such increasing upwelling and shoaling of oxycline, if more deoxygenated/near anoxic waters upwell, it may turn the future of the west coast comparable to the present-day east coast in terms of biogeochemistry under seasonal hypoxia/anoxia.

The impact of upwelling on oxygen concentration has a profound socio-economic impact too as it directly affects living resources and biodiversity (Panikkar and Jayaraman, 1966; Naqvi et al., 2006). Though the available information from the Arabian Sea is scanty, the mesopelagic fish populations appear to be impacted by a reduction in suitable habitat as respiratory stress increases due to deoxygenation (Naqvi et al., 2006). Benthic ecosystems along the eastern Arabian Sea are affected worst owing to the unusually large area of continental margins being exposed to hypoxic/anoxic waters (Helly and Levi, 2004). During this period, the density and diversity of larger benthic fauna (prawns, crabs, mollusks, etc.) become insignificant, and groups that are sensitive to hypoxia, like echinoderms, are either absent or least abundant (Parameswaran et al., 2018). However, macro-infaunal communities are overwhelmingly dominated by deposit-feeding opportunistic

polychaetes, particularly the proliferation of juveniles (Abdul Jaleel et al., 2015). The upwelling region of the Arabian Sea is a major ground for fishery potential in terms of their eggs laying and recruitment succession. The upwelling induced high primary production supports higher trophic level productivity but with less biodiversity. It is found that upwelling intensity and coastal currents during summer monsoon are highly influencing fish eggs transport, their recruitment success rate, and juveniles transport.

2.8 South Coast of Sri Lanka

The upwelling off the southern coast of Sri Lanka (which is slightly tilted towards the north in the east) begins with the onset of the SWM, during the last week of May or during the first of June, and continues through October. The coastal upwelling here is primarily caused by summer monsoon winds, which have a strong alongshore component along the southern coast of Sri Lanka (Vinayachandran et al., 2004). The SMC that flows eastward to the south of Sri Lanka and northeastward to the east of Sri Lanka (Vinayachandran et al., 1999, 2018; Webber et al., 2018; Rath et al., 2019) influences the advection of cold upwelled water. During the early part of the SWM, some advection of cooler water occurs towards the south, away from the coast. During the later half, most of the upwelled water flows into the BoB along with the SMC (Vinayachandran et al., 2004; Das et al., 2018; Vinayachandran et al., 2020). Numerical simulations have successfully reproduced the upwelling along the southern coast of Sri Lanka (Vos et al., 2014).

Satellite-derived chlorophyll data (**Figure 17)** during summer monsoon clearly shows that the coastal upwelling has a clear expression on the ecosystem (Vinayachandran et al., 2004; Vinayachandran 2009). The chlorophyll concentration is high near the coast in response to upwelling. In addition, the advection by SMC spreads water from near the coast towards the east of Sri Lanka, impacting a larger region. In situ sampling to quantify the physical and biological impacts of upwelling around Sri Lanka is yet to take place. The physical impact on the ecosystem in this upwelling zone is complex, owing to the simultaneous influence of multiple factors. The upwelled water advects to the southern coast of Sri Lanka from the southern tip of India and the Gulf of Mannar. There is additional advection along the path of the SMC. Finally, the currents along the east coast of Sri Lanka is southward during summer, being the eastern arm of the cyclonic gyre, associated with Sri Lanka Dome (SLD, Vinayachandran and Yamagata, 1998). There are indications from model simulations that the pCO2 distribution is impacted by the combined influence of upwelling and advection (Chakraborty et al., 2018). On the whole, satellite-derived SST and chlorophyll data clearly show an active upwelling zone along the southern coast of Sri Lanka, which draws out a definite response from the ecosystem and biogeochemistry.

Using shipboard observations, Jyothibabu et al. (2015) suggest that capping of the upper layer by low salinity water in this region can restrict the chlorophyll concentration in the near-surface layers. Using the glider data set, Thushara et al. (2019) has provided in situ observational evidence for the chlorophyll blooms associated with SLD. The observed bloom followed

a period of Ekman suction caused by cyclonic wind stress curl, and the decay was caused by the arrival of Rossby waves from the east. Model simulations (Thushara et al., 2019) support these processes and suggest that the Ekman pumping is capable of enriching the euphotic zone with nutrients, but there is a lack of corresponding in situ observations that are much needed to validate these processes.

2.9. East Coast of India

2.9.1 Background

Circulation in the Bay of Bengal (BoB) is driven by a rather intricate combination of local winds over the BoB and remote forcing originating from the equatorial Indian Ocean. During the southwest monsoon, strong southwesterly winds along the western boundary of the BoB (WBoB) makes conditions favourable for coastal upwelling (Shetye et al., 1991; Shankar et al., 1996; McCreary et al., 1996b; Vinayachandran et al., 1996; Shankar et al., 2002; Thushara and Vinayachandran, 2016). The winds are northeasterly during the northeast monsoon, which is favorable to coastal downwelling (Shetye et al., 1996). BoB is also known for high SST (average temperature greater than 28 C) (Vinayachandran and Shetye, 1991; Shenoi et al., 2002) and the formation of several low-pressure systems (Sikka 1980; Gadgil et al., 2004). A significant amount of freshwater influx from major river sources like Ganga, Brahmputra, etc., plays a dominant role in stratifying the upper layer affecting the strength and intensity of coastal upwelling (Vinayachandran et al., 2002; Behara and Vinayachandran, 2016; Thushara and Vinayachandran, 2016, Amol et al., 2019). Additionally, coastal processes in the WBoB are influenced by complex bathymetry, shallow mixed layer, the formation of mesoscale eddies, and propagations of large-scale planetary waves (Mukherjee et al., 2017). Detailed description of the East India Coastal Current (EICC) and its variability, based on moored observations, are given in Mukherjee et al. (2014) and Mukhopadhyay et al. (2020).

2.9.2 Observations

The first evidence of coastal upwelling along WBoB was observed between 1952–1965, during IIOE. The first published report, although insufficient to present evidence of coastal upwelling or downwelling for a season, along WBoB using hydrographic data, was by La Fond (1954, 1957, 1958, 1959). Evidence of coastal upwelling during summer monsoon along the east coast of India was reported by Varadachari (1961). Murty and Varadachari (1968) found stronger upwelling at Visakhapatnam compared to Chennai during both spring and summer. Similarly, upwelling at the northern part of the east coast of India (**Figure 18**) was also reported by several investigators (Murty, 1958; Murthy, 1981; Gopalakrishna and Sastry, 1984; Rao et al., 1986). Upwelling along the east coast of India have been described using hydrographic measurements (Shetye et al., 1991, 1993, 1996; Sanilkumar et al., 1997; Babu et al., 2003), Lagrangian drifters (Shenoi et al., 1999), satellite observed sea level (Shankar et al., 2002, Durand et al. 2009), current meter moorings (Mukherjee et al. 2014;

Mukhopadhyay et al., 2020) and high frequency HF Radar (Mukhopadhyay et al., 2017). The vertical extent of coastal upwelling can extend upto ~70 m (Shetye et al., 1991). During summer, both hydrography and moored observed current shows evidence of downwelling below upwelling along east coast of India (Shetye et al., 1991; Mukherjee et al., 2014; Francis et al., 2020).

Mesoscale eddies (both upwelling (cyclonic) and downwelling (anticyclonic) favorable) play a significant role in causing coastal upwelling/downwelling in the BoB (Ali et al., 1998; Gopalan et al., 2000; Chen et al., 2012; Nuncio and Kumar, 2012; Cheng et al., 2013; Mukherjee et al., 2019). However, the vertical structure of mesoscale eddies along WBoB is still unknown due to the lack of appropriate in-situ measurements. As cyclonic eddies upwell cold water from its lower base to upper depth and enhance vertical mixing (Falkowski et al., 1991; Kumar et al., 2004), and vertical structure of eddies affect the strength of upwelling and associated transport of heat, salt, and nutrients in the ocean (Chaigneau et al., 2011; Dong et al., 2014), it is required to understand the role of eddies in the upwelling along the east coast of India.

2.9.3: Mechanisms

Model simulations that began in the 1990s to investigate EICC found local wind-driven coastal upwelling along WBoB during the summer season compared to spring and northeast monsoon (McCreary et al., 1996b; Shankar et al., 1996; Vinayachandran et al., 1996). During spring, seasonal sea level variability along WBoB is dominated by remote forcing that originating from interior Ekman pumping in the BoB, the equatorial Indian Ocean, and alongshore wind along the eastern and northern boundary of the BoB (McCreary et al., 1996b; Vinayachandran et al., 1996; Aparna et al., 2012; Mukherejee et al., 2017). During the winter, seasonal coastal downwelling occurred due to the northeasterly winds (McCreary et al., 1996b; Shetye et al., 1996). Based on satellite and in-situ observations and models, Shankar et al. (2002) showed that the dynamics of sea level and associated upwelling along WBoB at seasonal time scales could be explained using linear theory.

At interannual time scales, dynamics of sea level and associated upwelling are dominated by El Niño-Southern Oscillation (ENSO) and Indian Ocean Dipole (IOD) (Saji et al., 1999). During ENSO and IOD events, interannual variability of sea level is influenced by remotely propagating waves from the equatorial Indian Ocean (Clarke and Liu, 1994; Rao et al., 2009; Aparna et al., 2012; Mukherejee and Kalita, 2019). At intraseasonal time scales, coastal upwelling or downwelling is dominated by mesoscale eddies formed due to instability of the ocean (Nuncio and Kumar, 2012; Chen et al., 2012; Cheng et al., 2013; Mukherejee et al., 2017).

Recent studies also showed that Andaman and Nicobar Islands (ANIs) play a dominant role in the dynamics of sea level and associated upwelling along WBoB (Chatterjee et al., 2017; Mukherjee et al., 2019) by influencing the wave propagation. While propagating in the interior BoB, the Rossby wave is significantly modified in the presence of ANIs (Chatterjee et al.,

2017) and generates coastal upwelling by the formation of mesoscale eddies in the WBoB (Mukherjee et al., 2019). Another significant force for modifying coastal upwelling comes from freshwater discharge by rivers (Behara and Vinayachandran, 2016). Owing to the presence of fresh river water, barrier layer formation is common in the northern Bay of Bengal (Vinayachandran et al., 2002), which has the potential to weaken upwelling (Behara and Vinayachandran, 2016). However, the impact of river runoff inhibits upwelling only towards the end of the summer monsoon (**Figure 19**), and the local winds sustain upwelling for most of the summer monsoon (Thushara and Vinayachandran, 2016)

In summary, coastal upwelling along WBoB is not simply local wind-driven but affected by several oceanic processes, which includes mesoscale eddies, remote forcing from equatorial Indian Ocean & interior BoB, freshwater forcing from rivers, etc. At the seasonal time scale, coastal upwelling along WBoB is dominated by linear processes either by local wind or remotely propagating waves. At interannual time scales, sea level variability along WBoB is dominated by remotely propagating waves from the equatorial Indian Ocean. At intraseasonal time scales, mesoscale eddies dominate sea level variability. More in-situ observations are necessary in order to understand the vertical structure of coastal upwelling at intraseasonal, seasonal, and interannual time scales. Additionally, ocean models need to be better parameterized for resolving vertical processes near the coast related to mixed layer, thermocline, barrier layer, vertical stratification, etc, based on in-situ observations.

2.9.4 Productivity and ecosystem impacts

Despite being situated at similar latitudes and experiencing similar monsoonal force, the Bay of Bengal is a low productive basin compared to the Arabian Sea. The large influx of freshwater l leads to the formation of the salinity-driven "barrier layer," (Vinayachandran et al., 2002) which restricts entrainment of nutrients into the upper sunlit layer. The inorganic nutrient (nitrate and phosphate) transport through rivers draining into the bay is also abysmal (Sengupta et al., 1981; Sengupta and Naqvi 1984). The salinity driven stratification is so strong that monsoonal winds are unable to erode them and inject nutrients from the subsurface layer. The surface chlorophyll concentration is therefore, always low in the Bay of Bengal. However, the basin is characterised by the perennial presence of sub-chlorophyll maximum (SCM), which is located at 40-90 m depth (Prasanna Kumar et al., 2007; Thushara et al., 2019). Cyclonic old-core eddies, which are predominantly present in the Bay of Bengal, do pump nutrients into the upper layer and can enhance the productivity by more than two-fold (Prasanna Kumar et al., 2007; Singh et al., 2015). Anticyclonic eddies, on the other hand, recharge the subsurface layer with dissolved oxygen and restrict the strengthening of the OMZ. Episodic atmospheric disturbances such as depressions and cyclones also erode the stratification by churning up the ocean and inject nutrients into the upper sunlit layer to fuel productivity (Gomes et al., 2000; Vinayachandran and Mathew 2003; Sarma et al., 2013; Vidya et al., 2017).

Though weak, the upwelling in the Bay of Bengal does drive regimes of high productivity in the southwestern region during the Southwest monsoon (Vinayachandran et al., 2004) and in the northeastern region during the northeast monsoon (Vinayachandran, 2009). The nitracline, usually situated at a depth of ~75 m, below the stratified layer, shoals upward by poleward flowing EICC during the pre-southwest monsoon and enhances productivity (Gomes et al., 2000). Additionally, high productivity was found due to eddies along the coast during the pre-monsoon. During the post-monsoon, although the wind-driven upwelling and river discharge increased the column chlorophyll concentration by nearly five-fold, the productivity decreased to half (Gomes et al., 2000) due to light limitation.

Vinayachandran et al. (2005) made the first attempt to use a four-component ecosystem model coupled with a general circulation model to simulate the evolution of phytoplankton bloom in the bay during the northeast monsoon. The biogeochemical simulation successfully captured the bloom evolution supported not only by the entrainment of nutrients but also through upward transport of significant amounts of chlorophyll from the sub-surface layer. It highlights the contribution of deep chlorophyll maxima in the observed surface bloom. Thushara and Vinayachandran (2016) later studied the evolution of phytoplankton bloom in the northwestern bay during the summer monsoon. Their chlorophyll simulations could successfully capture the seasonal distribution of biomass, including the coastal blooms at major river discharge mouths, and were in good agreement with the satellite-derived chlorophyll data. The bloom intensity, however, is more realistic in the east of Sri L anka and also in parts of the Andaman Sea. At other places, models tend to underestimate the chlorophyll values in comparison with the satellite chlorophyll. Thushara and Vinayachandran (2016) argued that the negative bias might be due to overestimation in the satellite-derived chlorophyll. Their biogeochemical simulations showed that as the river plumes were pushed away due to coastal upwelling, they did not change the biological production in model simulations. Surface winds appear to have significant control over governing bloom in the southwestern bay during the summer monsoon. Chakraborty et al. (2018), investigated the CO2 dynamics of the Sri Lanka dome region, which experiences intense upwelling during the southwest monsoon and showed that biological processes in the upwelling region contribute towards draw-down of the pCO2. Their simulations indicated that biological processes dominate over the physical upwelling in terms of the CO2 outgassing and lead to a net decrease (~11uatm) of pCO2. Shallower nitracline in the region pumps more nutrients into the upper layer and fuels biological production that compensates for the CO2 outgassing. In fact, the region becomes a sink for CO2 despite having significant upwelling.

2.10 Sumatra and Java

2.10.1 Background

The upwelling off the southern coasts of Sumatra and Java Islands is a remarkable and unique eastern boundary upwelling system (EBUS) in the Indian Ocean. The major EBUS in the Pacific and Atlantic Oceans are considered as the ocean component of an interacting system among the ocean, atmosphere, and land, and its existence and development are typically associated with drier conditions in atmosphere and on land (e.g. Chavez and Messie, 2009; Garcon et al., 2019). Compared with these major EBUS in the Pacific and Atlantic Oceans, however, the upwelling system in the Sumatra-Java coast develops under wetter atmospheric condition and forced mainly by monsoon variability modulated by other climate phenomena, such as ENSO and IOD. Despite its important roles in climate and ecosystem dynamics, the upwelling system in the Sumatra-Java coast had been overlooked until recently. This is because the average magnitude of the upwelling signals is smaller compared to the other major EBUS in the world, due partly to a strong seasonality associated with monsoonal wind forcing and partly to the existence of the Indonesian throughflow to the east and south of the upwelling region (Qu et al., 1994; Du et al., 2005). In addition, insufficient availability of in-situ data and complex geometry near the Indonesian Seas make detailed investigations difficult.

The Sumatra-Java upwelling region is embedded in rather complex upper-layer circulations in the southeastern tropical Indian Ocean between Indonesia and Australia (Fig.1). Seasonally changing South Java Coastal Current is associated with the monsoonal wind reversal and is directly linked with the upwelling system (Quadfasel and Cresswell, 1992; Sprintall et al., 1999). The westward flowing South Equatorial Current, a part of which is fed by the Indonesian throughflow from the Indonesian Archipelago, is located to the south of the upwelling region (e.g. Qu and Meyers, 2005a). Since the Sumatra-Java upwelling region sits close to the equator (from the equatorial region down to around 9°S), the equatorial and coastal wave guide affects variability in upwelling signatures significantly.

2.10.2 Mechanisms

A major feature of the upwelling in this region is the seasonal variation associated with the monsoonal wind along the coasts; the upwelling favorable southeasterly winds prevail during boreal summer while the northwesterly winds appear during boreal winter which generate downwelling conditions. Wyrtki (1962) was the first to demonstrate that the Ekman upwelling along the coast of Sumatra and Java occurs during the boreal summer associated with the local southeasterly monsoon over the region. Upwelling signatures in this region are well observed in in-situ measurements and satellite remote sensing

observations as in the other upwelling regions; e.g., cooler SST and subsurface temperature, shallower thermocline depth and lower sea surface height, and higher chlorophyll and nutrients concentrations compared to the surrounding area (e.g. Wyrtki, 1962; Susanto et al., 2001; Susanto and Marra, 2005; Iskandar et al., 2017) (**Figure 20**). The upwelling signatures propagate to the west in association with the westward movement of the along-shore winds (Susanto et al., 2001). However, locations of maximum amplitude of the upwelling signatures may differ in space due to dynamical upper-ocean responses to the wind forcing. One such example can be seen in a phase relation between the winds and SST along the Java coast; strong winds appear in the western area of the Java coast while the SST signal comes further east (Naulita et al., 2020). In addition to this local wind forcing, the Sumatra-Java coastal area is affected by remotely forced Kelvin waves propagating from regions further northwest along the Sumatra coast and from the equatorial Indian Ocean. Several studies have shown that both the local wind forcing and this remote wave influence play key roles in determining magnitude and area of the Sumatra-Java upwelling (e.g. Cheng et al., 2016; Horii et al., 2016; Delman et al., 2018).

The local and remote influences vary year-to-year, generating interannual variability of upwelling strength and spatial coverage. The most significant interannual variability is the Indian Ocean Dipole mode (IOD), whose center of action in the eastern pole appears over the Sumatra-Java upwelling region. During the positive IOD, the southeastern Indian Ocean, particularly along the Sumatra-Java coasts, are occupied by negative SST anomaly, which tends to be phase-locked to the seasonal upwelling during the boreal summer to fall. While the cool SST in seasonal variation is pronounced along the Java coast (see **Figure 20**), the interannual SST anomaly appears in both Sumatra and Java coastal regions. In addition, the upwelling variability in the interannual time-scale is also related to ENSO phenomena in the Pacific Ocean (Susanto et al., 2001; Susanto and Marra, 2005), partly due to co-occurrence of ENSO and IOD in some years and also to atmospheric teleconnections from the Pacific to modify strength of along coast component of the wind stress over Sumatra and Java.

There are attempts to investigate the ocean processes responsible for the seasonal and interannual variations in the mixed-layer or upper-layer temperature using heat/temperature budget analyses. Both the seasonal and interannual variations are dominated by vertical processes associated with the Ekman upwelling, with significant contributions from horizontal advection, including the one from the Indonesian throughflow (e.g. Qu et al., 1994; Du et al., 2005, 2008). The barrier layer is also affecting the seasonal SST variability, especially in the region off Sumatra coast (Du et al., 2005; Qu and Meyers, 2005b). For interannual time-scales, the SST variability is driven by both the local and remote wind forcing, both of which are strongly related to the IOD and to lesser extent to ENSO, while the thermocline depth variations are mostly due to the remote wave influences from the equatorial eastern Indian Ocean (Chen et al., 2016). There are several studies, including those under the IIOE-2 program, focusing on the roles of variability in the upwelling region on the evolution of IOD events. Initiation of positive IOD events is related to anomalous cooling off the coast of Sumatra-Java, which may be generated by local winds, particularly along the coast of Sumatra Island (Delman et al., 2016, 2018; Kämpf and Kavi, 2019), or remotely forced Kelvin wave signal originated in the equatorial Indian Ocean (Horii et al., 2008). During the mature stage of the

positive IOD, vertical upwelling processes as well as horizontal advection contribute in keeping anomalous cooling of the SST off the coasts of Sumatra and Java (Du et al., 2008; Chen et al., 2016). While the seasonal march to the northwesterly monsoon condition terminates this maintaining process forced by local and remote winds, oceanic eddy heat flux associated with mesoscale eddies generated by enhanced instability during the height of the positive IOD is also shown to facilitate disappearance of the anomalous conditions in the strong events (Ogata and Masumoto, 2010, 2011).

The upwelling off Sumatra and Java is also affected by intraseasonal variability in the ocean and atmosphere. These intraseasonal variability is, as in the case of seasonal and interannual variations, due both to the local winds and to remotely forced oceanic Kelvin waves (Iskandar et al., 2006; Horii et al., 2016). Even during the height of the positive IOD in 2008, strong intraseasonal upwelling signals are observed in temperature and salinity profiles obtained by Argo floats (Horii et al., 2018). In addition, a long-term trend in the upwelling strength is studied recently. For example, Varela et al. (2016) suggests the weakening of the upwelling while the SST shows a cooling trend due to cooler subsurface temperature. Sources of this upwelled water mass are not clearly determined yet. A study using a numerical model proposes the Indonesian throughflow as a possible source for the upwelling water off Java coast (Valsala and Maksyutov, 2010), while another study suggests that water mass from the northwest via South Java Current could be upwelled in this region (Varela et al., 2016).

2.10.3 Productivity and ecosystem impacts

The Java upwelling region off Indonesia is the only example of eastern boundary upwelling in the Indian Ocean. In contrast to the large eastern boundary upwelling in the Pacific and Atlantic Ocean, it occurs only seasonally during the SEM in association with the reversing South Java Current (Sprintall et al., 1999; Susanto et al., 2001) and, like the Bay of Bengal, is strongly influenced by freshwater inputs from the maritime Indonesian continent (Rixen et al., 2006). As in the other EBUS, high biological productivity is observed in the Sumatra-Java upwelling region during boreal summer and fall (Wei et al., 2012), with high nutrient and chlorophyll-a concentrations along the coasts (e.g. Wyrtki 1962; Tranter and Newell, 1962; Susanto et al., 2001; Asanuma et al., 2003; Iskandar et al., 2009). Spatial distributions and temporal variations of various biogeochemical parameters have been detected from in-situ observations, coral records, and sediment cores for the present situations and paleo-oceanographic conditions (e.g. Grumet et al., 2004; Murgese and De Deckker, 2005; Andruleit 2007; Andruleit et al., 2008; Baumgart et al., 2010; Ehlert et al., 2011). Satellites reveal that elevated Chl*a* (>2 mg m^{-3}) first appears off Java in June and persists into November (Lévy et al., 2006, 2007; Hood et al., 2017), with primary production estimates in August exceeding 1 mg C m^{-2} d^{-1} (Hood et al., 2017). Relaxation of SEM winds and downwelling Kelvin waves (Sprintall et al., 1999) suppress productivity in the fall. Zooplankton biomass increases by about an order of magnitude seasonally in the Java upwelling (Tranter and Kerr, 1969, 1977).

Recent in-situ observations in the Sumatra-Java upwelling region conducted during the IIOE-2 period indicate different phytoplankton composition and assemblages between upwelling and non-upwelling regions (Gao et al., 2018) and physical and biological processes that determine aragonite saturation state (Xue et al., 2016). Efforts to develop and improve biogeochemical model of the upwelling systems are also in progress (e.g. Sreeush et al., 2018). These researches on biogeochemistry are important to understand key processes operating in the Sumatra-Java upwelling system. However, these results are rather fragmentary at this stage and integrated studies on biophysical interactions, ecosystem dynamics, and marine food web in the Sumatra-Java upwelling region are needed.

2.11 West coast of Australia

2.11.1 Background

Unlike other eastern boundary systems, such as the highly productive Humboldt and Benguela upwelling systems, the west coast of Australia features a downwelling current that carries tropical water southward along the shelf-break (Pearce, 1991). In the late nineteenth century, the presence of tropical corals at the Abrolhos Islands (28°- 29°S 114° E) was observed by Saville-Kent (1897), and from sea temperature measurements, he postulated that there was an offshore, warm, southward-flowing current. A drift-card study conducted near Rottnest Island (32°S, 115°E) confirmed that during the austral winter, there was a southward flowing current (Rochford, 1969), and Gentilli (1972) explored the seasonal southward progression of "rafts" of warm water off the west coast of Australia.

The Leeuwin Current (LC) was named and described by Cresswell and Golding (1980) from the trajectories of satellite-tracked buoys and measurements of surface temperature and salinity from the shelf and slope stations. Other early studies of the LC used current meters, shipboard measurements, satellite imagery, steric height gradients, wind stress calculations and modelling. They identified the seasonal nature of the current, origins along the North West Shelf, eastward extension to the Great Australian Bight, frequent presence of meanders and eddies, and low nutrient status (Godfrey & Ridgway, 1985; Holloway & Nye, 1985; Pearce, 1991; Smith et al., 1991; Thompson, 1984; Thompson & Veronis, 1983; Weaver & Middleton, 1989). Essentially, the alongshore steric height gradient is set up by the Indonesian throughflow (which delivers warm, less saline waters from the Pacific into the Indian Ocean) and surface heat loss at higher latitudes (Smith et al., 1991). Later, using remote sensing and modeling, research attention centered on understanding the influence of the LC on the recruitment of puerulus larvae of the economically-important rock lobster *Panulirus cygnus* (e.g., Griffin et al., 2001; Phillips and Pearce, 1997).

More recent shipboard studies along the entire west coast of Australia (Weller et al., 2011; Woo and Pattiaratchi, 2008) provided more detailed information on the trajectory and features of the LC, including the chemistry, primary production, zooplankton and larval fishes (Buchanan and Beckley, 2016; Holliday et al., 2012; Lourey et al., 2012; Sutton and Beckley, 2016; Thompson et al., 2011). Further, remote sensing and modeling have confirmed the seasonal nature of the LC and the influence of the El Niño Southern Oscillation with stronger LC flows occurring during La Niña years (Domingues et al., 2007; Feng et al., 2003). The ecological significance of the LC eddy field was investigated with two dedicated voyages (Paterson et al., 2008; Waite et al., 2007b). The most recent ecological work explored the significance of the LC and its eddy field on the ecology of the planktonic phyllosoma of *P. cygnus* in the wake of a drastic decline in puerulus settlement (Saunders et al., 2012; Säwström et al., 2014; Waite et al., 2019).

Many of the early studies on the LC noted the occurrence of inshore northward-flowing currents during the summer months (e.g., Thompson and Veronis, 1983; Thompson, 1984) with Holloway and Nye (1985) specifically mentioning upwelling along the northwest coast. Subsequent studies highlighted regional upwelling nodes (see below) and, using an upwelling index developed from 15 years of satellite data, (Rossi et al., 2013b) produced a synopsis covering the development of sporadic upwelling events (generally lasting 3-10 days) along the entire western coast of Australia (**Figure 21 and 22**). Although such upwelling generally occurs from September to April (austral summer) sporadic events can occur at any time north of 30°S (**Figure 23**). Upwelling favorable winds, local topography, and the characteristics of the LC such as onshore geostrophic flow, stratification, mesoscale eddies, and meanders influence the intensity of intermittent upwelling. For this review of upwelling along the western coast of Australia, we have separated the coast into three nodes of upwelling, namely, the South West (35º-30º S), Central (30º-25º S), Gascoyne (25º- 22º S) and will also cover upwelling in the eddy field.
The vast eddy-field associated with the LC is well-known and has been investigated by numerous oceanographers and shown to influence regional biogeochemistry and pelagic ecology (e.g., Andrews, 1977; Feng et al., 2007; Waite et al., 2007b; Moore et al., 2007; Paterson et al., 2008; Holliday et al., 2011; Dufois et al., 2014). Though the warm, anticyclonic eddies have been explored in greater detail than the cyclonic eddies, it is the latter which are cold-core upwelling systems and deserve mention here as they have been shown to drive a significant fraction of cross-shelf transport and enhance local and regional productivity (Waite et al., 2016).

A study contrasting a dipole pair of eddies off Western Australia revealed many differences in the biota between the two eddies (Muhling et al., 2007; Strzelecki et al., 2007) as a result of the differences in physical and chemical properties. Warm-core eddies (WCEs; anticyclonic) have greater surface chlorophyll signatures compared to cold-core eddies (CCEs; cyclonic) in the eastern Indian Ocean (Dufois et al., 2014; Waite et al., 2016). Yet, Waite et al. (2019) showed that CCEs actually have greater depth-integrated primary productivity as their shallower mixed layers are closer to the nutricline and across pycnocline mixing then increases the upward flux of dissolved inorganic nutrients. This results in greater flagellate and dinoflagellate populations in CCEs, which provide a high-quality food source for zooplankton, and consequently

increases their lipid stores (Waite et al., 2019). Earlier work showed no significant differences between the fractionated isotopic zooplankton analyses between CCEs and WCEs but highlighted that micro-heterotrophs are positioned on a trophic level as third and fourth-order consumers (Waite et al., 2007a). The high position of micro-heterotrophs again confirms the rapid recycling of particulate organic matter in this system in general, as outlined previously (Hanson et al., 2005; Raes et al., 2014; Twomey et al., 2007). Further, upwelling eddies generated by the Leeuwin Undercurrent in the Perth Canyon have been implicated in the abundance of krill in the area and consequent feeding of migrating blue whales (Rennie et al., 2007).

2.11.2 Upwelling nodes

South West. A northward-flowing inshore current along parts of the southwest coast was indicated by several early LC studies (Cresswell et al., 1989; Cresswell and Peterson, 1993; Cresswell and Golding, 1980; Pearce, 1991; Thompson, 1987). For example, Cresswell and Peterson (1993) noted in the austral summer of 1986-87 that a cold upwelling plume (~17.5°C) extended westward along the shelf from the southern coast of Western Australia around Cape Leeuwin and northward to Cape Naturaliste. They speculated that the absence of the LC south of 34°S might have allowed upwelling-favorable easterly winds on the south coast to drive this upwelling. From a detailed analysis of satellite imagery (1987-1993) and environmental data, Pearce and Pattiaratchi (1999) described the narrow, northward flowing counter-current between Cape Leeuwin and Cape Naturaliste during the austral summer months and named it the Capes Current. They indicated that strong northward wind stresses between November and March slowed the LC and drove the Capes Current and that localized upwelling also contributed to it. This upwelling was examined by Gersbach et al. (1999) using XBT, CTD, nutrient, and ADCP data from summer sections off Cape Mentelle (located between Cape Leeuwin and Cape Naturaliste) and several sections between Albany and Perth, as well as wind data and satellite imagery. They concluded that northward wind stress in summer could overcome the alongshore steric height gradient on the continental shelf, inducing the thermocline to lift and sporadic upwelling to occur 5-9 times per summer. Interestingly, the T/S characteristics of the water upwelled at Cape Mentelle were slightly different from that of the current setup from the south (Gersbach et al., 1999). Rossi et al. (2013b) indicated that, overall, the transient upwelling events in this southwest region last 3-10 days, and shelf regions between 34°S and 31.5°S exhibit up to 12 upwelling days per month during the austral spring/summer (Figure 22). Historical current measurements near Perth suggest that the Capes Current continues northwards past Rottnest Island, and there may also be links with shelf counter-currents well past the Abrolhos Islands at 29ºS (Cresswell et al., 1989).

Central coast. Along the central Western Australian shelf inshore of the Leeuwin Current, there is a general northward flow during the austral summer months based on current measurements across the shelf near the Houtman Abrolhos Islands (Cresswell et al., 1989; Rochford, 1969). Rossi et al. (2013b) indicated a high upwelling index along the central coast with locations around 28ºS and 26º S producing elevated mean numbers of upwelling days per year. Interestingly, both show peaks in upwelling from March to May, with upwelling at 28º S continuing through the austral winter.

Gascoyne coast. The Gascoyne coast is characterised by a northward flowing inshore current known as the Ningaloo Current. Various studies have revealed that the Ningaloo Current consists of water sourced from upwelling of shallow water (~100 m) from the base of the LC (Hanson et al., 2005; Taylor and Pearce, 1999; Woo and Pattiaratchi, 2008; Woo et al., 2006a, 2006b). Previously, it was understood to be strongly seasonal in the austral summer, but recent investigations have shown autumn upwelling events as well (Lowe et al., 2012; Xu et al., 2013; Rossi et al., 2013a). The source water in autumn may be from a greater depth (150m) under the increased mixed layer depth (Rossi et al., 2013a). The Ningaloo upwelling region around 22.5ºS has the highest number of upwelling days per year (140), and the events are often longer in duration than elsewhere on the west coast (Rossi et al., 2013b).

2.11.3 Productivity and ecosystem impacts

Nutrients, primary productivity, pro- and micro- eukaryotes. Regional dynamics along the west coast of Australia controls the spatio-temporal variability of biogeochemical cycles, such as primary productivity and nutrient cycles in general. Water column productivity along the west coast of Australia (generally <200 mg C m^{-2} d^{-1}; Hanson et al., 2005) peaks at the deep chlorophyll maximum (DCM), which is closely aligned with the base of the nutricline. Productivity at the DCM in this system is strongly influenced by the mixed layer depth (MLD), with deeper DCMs having lower productivity and shallower DCMs resulting in higher productivity rates (Hanson et al., 2007a; Johannes et al., 1994).

Furnas (2007) argued that intermittent bursts of high productivity could occur in specific locations or under certain circumstances along this coast. The strength of the LC is controlled by the weakening of southerly winds in the austral autumn and winter. Modeling results from Feng et al. (2003) suggest that an increase in the southward transport of the LC has been linked to an erosion of the thermocline, which then brings NO_3^- into the euphotic zone, thereby enhancing primary productivity in early autumn (Feng et al., 2009; Rousseaux et al., 2012). Satellite observations across the shelf and LC confirmed these results with the highest chlorophyll levels in autumn and winter (Lourey et al., 2006; Lourey et al., 2012). Similarly, in summer, the wind-driven Capes Current locally enhances productivity near the shelf (Pearce and Pattiaratchi, 1999), yet, generally, the oligotrophic nature of this system limits NO_3^- driven new production throughout the year (Hanson et al., 2005; Twomey et al., 2007). The recycling of organic matter, however, via microbial regeneration has been shown to primarily control the rates of primary production in this system (Hanson et al., 2007b; Pearce et al., 2006; Twomey et al., 2007) rather than the strong upwelling as seen in other eastern boundary systems, such as the Humboldt and Benguela systems (Hood et al., 2017).

The inputs of new N derived from N_2 fixation is also an important pathway supporting primary productivity in this region. Along the Western Australian shelf from 32ºS northwards to 12ºS, and west to 110ºE, the contribution of new N from N_2 fixation towards the total dissolved inorganic nitrogen (DIN) assimilation pool can be ~ 20% and up to 50% during the winter months (with N_2 fixation rates ranging from 0.01 up to 12 $nmol^{-1}$ L^{-1} h^{-1}), making N_2 fixation equal to NO_3^- in terms of N assimilation into this ecosystem (Raes et al., 2015; Raes et al., 2014). Waite et al. (2013) and Raes et al. (2015) also noted that the small diffusive deep-water NO_3^- fluxes are not able to support the measured NO_3^- assimilation rates. Their data suggest that nitrification above the nutricline (referred to as "shallow nitrification"; see also Thompson et al., 2011) could be an important pathway of the N-cycle along the southwest coast of Australia. Waite et al. (2016) suggested that the persistent layers of low oxygen, high dissolved nitrogen (LDOHN; O_2 ~150 µmol L^{-1} and NO_3^- ~2-10 µmol L^{-1}) just below the euphotic zone (~150-250m; Thompson et al., 2011; Weller et al., 2011) are hotspots for the mineralization of organic material from local sources (< 500 km away). In addition, Waite et al. (2016) noted that the depletion of oxygen in these isolated layers along with the release of NO_3^-, could happen on a time-scale of ~2 weeks. Warren (1981), on the other hand, originally suggested that the isolated nature of the lower oxygen features is created by density gradients, which prevent the mixing of deep O_2 rich water. According to Thompson et al. (2011) and Weller et al. (2011), the source of the oxygen minimum layer is associated with multiple water masses further upstream, possibly at lower latitudes north of Australia. Overall, a number of studies point to the conclusion that an active microbial loop (Azam et al., 1983) controls the biogenic C and N fluxes through heterotrophic recycling via ammonification, nitrification, and N_2 fixation in this vast region (Hanson et al., 2007b; Raes et al., 2015; Waite et al., 2016).

The west coast of Australia has a subtropical phytoplankton cycle, with a winter bloom, similar to the open ocean waters of the subtropical South Indian Ocean (**Figure 24).** Picoplankton (unicellular cyanobacteria and prochlorophytes) have been shown to contribute >40% of the pigment biomass (Hanson et al., 2007b). In terms of bio-volume, the Dinophyceae, including large gymnoids and other Dinophyceae (e.g., *Gyrodinium* spp., *Prorocentrum* spp.), are the most abundant microplankton and can account for up to 50% of the microplankton component in this region (Raes et al., 2014). Sightings of N_2-fixing microorganisms (such as *Trichodesmium*) in the oligotrophic waters off the west coast of Australia date back to voyages of Captain Cook and Charles Darwin (Cook et al., 1999; Darwin, 1889). *Trichodesmium* occurrences have been measured at the Australian National Reference stations from the tropics (Darwin) to the temperate waters off Rottnest Island.

Amplicon sequencing of the nitrogenase (*nifH*) gene, however, has shown a low diazotrophic evenness across a transect along the shelf from Perth (32ºS) to Darwin (10°S). One operational taxonomic unit (OTU) made up 65–95% of the *nifH* enzyme diversity along the transect, and was identified as a Gamma 4 proteobacteria (Raes et al., 2018). This dominant *nifH* OTU was nearly identical (one nucleotide difference) to the gamma 4 proteobacteria (HM201363.1) found by Halm et al. (2012) in the oligotrophic South Pacific Gyre. The ubiquitous finding of these gamma proteobacterial *nifH* genes is consistent with the results from Schmidt et al. (1991) and Langlois et al. (2015) in open, oligotrophic oceanic waters.

Zooplankton. Ecological studies about zooplankton community structure along the west coast of Australia are few, and most studies have examined specific taxa (e.g., larval fishes, chaetognaths, or krill) particularly in relation to the effect of the LC on dispersal (Beckley et al., 2009; Buchanan & Beckley, 2016; Holliday et al., 2012; Sutton & Beckley, 2016). Although inshore stations (50 m depth) were sampled during the voyage when most of these studies were made (extending from 22°S - 34°S), there was no evidence of coastal upwelling, likely because it was conducted in the austral autumn (May 2007). Recently, meso-zooplankton abundance, composition, and diversity data from the three years (2010-2012) that the IMOS Australian National Reference Stations (Ningaloo, Rottnest Island, and Esperance) were concurrently sampled were analyzed (McCosker et al., 2020). Besides the obvious influence of the LC in winter, there were clear dissimilarities between the copepod assemblages, particularly during the summer months when coastal upwelling-associated currents such as the Capes and Ningaloo Currents influenced the biota.

Specific effects of coastal upwelling on zooplankton have not been explored in the South West, but concurrent with the phytoplankton study of Koslow et al. (2008) across the Two Rocks transect north of Perth, mesozooplankton assemblages were examined (Strzelecki and Koslow, 2006). During the summer, the inshore shelf stations were found to have significantly higher zooplankton abundance than the offshore sampling stations, but this was reversed in the winter months when the LC was flowing strongly. Copepod production ranged from 0.4-10 mg C m^{-2} d^{-1} (Strzelecki and Koslow, 2006), which is low compared to upwelling regions elsewhere in the world but comparable to copepod production in the North West Cape region (McKinnon and Duggan, 2003). Along the same cross-shelf transect, Muhling and Beckley (2007) and Muhling et al. (2008b) found clear seasonal differences in the diversity and abundance of inshore larval fish assemblages when the cool Capes Current was flowing northwards during the austral summer compared to the austral winter months when the LC strongly influenced larval fish assemblages on the continental shelf.

Little is known about the effect of coastal upwelling on zooplankton along the central part of the Western Australian coast, and the only extensive zooplankton survey in the region targeted the phyllosoma larvae of the rock lobster, *Panulirus cygnus*. Nevertheless, the study highlighted the presence of the Abrolhos front separating the tropical waters of the LC from the dominant oligotrophic subtropical surface water (STSW), and the LC waters had much higher chlorophyll *a* and zooplankton concentrations than the STSW (Säwström et al., 2014).

In the north, the coastal copepod communities at Ningaloo are diverse (> 120 species; McKinnon and Duggan 2001). They are characterized by small "upwelling- ready" species, which can react quickly to pulses of sporadic upwelling and phytoplankton blooms, but, unlike the high primary production rates, copepod production rates are generally low (~ 13 mg C m^{-2} d^{-1}; Hanson and McKinnon, 2009). Interestingly, *Calanoides carinatus*, a copepod that is characteristic of upwelling regimes elsewhere, was absent, and they proposed that upwelling was too infrequent and episodic to sustain zooplankton

specific to upwelling regimes. Of the macro-zooplankton, krill, especially *Pseudeuphausia latifrons* has been investigated in coastal waters at Ningaloo (Wilson et al., 2003), and seasonal occurrence of whale sharks has been linked to aggregations of this species during the austral autumn months (Hanson and McKinnon 2009).

Fisheries. Investigations into the spawning of sardines (*Sardinops sagax*) off southwestern Australia have highlighted advective transport (Fletcher et al., 1994; Gaughan et al., 2001b) and variation in the growth rate of larvae from areas with different levels of productivity (Gaughan et al., 2001a). Muhling et al. (2008a) showed that, although adult sardines had a winter spawning peak coinciding with the seasonal peak in chlorophyll *a* (Koslow et al., 2008), it also matched the seasonal peak in the southward flow of the LC, resulting in low retention of the early life history stages. Thus, egg and larval concentrations were lower than expected in winter but higher in summer when retention conditions were more favorable. They postulated that, as larval growth rates were actually high, the insignificant catches of adults in the fishery compared to other eastern boundary upwelling systems was due to a combination of suppression of large-scale upwelling and the modest seasonal maximum in primary productivity occurring during the time least favourable for pelagic larval retention.

There have been commentaries on the role of the Capes Current in assisting migrations of south coast fish species such as *Arripis truttaceus* and *Arripis georgianus* in their migrations to autumn spawning areas in southwestern Australia and subsequent return transport of early life stages by the LC during winter (Pearce and Pattiaratchi, 1999). Both Caputi et al. (1996) and Lenanton et al. (2009) have reviewed the importance of the LC with respect to Western Australian fisheries and have noted the likely role of the Capes Current for several species, including the economically important rock lobster. Through modeling, Feng et al. (2010) examined dispersal and retention areas along the west coast. Although the LC was dominant in winter, northward flow in summer was linked with recruitment success of scallops (*Amusium balloti)*, abalone (*Haliotis roei),* and tropical sardines (*Sardinella lemuru)*.

3. Open Ocean Upwelling: Seychelles-Chagos Thermocline Ridge

3.1 Background

The Seychelles-Chagos Thermocline Ridge (SCTR, Xie et al, 2002; Hermes and Reason, 2008; Yokoi et al., 2008; Vialard et al., 2009b) is an upwelling region across the southern tropical Indian Ocean between ~ 5-15°S and ~50-80°E (Figure 25). It is characterized by a thin mixed layer (~30m) and a relatively shallow thermocline. The ridge, and the upwelling associated with it, is set up by wind stress curl patterns, and it has significant variability on seasonal and interannual time scales due to both remote and local and forcing (Xie et al., 2002; Hermes and Reason, 2008; Yokoi et al., 2008; McPhaden and Nagura, 2014; Nyadjro et al., 2017). It is coincident with the southernmost latitudes of monsoon-driven circulation in the Indian

Ocean, south of which a steadier trade wind regime prevails (Figure 1). During boreal winter, the Intertropical Convergence Zone (ITCZ) is located over the SCTR. The ITCZ and associated rainfall migrate northwards to the Indian subcontinent as the year progresses, where it is the source of precipitation during the summer monsoon.

Upwelling along the SCTR affects sea surface temperature (SST, Figure 26), biogeochemistry (Figure 26), and fisheries (Figure 27), and drives strong ocean-atmosphere coupling (Vinayachandran and Saji, 2008, Vialard et al., 2009; Resplandy et al., 2009; Robinson et al., 2010; Dilmahamod et al., 2016). As discussed previously, upwelling centers in the monsoon-dominated Indian Ocean are found in off-equatorial regions because the mean winds along the equator are westerly, unlike in the easterly trade wind-forced Pacific and Atlantic Oceans (Schott et al., 2009; Wang and McPhaden, 2017). The SCTR is the largest and most persistent upwelling region in the Indian Ocean.

3.**2. Mechanisms**

The SCTR represents the ascending branch of the subtropical circulation cell in the southern hemisphere, where upwelling is balanced primarily by meridionally divergent flow in the surface layer (Lee, 2004; Figure 28). Horizontal flow in the upper ocean circulates cyclonically around the SCTR axis, with the westward-flowing South Equatorial Current (SEC) to the south and the eastward-flowing South Equatorial Countercurrent (SECC) to the north (Figure 25). The westward-flowing SEC in the SCTR region provides the conduit for interbasin exchanges that link the Pacific Ocean to the Atlantic Ocean through the Indonesian Seas and the Agulhas Current.

SST varies substantially in the SCTR on intraseasonal to interannual time scales because the shallow mixed layer is sensitive to changes in upwelling, vertical mixing, air-sea heat fluxes, and horizontal advection (Vialard et al., 2008; Foltz et al., 2010). On intraseasonal time scales, pronounced SST variations in the SCTR happen in response to forcing from the Madden-Julian Oscillation (MJO, Madden and Julian 1972), which is generated in this region. This variability feeds back to the atmosphere, which helps to organize the MJO convective cells. Large SST variations on interannual time scales are associated with the El Nino Southern Oscillation (ENSO) and the Indian Ocean Dipole (IOD; Webster et al., 1999; Saji et al., 1999). This year-to-year SST variability affects the frequency of Indian summer monsoon rainfall (Izumo et al., 2008), tropical storms in the southwestern Indian Ocean (Xie et al., 2002), and the climate of East Asia (Yamagata et al., 2004).

3.3 Productivity and ecosystem impacts

The nutricline shoals sharply due to upwelling in the SCTR where average nitrate concentration between the surface and 80 m depth exceed 5 μM in a bullseye centered at about 62°E, 8°S (Resplandy et al., 2009). Satellite observations and model

results reveal elevated near-surface Chla and primary production in the SCTR region with the highest values in austral winter (June-August; >0.20 mg m^{-3} and >600 mg C m^{-2} d^{-1}, respectively, see Figures 5 and 6 in Hood et al., 2017) due to the strong southeasterly winds that increase wind stirring and induce upwelling (Resplandy et al., 2009; Dilmahamod, 2014). Meridional sections through the SCTR region reveal a deep Chl*a* maximum that shoals from >100 m further south to ~50 m due to upwelling (George et al., 2013). Wind-induced mixing during MJO episodes (which typically occur between January and March) can also lead to enhanced Chl*a* at intra-seasonal time scales in the SCTR region (Resplandy et al., 2009; Dilmahamod et al., 2016). Zooplankton biomass is relatively low in the SCTR for most of the year with a pronounced 4-5X peak during the SWM upwelling in August (austral winter). Observational studies have revealed concentrated tuna fishing activities in the SCTR (Fonteneau et al. 2008) which are associated with the aforementioned regions of elevated Chl*a*, primary production and zooplankton biomass, demonstrating a strong connection between the food webs that respond to enhanced production in the SCTR the prey required by large tuna. The IOD also profoundly affects this tuna fishery, which is well developed in the SCTR region during normal years (Figure 27). However, during the positive IOD events, when upwelling is weakened in the SCTR and strengthened off the coast of Java and Sumatra, tuna migrate eastward, apparently in search of more favorable foraging grounds (Figure 27, Robinson et al., 2010).

The extent to which iron may be a limiting primary production in the SCTR is unknown, though independent modeling studies and remote sensing-based analyses both suggest it may be (Wiggert et al., 2006; Behrenfeld et al., 2009). Finally, there is still considerable uncertainty in whether the Indian Ocean is a net source or sink of carbon to the atmosphere because the variability in pCO_2 fluxes across the air-sea interface is poorly constrained by existing observations, particularly in active upwelling zones like the SCTR.

4. Summary

The unique features of the oceanography of the Indian Ocean and the complexities associated with its circulation, boundary currents, climate, and ecosystem response, driven and modulated by the monsoons, have been a matter of extensive discussion in the past reviews of the Indian Ocean (Shetye and Gouveia, 1998, Schott and McCreary, 2001 Shankar et al., 2002, Hood et al. 2015). The coastal upwelling, despite its importance for the ecosystem and economic impacts, however, has not received sufficient attention (Hood et al., 2015). Several new research programs were launched in the last decade, which has shed considerable new light on the coastal upwelling system in the Indian Ocean. The WIOURI was initiated to study nine upwelling systems in the western Indian Ocean (Roberts, 2015). Similarly, EIOURI was planned to study a large spectrum of processes affecting the upwelling in the eastern half of the Indian Ocean (Yu et al., 2016). Along the coasts of India, an array of ADCP mooring deployed since 2008 (Mukhopadhyay et al., 2017, Chaudhari et al., 2020). Such programs have contributed significantly to enhancing our knowledge of the science of the upwelling in the Indian Ocean, ecosystem

impacts, and sensitivity to changes in the environment. The prime goal of this paper is to review the present understanding of upwelling in the Indian Ocean, extending from the Agulhas region to the western coast of Australia.

The Upwelling. While some of the upwelling systems, such as that along the Somali coast, were surveyed early (during IIOE or before), others such as Mozambique were sampled much later. The surveys, particularly those in the recent period, have revealed multiple processes that trigger and control upwelling, the combination varying for each of the systems. Salient features of their progress are summarized in this paper. The northeast monsoon winds are favourable for upwelling along the western boundary in the southern hemisphere, up to about 20˚S. Along the coast of Kenya, in addition to an Ekman type of mechanism, shelf-break upwelling induced by topography is a driving force. Along the coast of Tanzania, the additional forcing for upwelling is drawn from the shear instability of EACC. In the Mozambique channel, competing roles of local winds and eddies drive upwelling in the channel. South of Madagascar, upwelling is caused by local winds, the interaction of the currents with the continental margin and eddies. Eddies associated with Natal pulses cause subsurface upwelling in the Agulhas region, and surface-reaching upwelling occurs in its inshore edge due to dynamical processes and wind forcing.

The distinct feature of the Somali upwelling system is the cold wedges. One wedge forms in May on the shoreward edge of the Southern Gyre during May and the other along the northern flank of the Great Whirl, during the peak of the summer monsoon. The presence of multiple gyres and the intense current present a complicated upwelling system in this region. In addition to alongshore winds, Rossby wave radiation from the east by Ekman pumping du to anticyclonic wind stress curl drive upwelling in this region. The downwelling of the thermocline due to the wind stress curl, however, can lead to a weakening of the upwelling as the deepening reaches up to the coastal region during the fully developed phase of the SWM. Consequently, upwelling is limited to frontal regions dominated by eddies. The coast of Oman, on the other hand, presents a classical Ekman type of upwelling system. The intensity of the upwelling increases with the progress in the SWM. However, the influence of Rossby wave radiation has been suggested to affect the timing of the peak phase of the SST decrease associated with upwelling. Generation of eddies and filaments are well-known features associated with the currents and upwelling along the coast of Oman.

Along the west coast of India, upwelling is more prominent along the southern part of the coast and begins about 4 months before the onset of the summer monsoon. The alongshore winds are weak and are only partly responsible for the upwelling. The major driving force is the coastally trapped wave propagation originating from the Bay of Bengal. The alongshore winds are unidirectional, but the currents reverse, confirming the dominant role of remote forcing. Winds along the southern tip of India and along the southern coast of Sri Lanka drive Ekman type of upwelling during the summer monsoon. Upwelling along the east coast of India is weak and available evidences suggest the presence of upwelling during the summer monsoon. The intricate combination of forcing by local winds, Kelvin waves originating from either EIO or the eastern boundary of

the BoB, Rossby wave propagation all affect the upwelling. At interannual time scales, ENSO and IOD dominate the variability, whereas at intraseasonal time scales, mesoscale eddies appear to be important.

The upwelling along the Sumatra and Coasts is mainly driven by alongshore winds during the summer monsoon but affected by Kelvin wave propagations and circulation in the Equatorial Indian Ocean, Indonesian throughflow and the subtropical Indian Ocean. It is affected severely by IOD events and modified significantly by intraseasonal events. The circulation along the west coast of Australia is dominated by the LC but upwelling occurs at several nodes along the coast. Transient wind-driven upwelling that lasts for 3-20 days occurs along the southwest part of the coast. Along the central coast, upwelling takes place during March-May. Along the Gascoyne coast, Ningaloo upwelling takes place during austral summer and autumn.

Ecosystem Impacts. It is evident that in all regions, the upwelling stimulates an ecosystem response and the facilitation of this response is achieved by different processes in different regions. In the Mozambique channel, peripheries of the cyclonic eddies are centers of biological activity in terms of increased productivity, aggregation of small organisms and foraging bird populations. Along the southern coast of Madagascar, upwelling nodes enhance primary productivity, fish catch and whale sightings. The interannual variability of the cyanobacteria bloom here is modulated by the detachment of the South-East Madagascar current. The chlorophyll concentration is high along the coasts of Somalia and Oman, during the summer monsoon, which has been known since a long time. Recent advances in this region have been slow and a modeling study suggests that the influence of upwelling is restricted to limited areas and the strong currents spread the effect to larger spatial coverage. Off the coast of Oman, advection of nutrient-rich water can give rise to blooms in the offshore region.

Recent research has revealed the high impact of upwelling on the biogeochemistry of the eastern Arabian Sea. Most significantly, the strong Ekman transport from the western Arabian Sea upwelling affects the OMZ and its spatial and temporal limits more closer to the eastern Arabian Sea, and forms the source for upwelling over its eastern shelf, thus making a tele-connection between upwelling over both the coasts of Arabian Sea This has an impact on the mesopelagic fish population, benthic ecosystems, macro infaunal communities and biodiversity. The upwelling in the Bay of Bengal, on the other hand, is weak and it is not clear what the ecosystem responses are to upwelling. The productivity appears to be more under the control of eddies and the stratification imposed by rainfall and river runoff. The upwelling along the coasts of Sumatra and Java enhances productivity and the phytoplankton composition here is distinctly different during upwelling compared to that during downwelling. Along the west coast of Australia, upwelling has a lesser role in controlling the rates of primary productivity compared to that of remineralization. However, there are indications that summertime zooplankton biota is affected by upwelling. The SCTR is a prominent open ocean upwelling region in the Southern Topical Indian Ocean that is caused primarily by the persistent wind stress curl and this upwelling has a clear expression on the surface chlorophyll distribution. This region also has a significant role in the air-sea interaction in this region.

During the IIOE-2 period, Argo float measurements and satellite remote sensing data have been accumulated significantly and there were several *in-situ* observations of physical and biogeochemical aspects of the upwelling systems. These data provide us better understanding of physical processes responsible for the upwelling variability in various time-scales and their impact on distributions of biogeochemical variables. However, *in-situ* measurements are still quite limited to obtain a synthetic view of upwelling systems, particularly on biogeochemical parameters. Understanding of mixed-layer dynamics and mixing processes in this unique region that affect subsurface oceanic variability and SST need to be investigated in more detail. Further observations and accumulation of additional evidences are necessary to obtain a comprehensive view of the upwelling systems in the Indian Ocean.

Future prospects. Some of the upwelling zones have registered significant progress during the period of IIOE-2 (2015 onwards) while some others have rather been left behind. Agulhas current, Mozambique channel, Madagascar Coasts and coasts of India, Sumatra-Java and Africa belong to the former category whereas Somali and Oman costs to the latter. In addition, the northern coast of the Arabian Sea and the eastern boundary of the Bay of Bengal still remain poorly observed and understood. The spatial and temporal variability of upwelling is not sufficiently documented for most parts of the Indian Ocean coastline. This emphasizes the importance of sustained observations and modelling, and a combination of them.

The new knowledge that has been acquired from the recent research has posed new questions and challenges. One of them is related to the variability of upwelling. There is a considerable gap in the space-time variability of upwelling in almost all the regions, primarily owing to the lack of systematic long-term data sets with sufficient spatial resolution and coverage. Second, the processes that drive upwelling are complicated in several regions and there is no consensus or quantitative account of the relative roles of each process; the role of eddies in the Mozambique channel, impact of currents along the southern coast of Madagascar and coastally trapped waves are good examples for the dichotomy. A combination of focused modelling studies and systematic observations are required to address such issues. The required *in-situ* observations need to be with high spatial and temporal resolutions and with the capability for long-term monitoring. In addition, intensive process-oriented observational programs are required to understand physical processes and their interconnection to the ecosystem. Such observing strategies together with high-resolution regional and global models that include both physical and biogeochemical/ecosystem components have the potential to develop strategies for sustainable uses of coastal resources. A related and more sophisticated issue is the ecosystem response and fisheries. While definite progress has been made in the Eastern Arabian Sea and off the coast of Australia, a complete picture regarding the dependence of marine biota on upwelling is yet to emerge for the entire upwelling system along the periphery of the Indian Ocean.

Author contributions: PNV planned the outline of the paper and led the paper preparation. All authors contributed to the paper preparation.

Competing interests: The authors declare that they have no conflict of interest.

Acknowledgments

This is a contribution from the Science Theme - 2 of the IIOE-2. Partial financial support from SCOR is gratefully acknowledged. PNV acknowledges partial financial support from J C Bose National Fellowship, SERB, DST, Govt. India and BoBBLE project funded by the Ministry of Earth Sciences, Govt. of India under its Monsoon Mission program. NIO contribution number of this paper is 10473. Thanks to Dr. D. Shankar for his comments on the manuscript and to Dr. C. P. Neema for help with manuscript preparation. We gratefully acknowledge the contribution of our co-author Dr. Satya Prakash to IIOE-2 before his untimely passing away in July 2021. This paper is dedicated the memory of Dr. Satya Prakash.

References

Abdul Jaleel, K. U., Parameswaran, U. V., Gopal, A., Khader, C., Ganesh, T., Sanjeevan, V. N., Shunmugaraj, T., Vijayan, A. K., and Gupta, G. V. M.: Evaluation of changes in macrobenthic standing stock and polychaete community structure along the south eastern Arabian Sea shelf during the monsoon trawl-ban, *Cont. Shelf Res.* 102, 9–18,doi: 10.1016/j. Csr.2015.04.011, 2015.

Ali, M. M., Sharma, R., and Cheney, R.: An atlas of the north Indian Ocean eddies from TOPEX altimeter derived sea surface heights, Spec. Publ., ISRO-SAC-SP-69-98, Indian Space Res. Organ., Bangalore, India, 69–98, 1998.

Allen, J. S.: Upwelling and coastal jets in stratified ocean, J. Phys. Oceanography, 3, 245-257, doi: https://doi.org/10.1175/1520-0485(1973)003%3C0245:UACJIA%3E2.0.CO;2, 1973.

Alvheim, O., Torstensen, E., Fennessy, S., MacKay, F., Zaera, D., and Bemiasa, J.: West Madagascar: Cruise Reports Dr Fridtjof Nansen. Pelagic Ecosystem Survey SWIOFP/ASCLME/FAO, Cruise 2, 25 August–3 October 2009, Preliminary report, Institute of Marine Research, Bergen, Norway, 2009.

Amol, P., Vinayachandran, P. N., Shankar, D, Thushara, V., Vijith, V., and Abhisek Chatterjee: Effect of freshwater advection and winds on the vertical structure of chlorophyII in the northern Bay of Bengal, Deep-Sea Res (Part II)., 179 104622), doi.org/10.1016/j.dsr2.2019.07.010, 2019.

Amol, P., Shankar, D., Fernando, V., Mukherjee, A., Aparna, S. G., Fernandes, R., Michael, G. S., Khalap, S. T., Satelkar, N. P., Agarvadekar, Y., Gaonkar, M. G., Tari, A. P., Kankonkar, A., and Vernekar, S. P.: Observed intraseasonal and seasonal variability of the West India Coastal Current on the continental slope, J. Earth Syst. Sci., 123, 1045–1074, doi:10.1007/s12040-014-0449-5, 2014.

Amol, P., Suchandan Bemal, Shankar, D., Jain, V., Thushara, V., Vijith, V. and Vinayachandran, P. N.: Modulation of chlorophyll concentration by downwelling Rossby waves during the winter monsoon in the southeastern Arabian Sea, Prog. Oceanogr., 186, 102365, doi.org/10.1016/j.pocean.2020.102365, 2020.

Amol, P.: Impact of Rossby waves on chlorophyll variability in the southeastern Arabian Sea, Remote Sens. Lett., 9, 1214–1223, doi.org/10.1080/2150704X, 2018.

742 Anderson, D. L. T., and Moore, D. W.: Cross-equatorial inertial jets with special relevance to very remote forcing of the
743 Somali Current, Deep-Sea Res., 26, 1–22, https://doi.org/10.1016/0198-0149(79)90082-7, 1979.

744 Andrews, J. C.: Eddy structure and the West Australian current, Deep Sea Res., 24(12), 1133-1148, doi:10.1016/0146-
745 6291(77)90517-3, 1977.

746 Andruleit, H.: Status of the Java upwelling area (Indian Ocean) during the oligotrophic northern hemisphere winter
747 monsoon season as revealed by coccolithophores, Mar. Micropaleontol., 64, 36–51, doi:10.1016/j.marmicro.2007.02.001,
748 2007.

749 Andruleit, H., A. Lückge, M. Wiedicke, and S. Stäger: Late Quaternary development of the Java upwelling system
750 (eastern Indian Ocean) as revealed by coccolithophores, Mar. Micropaleontol., 69, 3–15,
751 doi:10.1016/j.marmicro.2007.11.005, 2008.

752 Anonymous: World atlas of sea surface temperatures, 2nd ed., U. S. Hydrographic Office, Washington D. C. , Reprinted
753 1948, 1944.

754 Anonymous: Temperature and monthly maps for the Indian Ocean, Edition 135, Royal Netherlands Meteorological
755 Institute, Den Haag, 1952.

756 Aparna, S. G., McCreary, J. P., Shankar, D., and Vinayachandran, P. N.: Signatures of the Indian Ocean Dipole and El
757 Nino-Southern Oscillation events in sea level variations in the Bay of Bengal, J. Geophys. Res., 117:C10012, doi:
758 10.1029/2012JC008055, 2012.

759 Arístegui, J., Barton, E. D., Álvarez Salgado, X. A., Santos, A. M. P., Figueiras, F. G., Kifani, S., Hernndez-Len, S.,
760 Mason, E., Mach, E., and Demarcq, H.: Sub-regional ecosystem variability in the Canary Current upwelling, Prog.
761 Oceanogr., 83 , 33–48, doi:10.1016/j.pocean.2009.07.031, 2009.

762 Asanuma, I., Matsumoto, K., Okano, H., Kawano, T., Hendiarti, N., and Sachoemar, S. I.: Spatial distribution of
763 phytoplankton along the Sunda Islands: The monsoon anomaly in 1998, J. Geophys. Res., 108 (C6), 3202,
764 doi:10.1029/1999JC000139, 2003.

765 Augustyn, C. Lipinski, M., Sauer, Whh, Roberts, M. and Mitchell-Innes, B.A.: Chokka squid on the Agulhas Bank: Life
766 history and ecology, S. Afr. J. Sci.. 90, 143-154, 1994.

767 Azam, F., Fenchel, T., Field, J. G., Gray, J., Meyer-Reil, L., and Thingstad, F.: The ecological role of water-column
768 microbes in the sea, Mar. Ecol. Prog. Ser., 10, 257-263, doi: 10.3354/meps010257, 1983.

769 Babu, M. T., Sarma, Y. V. B., Murty, V. S. N., and Vethamony, P.: On the circulation in the Bay of Bengal during
770 northern spring inter-monsoon (march april 1987), Deep–Sea Res. (Part II), 5, 855–865, doi:10.1016/S0967–
771 0645(02)00609–4., 2003.

772 Bakun, A., Roy, C., and Lluch-Cota, S. E.: Coastal upwelling and other processes regulating ecosystem productivity and
773 fish production in the western Indian Ocean, in Large marine ecosystems of the Indian Ocean: Assessment, sustainability,
774 and management, Edited by Sherman K., Okemwa, EN and Ntiba MJ, 103–141, Blackwell Science Inc., 1998.

775 Banse, K.: On upwelling and bottom-trawling off the southwest coast of India, J. mar. biol. Ass. India, 1, 33–49, 1959.

776 Banse, K.: Hydrography of the Arabian Sea Shelf of India and Pakistan and effects on demersal fishes, Deep Sea Res.
777 Oceanogr. Abstr., 15 , 45–79, doi:10.1016/0011-7471(68)90028-4, 1968.

Barlow, R., Lamont, M.-J., Gibberd, R., Airs, L., Jacobs, and Britz, K.: Phytoplankton communities and acclimation in a cyclonic eddy in the southwest Indian Ocean, Deep Sea Res. Part I Oceanogr. Res., 18–30, doi:10.1016/j.dsr.2017.03.013, 2017.

Baumgart, A., Jennerjahn, T., Mohtadi, M., and Hebbeln, D.: Distribution and burial of organic carbon in sediments from the Indian Ocean upwelling region off Java and Sumatra, Indonesia, Deep Sea Res.I, 157, 458-467, doi:10.1016/j.dsr.2009.12.002, 2010.

Beal, L. M., Chereskin, T. K., Lenn, Y. D., and Elipot, S.: The Sources and Mixing Characteristics of the Agulhas Current, J. Phys. Oceanogr., 36(11), 2060–2074, https://doi.org/10.1175/JPO2964.1, 2006.

Beal, L. M., De Ruijter, W. P. M., Biastoch, A. , Zahn, R., and SCOR/WCRP/IAPSO Working Group 136: On the role of the Agulhas system in ocean circulation and climate, Nature 472, 429-436, https://doi.org/10.1038/nature09983, 2011.

Beal, L. M., and Donohue, K. A.: The Great Whirl: Observations of its seasonal development and interannual variability, J. Geophys. Res. Oceans, 118, 1–13, https://doi.org/10.1029/2012JC008198, 2013.

Beal, L. M., Elipot, S., Houk, A., and Leber, G. M. : Capturing the Transport Variability of a Western Boundary Jet: Results from the Agulhas Current Time-Series Experiment (ACT)*, J. Phys. Oceanogr., 45(5), 1302–1324, https://doi.org/10.1175/JPO-D-14-0119.1, 2015.

Beckley, L.E., Muhling, B.A. and Gaughan, D.J.: Larval fishes off Western Australia: influence of the Leeuwin Current, J R Soc West Aus, 92(2), 101-109, 2009.

Behara, A., and Vinayachandran, P. N.: An OGCM study of the impact of rain and river water forcing on the Bay of Bengal, J. Geophys. Res., 121, 2425–2446, doi: :10.1002/2015JC011325, 2016.

Behrenfeld, M. J., Westberry, T. K., Boss, E. S., O'Malley, R. T., Siegel, D. A., Wiggert, J. D., Franz, B. A., McClain, C. R., Feldman, G. C., Doney, S. C., Moore, J. K., Dall'Olmo, G., Milligan, A. J., Lima, I., and Mahowald, N.: Satellite-detected fluorescence reveals global physiology of ocean phytoplankton, Biogeosciences, 6, 779–794, https://doi.org/10.5194/bg-6-779-2009, 2009.

Bennett, B. A. : Aspects of the biology and life history of white steenbras Lithognathuslithognathus in southern Africa, South Afr. J. Mar. Sci., 13(1), 83-96, DOI: 10.2989/025776193784287257, 1993.

Biastoch, A., Böning, C. W., Lutjeharms, J. R. E.: Agulhas Leakage dynamics affects decadal variability in Atlantic overturning circulation, Nature, 456, 489–492, doi: 10.1038/nature07426, 2008.

Braby, L.: Dynamics, interactions and ecosystem implications of mesoscale eddies formed in the southern region of Madagascar, MSc thesis, University of Cape Town, South Africa, 54 pp, 2014.

Breitburg, D., Levin, L. A., Oschlies, A., Grégoire, M., Chavez, F. P., Conley, D. J., Garçon, V., Gilbert, D., Gutiérrez, D., Isensee, K., Jacinto, G. S., Limburg, K. E., Montes, I., Naqvi, S. W. A., Pitcher, G. C., Rabalais, N. N., Roman, M. R., Rose, K. A., Seibel, B. A., and Zhang, J.: Declining oxygen in the global ocean and coastal waters, *Science*, *359*(6371), https://doi.org/10.1126/science.aam7240, 2018.

Brinca, L., Rey, F., Silva, C., and Sætre, R.: A survey on the marine fish resources of Mozambique. October–November 1980., Institute of Marine Research, Bergen, Norway, 1981.

Brown, S. L., M. R. Landry, R. T. Barber, L. Campbell, D. L. Garrison, and Gowing, M. M.: Picophytoplankton dynamics and production in the Arabian Sea during the 1995 Southwest Monsoon, Deep Sea Res., Part II, 46, 1745 – 1768, https://doi.org/10.1016/S0967-0645(99)00042-9, 1999.

Bryden, H. L., Beal, L. M. and Duncan, L. M.: Structure and Transport of the Agulhas Current and Its Temporal Variability, J Oceanogr 61, 479–492. https://doi.org/10.1007/s10872-005-0057-8, 2005.

Buchanan, P., and Beckley, L. E.: Chaetognaths of the Leeuwin Current system: oceanographic conditions drive epi-pelagic zoogeography in the south-east Indian Ocean, Hydrobiologia, 763(1), 81-96, doi:10.1007/s10750-015-2364-4, 2016.

Capet, X., Colas, F., McWilliams, J. C., Penven, P., and Marchesiello, P: Eddies in Eastern Boundary Subtropical Upwelling Systems, Ocean Modeling in an Eddying Regime, Geophysical Monograph SeDilmahamod, A. 2014. Links between the Seychelles-Chagos thermocline ridge and large scale climate modes and primary productivity; and the annual cycle of chlorophyll-a. University of Cape Town.ries 177, AGU, 131-147, doi: 10.1029/177GM10, 2008.

Capone, D. G., Subramaniam, A., Montoya, J. P., Voss, M., Humborg, C., Johansen, A. M., Siefert, R. L., and Carpenter, E. J.: An extensive bloom of the N_2-fixing cyanobacterium Trichodesmium erythraeum in the central Arabian Sea, Mar. Ecol. Prog. Ser., 172, 281–292, doi: 10.3354/meps172281, 1998.

Caputi, N., Fletcher, W., Pearce, A., and Chubb, C.: Effect of the Leeuwin Current on the recruitment of fish and invertebrates along the Western Australian coast, Mar. Freshw. Res., 47(2), 147-155, doi:10.1071/MF9960147, 1996.

Carr, M.-E. and Kearns, E. J.: Production regimes in four Boundary Current Systems, Deep-Sea Res. Part II: Topical Studies in Oceanography, 50, 3199-3221.,doi:10.1016/j.dsr2.2003.07.015, 2003.

Chaigneau, A., Le Texier, M., Eldin, G., Grados, C., and Pizarro, O.: Vertical structure of mesoscale eddies in the eastern South Pacific Ocean: A composite analysis from altimetry and Argo profiling floats, J. Geophys. Res. , 116(C11), C11025, https://doi.org/10.1029/2011JC007134, 2011.

Chakraborty, K., Valsala, V., Gupta, G.V.M. and Sarma, V.V.S.S. :Dominant biological control over upwelling on pCO2 in sea east of Sri Lanka, J. Geophys. Res., 123, doi:10.1029/2018JG004446, 2018.

Chatterjee, A., Shankar, D., Shenoi, S. S. C., Reddy, G. V., Michael, G. S., Ravichandran, M., Gopalkrishana, V. V., Rama Rao, E. P., Udaya Bhaskar, T. V. S., and Sanjeevan, V. N.: A new atlas of temperature and salinity for the North Indian Ocean, J. Earth Syst. Sci., 121, 559–593, doi:10.1007/s12040-012-0191-9, 2012.

Chatterjee, A., Shankar, D., McCreary, J. P., and Vinayachandran, P. N.: Yanai waves in the western equatorial Indian Ocean, J. Geophys. Res.: Oceans, 118, 1556–1570, https://doi.org/0.1002/jgrc.20121, 2013.

Chatterjee, A., Shankar, D., McCreary, J. P., Vinayachandran, P. N., and Mukherjee, A.: Dynamics of Andaman Sea circulation and its role in connecting the equatorial Indian Ocean to the Bay of Bengal, J. Geophys. Res., 122,1–19, doi: 10.1002/2016JC012300, 2017.

Chatterjee, A., Kumar, B. P., Prakash, S., and Singh, P.: Annihilation of the Somali upwelling system during summer monsoon, Sci. Rep, 9(1), 7598., https://doi.org/10.1038/s41598-019-44099-1, 2019.

Chaudhuri, A., Shankar, D., Aparna, S. G., Amol, P., Fernando, V., Kankonkar, A., Michael, G. S., Satelkar, N. P., Khalap, S. T., Tari, A. P., Gaonkar, M. G., Ghatkar, S., and Khedekar, R. R.: Observed variability of the West India

Coastal Current on the continental slope from 2009–2018, J. Earth Syst. Sci., 129 , 57, doi:10.1007/s12040-019-1322-3, 2020.

Chavez, F. P. and Toggweiler, J. R.: Physical estimates of global new production: The upwelling contribution, in: C. P. Summerhayes, K.-C. Emeis, M. V. Angel, R. L. Smith & B. Zeitzschel (Eds) Upwelling in the ocean: Modern processes and ancient records, New York, John Wiley & Sons, 313-320, 1995.

Chavez, F.P. and Messie, M.: A comparison of eastern boundary upwelling ecosystems, Prog. Oceanogr., 83, 80-93, doi: 10.1016/j.pocean.2009.07.032, 2009.

Checkley, D. M., and Barth, J. A.: Patterns and processes in the California Current System, Prog. Oceanogr., 83 , 49–64, doi:10.1016/j.pocean.2009.07.028, 2009.

Chen, G., Wang, D., and Hou, Y.: The features and interannual variability mechanism of mesoscale eddies in the Bay of Bengal, Cont. Shelf. Res., 47, 178–185, doi:10.1016/j.csr.2012.07.011, 2012.

Chen, G., Han, W., Shu, Y., Li, Y., Wang, D., and Xie, Q.: The role of Equatorial Undercurrent in sustaining the Eastern Indian Ocean upwelling, Geophys. Res. Lett., 43(12), 6444–6451. https://doi.org/10.1002/2016GL069433, 2016.

Cheng, X., Xie, S.-P., McCreary, J. P., Qi, Y., and Du, Y.: Intraseasonal variability of sea surface height over the Bay of Bengal, J. Geophys. Res., 118, 1–15, doi: 10.1002/jgrc.20075, 2013.

Cheng, G., Han, W., Li, Y., and Wang, D.: Interannual variability of equatorial eastern Indian Ocean upwelling: Local versus remote forcing, J. Phys. Oceanogr., 46, 789-807, doi:10.1175/JPO-D-15-0117.1, 2016.

Clarke, A. J., and X. Liu.: Interannual sea level in the northern and eastern Indian ocean, J. Phys. Oceanogr., 24, 1224–1235, doi: 10.1017/1520-0485, 1994.

Collins, M.: Upwelling on the southeast Madagascan shelf: frequency, extent, and driving mechanisms, MSc thesis, Nelson Mandela University, Port Elizabeth, South Africa, 126pp, 2020.

Cook, J., Cook, J. R., and Beaglehole, J. C.: The Journals of Captain Cook, Penguin UK, 1999.

Cossa, O., Pous, S., Penven, P., Capet, X., and Reason, C. J. C.: Modelling cyclonic eddies in the Delagoa Bight region, Cont. Shelf. Res., 119, 14-29, doi:10.1016/j.csr.2016.03.006, 2016.

Cox, M. D.: A numerical study of Somali Current eddies. J. Phys. Oceanogr., 9(2), 311–326, https://doi.org/10.1175/1520-0485(1979)009%3C0311:ANSOSC%3E2.0.CO;2, 1979.

Cresswell, G. R., and Golding, T.: Observations of a south-flowing current in the southeastern Indian Ocean, Deep Sea Res. Part I Oceanogr. Res. Pap., 27(6), 449-466, doi:10.1016/0198-0149(80)90055-2, 1980.

Cresswell, G., Boland, F., Peterson, J., and Wells, G.: Continental shelf currents near the Abrolhos Islands, Western Australia, Mar. Freshw. Res., 40(2), 113-128, doi:10.1071/MF9890113, 1989.

Cresswell, G., and Peterson, J.: The Leeuwin Current south of Western Australia, Mar. Freshw. Res., 44(2), 285-303, doi:10.1071/MF9930285, 1993.

Cutler, A. N., and Swallow, J. C.: Surface currents of the Indian Ocean (to 25S, 100E), Technical Report 187 (8 pp. and 36 charts). Brachnell: Meteorological Office, UK Institute of Oceanographic Science, 1984.

Darwin, C.: Journal of Researches Into the Natural History and Geology of the Countries Visited During the Voyage of HMS 'Beagle' Round the World: Under the Command of Capt. Fitz Roy, R.N, 5th ed., London: Ward, Lock and co., 1889.

Das, U., Vinayachandran, P. N., and Behara, A.: Formation of the southern Bay of Bengal cold pool, Clim Dyn, 47(5–6), 2009–2023, https://doi.org/10.1007/s00382-015-2947-9, 2018.

De Ruijter, W.P.M, Leeuwen,P and Lutjeharms, J.: Generation and Evolution of Natal Pulses: Solitary Meanders in the Agulhas Current, J. Phys. Oceanography, 29, 3043-3055, doi:https://doi.org/10.1175/1520-0485%281999%29029%3C3043%3AGAEONP%3E2.0.CO%3B2, 1999.

De Ruijter, W.P.M., Ridderinkhof, H., Lutjeharms, J.R.E., Schouten, M.W., and Veth, C.: Observations of the flow in the Mozambique Channel, Geophys. Res. Lett., 29 (10), 1502, doi:10.1029/2001GL013714, 2002.

Delman, A. S., Sprintall, J., McClean, J. L., and Talley, L. D.: Anomalous Java cooling at the initiation of positive Indian Ocean Dipole events, J. Geophys. Res. Oceans, 121, 5805–5824, doi:10.1002/2016JC011635, 2016.

Delman, A. S., McClean, J. L., Sprintall, J., Talley, L. D., and Bryan, F. O.: Process-specific contributions to anomalous Java mixed layer cooling during positive IOD events, J. Geophys. Res. Oceans, 123, 4153–4176, doi:/10.1029/2017JC013749, 2018.

Deutsch, C., Sarmiento, J. L., Sigman, D. M., Gruber, N., and Dunne, J. P.: Spatial coupling of nitrogen inputs and losses in the ocean, Nature, 445(7124), 163–167, doi: 10.1038/nature05392, 2007.

Dilmahamod, A. : Links between the Seychelles-Chagos thermocline ridge and large scale climate modes and primary productivity; and the annual cycle of chlorophyll-a, University of Cape Town, 2014.

Dilmahamod, A. F., Hermes, J. C., and Reason, C. J. C. : Chlorophyll-a variability in the Seychelles–Chagos Thermocline Ridge: Analysis of a coupled biophysical model. J. Mar. Syst., 154, 220–232, https://doi.org/10.1016/j.jmarsys.2015.10.011, 2016.

Dilmahamod, A. F., Penven, P., Aguiar-González, B., Reason, C. J. C., and Hermes, J. C.: A new definition of the South-East Madagascar Bloom and analysis of its variability, J. Geophys. Res. : Oceans, 124, doi:10.1029/2018JC014582, 2019.

DiMarco, S.F., Chapman, P., and Nowlin, W.D. Jr.: Satellite observations of upwelling on the continental shelf south of Madagascar, Geophys. Res. Lett., 27(24), 3965-3968, doi:10.1016/j.dsr2.2013.10.021, 2000.

Domingues, C. M., Maltrud, M. E., Wijffels, S. E., Church, J. A., and Tomczak, M.: Simulated Lagrangian pathways between the Leeuwin Current System and the upper-ocean circulation of the southeast Indian Ocean, Deep Sea Res. Part II: Top. Stud. Oceanogr., 54(8-10), 797-817, doi:10.1016/j.dsr2.2006.10.003, 2007.

Dong, C., McWilliams, J., Liu, Y. And Chen, D.: Global heat and salt transports by eddy movement, *Nat Commun.,* 5**,** 3294, https://doi.org/10.1038/ncomms4294, 2014.

Donners, J., and Drijfhout, S. S.: The Lagrangian view of South Atlantic interocean exchange in a global ocean model compared with inverse model results., J. Phys. Oceanogr. 34, 1019–1035, https://doi.org/10.1175/1520-0485(2004)034%3C1019:TLVOSA%3E2.0.CO;2, 2004.

Du, Y., Qu, T., Meyers, G., Masumoto, Y., and Sasaki, H.: Seasonal heat budget in the mixed layer of the southeastern tropical Indian Ocean in a high-resolution ocean general circulation model, J. Geophys. Res., 110, C04012, doi:10.1029/2004JC002845, 2005.

Du, Y., Qu, T., Meyers, and Meyers, G.: Interannual variability of sea surface temperature off Java and Sumatra in a global GCM, J. Climate, 21, 2451-2465, doi:10.1175/2007JCLI1753.1, 2008.

Dufois, F., Hardman-Mountford, N. J., Greenwood, J., Richardson, A. J., Feng, M., Herbette, S., and Matear, R.: Impact of eddies on surface chlorophyll in the South Indian Ocean, J. Geophys. Res. Oceans, 119(11), 8061-8077, doi:10.1002/2014jc010164, 2014.

Düing, W., Molinari, R., and Swallow, J.: Somali Current: Evolution of surface flow. Science, 209(4456), 588–590, 10.1126/science.209.4456.588-a, 1980.

Durand, F., Shankar, D., Birol, F. and Shenoi, S. S.C.: Spatiotemporal structure of the East India Coastal Current from satellite altimetry; J. Geophys. Res., 114, CO2013, doi: 10.1029/2008JC004807, 2009.

Ehlert, C., Frank, M., Haley, B. A., Böniger, U., De Deckker, P., and Gingele, F. X.: Current transport versus continental inputs in the eastern Indian Ocean: Radiogenic isotope signatures of clay size sediments, Geochem. Geophys. Geosyst., 12, Q06017, doi:10.1029/2011GC003544, 2011.

Ekman, V. W.: On the influence of the Earth's rotation on ocean currents, Arch. Math. Astron. Phys., 2, 1-52, 1905.

Elipot, S., and Beal, L. M.: *Characteristics, Energetics, and Origins of Agulhas Current Meanders and their Limited Influence on Ring Shedding*, J. Phys. Oceanogr., 45, 2294-2314,doi:10.1175/JPO-D-14-0254.1, 2015.

Falkowski, P., Ziemann, D., Kolber, Z. and Beinfang, P. K.:Role of eddy pumping in enhancing primary production in the ocean, *Nature,* 352**,** 55–58, https://doi.org/10.1038/352055a0, 1991.

Feng, M., Meyers, G., Pearce, A., and Wijffels, S.: Annual and interannual variations of the Leeuwin Current at 32°S, J. Geophys. Res. Oceans, 108(C11), doi:10.1029/2002jc001763, 2003.

Feng, M., Majewski, L. J., Fandry, C. B., and Waite, A. M: Characteristics of two counter-rotating eddies in the Leeuwin Current system off the Western Australian coast, Deep Sea Res. Part II: Top. Stud. Oceanogr., 54(8), 961-980. doi:10.1016/j.dsr2.2006.11.022, 2007.

Feng, M., Waite, A., and Thompson, P.: Climate variability and ocean production in the Leeuwin Current system off the west coast of Western Australia, J R Soc West Aus, 92, 67-82, 2009.

Feng, M., Slawinski, D., Beckley, L. E., and Keesing, J. K.: Retention and dispersal of shelf waters influenced by interactions of ocean boundary current and coastal geography, Mar. Freshw. Res., 61(11), 1259-1267, doi:10.1071/MF09275, 2010.

Findlater, J.: A major low-level air current near the Indian Ocean during the northern summer, Q J R Meteorol Soc, 95(404), 362–380, https://doi.org/10.1002/qj.49709540409, 1969.

Fischer, J., F. Schott, and Stramma, L.: Currents and transports of the Great Whirl-Socotra Gyre system during the summer monsoon, August 1993, J. Geophys. Res., 101, 3573–3587, https://doi.org/10.1029/95JC03617, 1996.

Fletcher, W., Tregonning, R., and Sant, G.: Interseasonal variation in the transport of pilchard eggs and larvae off southern Western Australia, Mar. Ecol. Prog. Ser., 111(3), 209-224, doi:10.3354/meps111209, 1994.

Foltz, G. R., Vialard, J., Praveen Kumar, B., and McPhaden, M. J.: Seasonal Mixed Layer Heat Balance of the Southwestern Tropical Indian Ocean, J. Clim, 23(4), 947–965. https://doi.org/10.1175/2009JCLI3268.1, 2010.

Fonteneau, A. , Lucas, V. , Tew Kai, E. , Delgado, A. and Demarcq, H.: Mesoscale exploitation of a major tuna concentration in the Indian Ocean, http://dx.doi.org/10.1051/alr:2008028. 21. 10.1051/alr:2008028, 2008.

Francis, P. A., Jithin, A. K., Chatterjee, A., Mukherjee, A., Shankar, D., Vinayachandran, P. N. and Ramakrishna, S. S. V. S.: Structure and dynamics of undercurrents in the western boundary current of the Bay of Bengal, Ocean Dyn., 70, 387-404, doi: doi.org/10.1007/s10236-019-01340-9, 2020.

Furnas, M.: Intra-seasonal and inter-annual variations in phytoplankton biomass, primary production and bacterial production at North West Cape, Western Australia: Links to the 1997–1998 El Niño event, Cont Shelf Res., 27(7), 958-980, doi:10.1016/j.csr.2007.01.002, 2007.

Fye, P.M.: The International Indian Ocean Expedition, The Distinguished Lecture Series 1964-1965, sponsored by Science Bureau, Washington Board of Trade, presented at Georgetown University, 27 January 1965, doi:10.1575/1912/5872, 1965.

Gadgil, S., Vinayachandran, P. N., Francis, P. A., and Gadgil, S.: Extremes of the Indian summer monsoon rainfall, ENSO and equatorial Indian Ocean oscillation, Geophys. Res. Lett., 31(12), L12213, https://doi.org/10.1029/2004GL019733, 2004.

Gandhi, N., Singh, A., Prakash, S., Ramesh, R., Raman, M., Sheshshayee, M., and Shetye, S.: First direct measurements of N_2 fixation during a Trichodesmium bloom in the eastern Arabian Sea, Glob. Biogeochem. Cycles, 25, GB4014, doi:10.1029/2010GB003970, 2011.

Gao, C., Fu, M., Song, H., Wang, L., Wei, Q., Sun, P., Liu, L. and Zhang, X.: Phytoplankton pigment pattern in the subsurface chlorophyll maximum in the South Java coastal upwelling system, Indonesia, Acta Oceanol. Sin., 37, 97-106, doi: 10.1007/s13131-018-1342-x, 2018.

Garçon, V., B. Dewitte, I. Montes, and K. Goubanova, Land-sea-atmosphere interactions exacerbating ocean deoxygenation in Eastern Boundary Upwelling Systems (EBUS), In IUCN Report Ocean Deoxygenation: Everyone's Problem., (https://portals.iucn.org/library/sites/library/files/ documents/03.4%20DEOX.pdf), 2019.

Gaughan, D., Fletcher, W., and White, K.: Growth rate of larval Sardinops sagax from ecosystems with different levels of productivity, Mar. Biol, 139(5), 831-837, doi:10.1007/s002270100637, 2001a.

Gaughan, D., White, K., and Fletcher, W.: The links between functionally distinct adult assemblages of Sardinops sagax: larval advection across management boundaries, ICES J. Mar. Sci., 58(3), 597-606, doi:10.1006/jmsc.2001.1061, 2001b.

Gauns, M., Madhupratap, M., Ramaiah, N., Jyothibabu, R., Fernandes, V., Paul, J. T. and Prasanna Kumar, S.: Comparative accounts of biological productivity characteristics and estimates of carbon fluxes in the Arabian Sea and the Bay of Bengal, Deep-Sea Res. Part II: Topical Stud. Oceanogr, 52, 2003-2017, doi: 10.1016/j.dsr2.2005.05.009, 2005.

Guastella, L. A., Roberts, M. J.: Dynamics and role of the Durban cyclonic eddy in the KwaZulu-Natal Bight ecosystem, African Journal of Marine Science, 38:sup1, S23-S42, DOI: 10.2989/1814232X.2016.1159982, 2006.

Gentilli, J.: Thermal anomalies in the eastern Indian Ocean, Nat. Phys. Sci., 238(84), 93-95, doi:10.1038/physci238093a0, 1972.

George, J .V., Nuncio, M, Racheal, C., Anilkumar, N., Sharon, B. N., Shramik, M. P., Sini P., Denny, P. A., Krishnan, K.P., and Achuthankutty, C.T.: Role of physical processes in chlorophyll distribution in the western tropical Indian Ocean, J. Mar. Syst., Volumes 113–114, 2013.

1991 Gersbach, G. H., Pattiaratchi, C. B., Ivey, G. N., and Cresswell, G. R.: Upwelling on the south-west coast of Australia—
1992 source of the Capes Current?, Cont Shelf Res., 19(3), 363-400, doi:10.1016/S0278-4343(98)00088-0, 1999.

1993 Godfrey, J., and Ridgway, K.: The large-scale environment of the poleward-flowing Leeuwin Current, Western Australia:
1994 longshore steric height gradients, wind stresses and geostrophic flow, J. Phys. Oceanogr., 15(5), 481-495,
1995 doi:10.1175/1520-0485(1985)015<0481:TLSEOT>2.0.CO;2, 1985.

1996 Goes, J. I., Thoppil, P. G., Gomes, H. D. and Fasullo, J .T.: Warming of the Eurasian landmass is making the Arabian Sea
1997 more productive, Science, 308, 545-547, 2005.

1998 Goes, J. I., Tian, H., Gomes, H. D. R., Anderson, O. R., Al-Hashmi, K., deRada, S., Luo, H., Al-Kharusi, L., Al-Azri, A.,
1999 and Martinson, D. G.: Ecosystem state change in the Arabian Sea fuelled by the recent loss of snow over the Himalayan-
2000 Tibetan Plateau region, Sci. Rep, 10, 7422, 2020.

2001 Gomes, H.D.R., Goes, J. I., and Saino, T.: Influence of physical processes and freshwater discharge on the seasonality of
2002 phytoplankton regime in the Bay of Bengal, Cont. Shelf Res., 20, 313–330, doi: 10.1016/S0278-4343(99)00072-2, 2000.

2003 Gomes, H.D.R., Goes, J. I., Matondkar, S. P., Parab, S. G., Al-Azri, A. R., and Thoppil, P. G.: Blooms of Noctiluca
2004 miliaris in the Arabian Sea—An in situ and satellite study, Deep Sea Res. Part I Oceanogr., 55(6), 751–765,
2005 doi:10.1016/j.dsr.2008.03.003, 2008.

2006 Gomes, H.D.R., Goes, J. I., Matondkar, S. P., Buskey, E. J., Basu, S., Parab, S., and Thoppil, P.: Massive outbreaks of
2007 Noctiluca scintillans blooms in the Arabian Sea due to spread of hypoxia, Nat. Commun., 5, 4862, doi:
2008 10.1038/ncomms5862, 2014.

2009 Gopalakrishna, V. V., and Sastry, J. S.: Hydrography of the western Bay of Bengal during SW monsoon, Indian J. Mar.
2010 Sci., 14,62–65, 1984.

2011 Gopalan, A. K. S., Gopalakrishna, V. V., Ali, M. M, and Sharma, R.: Detection of BoB eddies from TOPEX and sea
2012 truth observations. J. Mar. Res., 58,721–734, 2000.

2013 Goschen, W. S., Bornman, T. G., Deyzel, S., and Schumann, E. H.: Coastal upwelling on the far eastern Agulhas Bank
2014 associated with large meanders in the Agulhas Current, Cont. Shelf Res., 101, 34-46, 2015.

2015 Govender, A. and Rabede P. V.: Status report: seventy four (Polysteganus undulosus), In Status Reports for Key Linefish
2016 Species, Mann, B. Q. (Ed.). Spec. Publ. oceanogr. Res. Inst. S. Afr. 7,174-175, 2000.

2017 Griffin, D. A., Wilkin, J. L., Chubb, C. F., Pearce, A. F., and Caputi, N.: Ocean currents and the larval phase of Australian
2018 western rock lobster, Panulirus cygnus, Mar. Freshw. Res., 52(8), 1187-1199, doi:10.1071/MF01181, 2001.

2019 Griffiths, M. H. and Hecht,T.: On the life-history of Atractoscion aequidens, a migratory sciaenid off the east coast of
2020 southern Africa, J. Fish Bioi., 47, 962-985, 1995.

2021 Griffiths, C. L., Robinson, T. B., Lange, L., and Mead, A.: Marine biodiversity in South Africa: an evaluation of current
2022 states of knowledge, Plos one, 5(8):e12008, doi: 10.1371/journal.pone.0012008, 2010.

2023 Grumet, N. S., Abram,N. J., Beck, J. W., Dunbar,R. B., Gagan, M. K., Guilderson, T. P., Hantoro, W. S. and Suwargadi,
2024 B. W.: Coral radiocarbon records of Indian Ocean water mass mixing and wind-induced upwelling along the coast of
2025 Sumatra, Indonesia, J. Geophys. Res., 109, C05003, doi:10.1029/2003JC002087, 2004.

Guastella, L. A., Roberts, M. J.: Dynamics and role of the Durban cyclonic eddy in the KwaZulu-Natal Bight ecosystem, Afr. J. Mar. Sci., 38:sup1, S23-S42, doi: 10.2989/1814232X.2016.1159982, 2016.

Gupta, G., Sudheesh, V., Sudharma, K., Saravanane, N., Dhanya, V., Dhanya, K., Lakshmi, G., Sudhakar, M., and Naqvi, S.: Evolution to decay of upwelling and associated biogeochemistry over the southeastern Arabian Sea shelf, J. Geophys. Res. Biogeosci., 121(1), 159–175, doi: 10.1002/2015JG003163, 2016.

Halm, H., Lam, P., Ferdelman, T.G., Lavik, G., Dittmar, T., Laroche, J., D'Hondt, S., and Kuypers, M.M.: Heterotrophic organisms dominate nitrogen fixation in the South Pacific Gyre, ISME J., 6(6), 1238-49, doi:10.1038/ismej.2011.182, 2012.

Halo, I., Backeberg, B., Penven, P., Ansorge, I., Reason, C., and Ullgren, J.E.: Eddy properties in the Mozambique Channel: A comparison between observations and two numerical ocean circulation models, Deep-Sea Res. II, 100, 38–53, doi:10.1016/j.dsr2.2013.10.015, 2014.

Halo, I., Sagero, P., Manyilizu, M., and Shigalla M.: Biophysical modelling of the coastal upwelling variability and circulation along the Tanzanian and Kenyan coasts. WIO, Journal of Marine Science, 1, 43-61, doi:10.4314/wiojms.si2020.1.5, 2020 .

Hanson, C. E., Pattiaratchi, C. B., and Waite, A. M.: Seasonal production regimes off south-western Australia: influence of the Capes and Leeuwin Currents on phytoplankton dynamics, Mar. Freshw. Res., 56(7), 1011-1026, doi:10.1071/MF04288, 2005.

Hanson, C. E., Pesant, S., Waite, A. M., and Pattiaratchi, C. B.: Assessing the magnitude and significance of deep chlorophyll maxima of the coastal eastern Indian Ocean, Deep Sea Res. Part II: Top. Stud. Oceanogr., 54(8-10), 884-901, doi:10.1016/j.dsr2.2006.08.021, 2007a.

Hanson, C. E., Waite, A. M., Thompson, P. A., and Pattiaratchi, C. B.: Phytoplankton community structure and nitrogen nutrition in Leeuwin Current and coastal waters off the Gascoyne region of Western Australia, Deep Sea Res. Part II: Top. Stud. Oceanogr., 54(8-10), 902-924, doi:10.1016/j.dsr2.2006.10.002, 2007b.

Hanson, C., and McKinnon, A.: Pelagic ecology of the Ningaloo region, Western Australia: influence of the Leeuwin Current, J R Soc West Aus, 92, 129-138, 2009.

Harris, T. F. W., and van Foreest, D.: The Agulhas Current in March 1969, Deep Sea Res., 25(6), 549-550, https://doi.org/10.1016/0146-6291(78)90643-4, 1978.

Haugen, V. E., Johannessen, O. M., and Evensen, G.: Mesoscale modeling study of the oceanographic conditions off the southwest coast of India, J. Earth Syst. Sci., 111 , 321–337, doi:10.1007/BF02701978, 2002.

Heileman, S. and Scott, L.E.P.: The Somali coastal current large marine ecosystem. In: Sherman, K., Hempel, G. (Eds.), The UNEP Large Marine Ecosystem Report: A perspective on changing conditions in LMEs of the World's regional seas, UNEP, United States, 2008.

Heip C.H.R., Hemminga, M.A., and de Bie, M.J.M. (Eds): Monsoons and Coastal Ecosystems in Kenya, Cruise reports Netherlands Indian Ocean Programme, 5, National Museum of Natural History, Leiden, Netherlands, 122 pp, 1995.

Helly, J. J., and Levi, L. A.: Global distribution of naturally occurring marine hypoxia on continental margins, *Deep Sea Res., Part I*, *51*,1159–1168, 2004.

2062 Hermes, J. C., & Reason, C. J. C. : Annual cycle of the South Indian Ocean (Seychelles-Chagos) thermocline ridge in a
2063 regional ocean model, J. Geophys. Res., 113(C4), C04035, https://doi.org/10.1029/2007JC004363, 2008.

2064 Hitchcock, G. L., and Olson, D.: NE and SW monsoon conditions along the Somali coast during 1987, In B. N. Desai
2065 (Ed.), Oceanography of the Indian Ocean, New Delhi: Oxford & IBH, 1992.

2066 Hitchcock, G.L., Key, E., and Masters, J.: The fate of upwelled waters in the Great Whirl, August 1995, Deep-Sea Res. II
2067 47, 1605–1621, 2000.

2068 Ho, C.-R., Zheng, Q., and Kuo, N.-J.: SeaWiFs observations of upwelling south of Madagascar: long-term variability and
2069 interaction with East Madagascar Current, Deep-Sea Res. II Top. Stud. Oceanogr., 51(1), 59–67,
2070 doi:10.1016/j.dsr2.2003.05.001, 2004.

2071 Holliday, D., Beckley, L. E., and Olivar, M. P.: Incorporation of larval fishes into a developing anti-cyclonic eddy of the
2072 Leeuwin Current off south-western Australia, J. Plankton Res., 33(11), 1696-1708, doi:10.1093/plankt/fbr064, 2011.

2073 Holliday, D., Beckley, L. E., Millar, N., Olivar, M. P., Slawinski, D., Feng, M., and Thompson, P. A.: Larval fish
2074 assemblages and particle back-tracking define latitudinal and cross-shelf variability in an eastern Indian Ocean boundary
2075 current, Mar. Ecol. Prog. Ser., 460, 127-144, doi:10.3354/meps09730, 2012.

2076 Holloway, P. E., and Nye, H.: Leeuwin Current and wind distributions on the southern part of the Australian North West
2077 Shelf between January 1982 and July 1983, Australian Journal of Mar. Freshw. Res., 36(2), 123-137,
2078 doi:10.1071/MF9850123, 1985.

2079 Hood, R.R., Bange, H.W., Beal, L., Beckley, L.E., Burkill, P., Cowie, G.L., D'Adamo, N., Ganssen, G., Hendon, H.,
2080 Hermes, J., Honda, M., McPhaden, M., Roberts, M., Singh, S., Urban, E., Yu, W.: Science Plan of the Second
2081 International Indian Ocean Expedition (IIOE-2): A Basin-Wide Research Program, Scientific Committee on Oceanic
2082 Research, Newark, Delaware, USA, 2015.

2083 Hood, R. R., Beckley, L. E., and Wiggert, J. D.: Biogeochemical and ecological impacts of boundary currents in the
2084 Indian Ocean, Prog. Oceanogr., 156, 290-325, doi:10.1016/j.pocean.2017.04.011, 2017.

2085 Horii, T., Hase, H., Ueki, I., and Masumoto, Y.: Oceanic precondition and evolution of the 2006 Indian Ocean dipole,
2086 Geophys. Res. Lett., 35, L03607, doi:10.1029/2007GL032464, 2008.

2087 Horii, T., Ueki, I., Syamsudin, F., Sofian, I., and Ando, K.: Intraseasonal coastal upwelling signal along the southern coast
2088 of Java observed using Indonesian tidal station data, J. Geophys. Res., 121, 2690-2708, doi: 10.1002/2015JC010886,
2089 2016.

2090 Horii, T., Ueki, I., and Ando, K.: Coastal upwelling events along the southern coast of Java during the 2008 positive
2091 Indian Ocean Dipole, J. Oceanogr., 74, 499–508, doi:10.1007/s10872-018-0475-z, 2018.

2092 Huggett, J. A.: Mesoscale distribution and community composition of zooplankton in the Mozambique Channel.,Deep-Sea
2093 Res. II, 100, 119–135, doi: 10.1016/j.dsr2.2013.10.021, 2014.

2094 Hutchings, L. Beckley, L. L. E., , Griffiths, M. H., Roberts, M. J., Sundby, S., van der Lingen, C. : Spawning on the edge:
2095 spawning grounds and nursery areas around the southern African coastline, Mar. Freshw. Res. 53, 307–318,
2096 doi:10.1071/MF01147, 2002.

2097 Hutchings, L., [van der Lingen], C., Shannon, L., Crawford, R., Verheye, H., Bartholomae, C., [van der Plas], A., Louw,
2098 D., Kreiner, A., Ostrowski, M., Fidel, Q., Barlow, R., Lamont, T., Coetzee, J., Shillington, F., Veitch, J., Currie, J., and
2099 Monteiro, P.: The Benguela Current: An ecosystem of four components, Prog. Oceanogr., 83 , 15–32,
2100 doi:10.1016/j.pocean.2009.07.046, 2009.

2101 IMR.: Cruise Report No. 1 of R/V Dr Fridtjof Nansen, Joint NORAD/Mozambique/FAO Project to investigate the fish
2102 resources off the coast of Mozambique, Institute of Marine Research, Bergen, Norway, 1977a.

2103 IMR.: Cruise Report No. 2 of R/V Dr Fridtjof Nansen, Joint NORAD/Mozambique/FAO Project to investigate the fish
2104 resources off the coast of Mozambique, October–December 1977.,Institute of Marine Research, Bergen, Norway, 1978a.

2105 IMR.: Cruise Report No. 3 of R/V Dr Fridtjof Nansen. Joint NORAD/Mozambique/FAO Project to investigate the fish
2106 resources off the coast of Mozambique, January–March 1978, Institute of Marine Research, Bergen, Norway, 1978b.

2107 IMR.: Cruise Report No. 4 of R/V Dr Fridtjof Nansen, Joint NORAD/Mozambique/FAO Project to investigate the fish
2108 resources off the coast of Mozambique, April–June 1978, Institute of Marine Research, Bergen, Norway, 1978c.

2109 IMR.: Fisheries resources survey, Madagascar. Cruise Report R/V Dr Fridtjof Nansen, 16–28 June 1983, Institute of
2110 Marine Research, Bergen, Norway, 1983a.

2111 Iskandar, I., Tozuka, T., Sasaki, H., Masumoto, Y., and Yamagata, T.: Intraseasonal variations of surface and subsurface
2112 currents off Java as simulated in a high-resolution ocean general circulation model, J. Geophys. Res., 111, C12015,
2113 doi:10.1029/2006JC003486, 2006.

2114 Iskandar, I., Rao, S. A., and Tozuka, T.: Chlorophyll-a bloom along the southern coasts of Java and Sumatra during 2006,
2115 Int. J. Remote Sens., 30, 663-671, doi:10.1080/01431160802372309, 2009.

2116 Iskandar, I., Sari, Q. W, Setiabudidaya, D., Yustian I., and Monger B.: The distribution and variability of chlorophyll-a
2117 bloom in the southeastern tropical Indian Ocean using Empirical Orthogonal Function analysis, Biodiversitas, 18, 1546-
2118 1555, doi: 10.13057/biodiv/d180433, 2017.

2119 Izumo, T., Montegut, C. D., Luo, J. J. , Behera, S. K., Masson, S., and Yamagata, T.: The role of the western Arabian
2120 Sea upwelling in Indian monsoon rainfall variability, J. Clim., 21(21), 5603 – 5623, doi:10.1175/2008JCLI2158.1, 2008.

2121 Jackson, J. M., Rainville, L., Roberts, M. J. , McQuaid, C. D., and Lutjeharms, J. R. E.: Mesoscale bio-physical
2122 interactions between the Agulhas Current and the Agulhas Bank, South Africa, Cont. Shelf Res., 49, 10–24, doi:10.1016/
2123 j.csr.2012.09.005, 2012.

2124 Jacobs, Z. L., Jebri, F., Raitsos, D. E., Popova, E., Srokosz, M., Painter, S. C., Nencioli, F., Roberts, M., Kamau, J.,
2125 Palmer, M., and Wihsgott, J.: Shelf-break upwelling and productivity over the North Kenya Banks: The importance of
2126 large-scale ocean dynamics, J. Geophys. Res. : Oceans, 125, e2019JC015519, https://doi.org/10.1029/2019JC015519,
2127 2020.

2128 Jochum, J. and Murtugudde, R.: Internal variability of Indian Ocean SST, J. Climate, 18, 3726–3738,
2129 https://doi.org/10.1175/JCLI3488.1, 2005.

2130 Johannes, R., Pearce, A., Wiebe, W., Crossland, C., Rimmer, D., Smith, D., and Manning, C.: Nutrient characteristics of
2131 well-mixed coastal waters off Perth, Western Australia, Estuar. Coast. Shelf Sci., 39(3), 273-285,
2132 doi:10.1006/ecss.1994.1064, 1994.

2133 Johannessen, O. M., Subbaraju, G. V., and Blindheim, J.: Seasonal variations of the oceanographic conditions off the
2134 southwest coast of India during 1971-1975, Fisk Dir Skr Ser Hav Unders, 18 , 247–261, 1981.

2135 Johnsen, E., Krakstad, J., Ostrowski, M., Serigstad, B., Strømme, T., Alvheim, O., Olsen, M., Zaera, D., André, E., Dias,
2136 N., Sousa, L., Sousa, B., Malauene, B., and Abdula, S.: Surveys of the living marine resources of Mozambique:
2137 Ecosystem survey and special studies, 27 September–21 December 2007, Report No. 8/2007–2007409, Institute of Marine
2138 Research, Bergen, Norway, 2007.

2139 Jorge da Silva, A., Mubango, A., and Sætre, R.: Information on oceanographic cruises in the Mozambique Channel,
2140 Revista de Investigação Pesquira, 2, Instituto de Desenvolvimento Pesqueiro, Maputo, República Popular de
2141 Moçambique, 89, 1981.

2142 Jyothibabu, R., Vinayachandran, P. N., Madhu, N. V., Robin, R. S., Karnan, C., Jagadeesan, L., and Anjusha, A. :
2143 Phytoplankton size structure in the southern Bay of Bengal modified by the Summer Monsoon Current and associated
2144 eddies: Implications on the vertical biogenic flux, J. Mar. Syst., 143, 98–119,
2145 https://doi.org/10.1016/j.jmarsys.2014.10.018, 2015.

2146 Kampf, J. and Chapman, P: Upwelling Systems of the World, 10.1007/978-3-319-42524-5, 2016.

2147 Kämpf, J. and Kavi, A.: SST variability in the eastern intertropical Indian Ocean – On the search for trigger mechanisms
2148 of IOD events, Deep Sea Res. Part II Top. Stud. Oceanogr., 166, 64-74, doi:10.1016/j.dsr2.2018.11.010, 2019.

2149 Kanuri, V. V., Rao, G.D., Munnooru,K., Sura, A., Patra, S.,Vinjamuri,R. R., and Karr. R.: Scales and drivers of seasonal
2150 pCO_2 dynamics and net ecosystem exchange along the coastal waters of southeastern Arabian Sea, *Marine poll. Bull.*,
2151 *121*(1-2), 372-380, 2017.

2152 Kawamiya, M.: Mechanism of offshore nutrient supply in the western Arabian Sea, J. Mar. Res., 59, 675–696,
2153 https://doi.org/10.1357/002224001762674890, 2001.

2154 Keen, T.R., Kindle, J.C., and Young, D.K.: The interaction of southwest monsoon upwelling, advection and primary
2155 production in the northwest Arabian Sea, J. Mar. Syst., 13, 61–82, https://doi.org/10.1016/S0924-7963(97)00003-1, 1997.

2156 Kindle, J. C., Arnone, R., and Smedstad, O. M.: On the generation of coastal filaments during the Spring Intermonsoon,
2157 EOS, Transactions of the AGU, 83, 37, 2002.

2158 Kolasinski, J., Kaehler, S., and Jaquemet, S.: Distribution and sources of particulate organic matter in a mesoscale eddy
2159 dipole in the Mozambique Channel (south-western Indian Ocean): Insight from C and N stable isotopes, J. Mar. Syst., 96–
2160 97, 122–131, doi: 10.1016/j.jmarsys.2012.02.015, 2012.

2161 Koné, V., Aumont, O., Lévy, and M., Resplandy, L.: Physical and biogeochemical controls of the phytoplankton seasonal
2162 cycle in the Indian Ocean: a modeling study, In: Indian Ocean Biogeochemical Processes and Ecological Variability,
2163 AGU, 147–166, doi.org/10.1029/2008GM000700, 2009.

2164 Koné, V., Lett, C., and Fréon, P.,: Modelling the effect of food availability on recruitment success of Cape anchovy
2165 ichthyoplankton in the southern Benguela upwelling system, Afr. J. Mar. Sci., 35 (2), 151-161, 2013.

2166 Koslow, J.A., Pesant, S., Feng, M., Pearce, A., Fearns, P., Moore, T., Matear, R., and Waite, A.: The effect of the Leeuwin
2167 Current on phytoplankton biomass and production off Southwestern Australia, J. Geophys. Res. Oceans, 113(C7),
2168 doi:10.1029/2007JC004102, 2008.

2169 Krakstad, J.-O., Mehl, S., Roman, R., Escobar-Porras, J., Stapley, J., Flynn, B., Olsen, M., and Beck, I.: Cruise Reports Dr
2170 Fridtjof Nansen, East Madagascar Current Ecosystem Survey ASCLME/FAO 2008 Cruise 1, 24 August–1 October 2008,
2171 Institute of Marine Research, Bergen, Norway, 2008.

2172 Kromkamp, J., de Bie, M., Goosen, N., Peene, J., van Rijswijk, P., Sinke, J., and Duineveld, G.C.A.: Primary production
2173 by phytoplankton along the Kenyan coast during the SE monsoon and November intermonsoon 1992, and the occurrence
2174 of *Trichodesmium,* Deep-Sea Res., Part 2, Top. Stud. Oceanogr., 44(6-7), 1195-1212, doi:10.1016/S0967-0645(97)00015-
2175 5, 1997.

2176 Krug, M., and Tournadre, J.: Satellite observations of an annual cycle in the Agulhas Current, Geophys. Res. Lett., 39(15),
2177 https://doi.org/10.1029/2012GL052335, 2012.

2178 Krug, M., Tournadre, J., and Dufois, F.: Interactions between the Agulhas Current and the eastern margin of the Agulhas
2179 Bank, Cont. Shelf Res., 81, 67–79, https://doi.org/10.1016/j.csr.2014.02.020, 2014.

2180 Krug, M., Swart, S., and Gula, J.: Submesoscale cyclones in the Agulhas current, Geophys. Res. Lett., 44(1), 346–354,
2181 https://doi.org/10.1002/2016GL071006, 2017.

2182 Kumar, S., Ramesh, R., Sardesai, S., Sheshshayee, M.S.: High new production in the Bay of Bengal: possible causes and
2183 implications, Geophys. Res. Lett. 31(L18304), doi:10.1029/2004GL021005, 2004.

2184 Kumar, P. K, Singh, A., Ramesh, R., and Nallathambi, T.: N_2 Fixation in the Eastern Arabian Sea: Probable Role of
2185 Heterotrophic Diazotrophs, Mar. Chem., 4, 80, doi:10.3389/fmars.2017.00080, 2017.

2186 Kurian, J., and Vinayachandran, P. N.: Mechanisms of formation of the Arabian Sea mini warm pool in a high-resolution
2187 Ocean General Circulation Model, J. Geophys. Res. Oceans, 112, C05009, doi:10.1029/2006JC003631, 2007.

2188 Kyewalyanga, M.S., Naik, R., Hegde, S., Raman, M., Barlow, R., and Roberts, M.: Phytoplankton biomass and primary
2189 production in Delagoa Bight Mozambique: Application of remote sensing, Estuar. Coast. Shelf Sci., 74, 429-436, doi:
2190 10.1016/j.ecss.2007.04.027, 2007.

2191 L´evy, M., Andr´e., J.-M., Shankar, D., Durand, F. and Shenoi, S.S.C.: A quantitative method for describing the seasonal
2192 cycles of surface chlorophyll in the Indian Ocean, SPIE Proceedings, Remote Sensing of the Marine Environment, R. J.
2193 Frouin, V. K.Agarwal, H. Kawamura, S. Nayak, D. Pan; Eds. , 6406, 640611, 8pp, 2006.

2194 La Fond, E. C.: On upwelling and sinking off the east coast of India, Andhra Univ. Mem. Oceanogr., 1, 117–121, 1954.

2195 La Fond, E. C.: Oceanographic studies in the Bay of Bengal, Proc. Indian Acad. Sci., 46, 1–46, doi:10.1007/BF03052445,
2196 1957.

2197 La Fond, E. C.: On the circulation of the surface layers on the east coast of India, Andhra Univ. Mem. Oceanogr., 2, 1–11,
2198 1958.

2199 La Fond, E. C: Sea surface features and internal waves in the sea, Indian J. Meterol. Geophys., 10, 415–419,
2200 https://metnet.imd.gov.in/mausamdocs/51047.pdf, 1959.

2201 Lakshmi, R. S., Chatterjee, A., Prakash, S., and Mathew, T.: Biophysical Interactions in Driving the Summer Monsoon
2202 Chlorophyll Bloom Off the Somalia Coast, J.Geophys. Res. Oceans, *125*(3), https://doi.org/10.1029/2019JC015549,
2203 2020.

2204 Lamont, T., Roberts, M. J., Barlow, R. G., Morris, T., and van den Berg, M. A.: Circulation patterns in the Delagoa Bight,
2205 Mozambique, and the influence of deep ocean eddies, Afr. J. Mar. Sci., 32 (3), 553–562, doi:
2206 10.2989/1814232X.2010.538147, 2010.

2207 Lamont, T., Barlow, R., Morris, T., and van den Berg, M.: Characterisation of mesoscale features and phytoplankton
2208 variability in the Mozambique Channel, Deep-Sea Res. II 100, 94–105, doi: 10.1016/j.dsr2.2013.10.019, 2014.

2209 Landolfi, A., Koeve, W., Dietze, H., Kähler, P., and Oschlies, A.: A new perspective on environmental controls of marine
2210 nitrogen fixation, Geophys. Res. Lett., 42, 4482–4489, doi:10.1002/2015GL063756, 2015.

2211 Langlois, R., Großkopf, T., Mills, M., Takeda, S., and LaRoche, J.: Widespread distribution and expression of gamma A
2212 (UMB), an uncultured, diazotrophic, γ-proteobacterial nifH phylotype, PLoS One, 10(6),
2213 doi:10.1371/journal.pone.0128912, 2015.

2214 Leber, G. M., and Beal, L. M.: Local water mass modifications by a solitary meander in the A gulhas Current, J. Geophys.
2215 Res. : Oceans, 120(6), 4503–4515. https://doi.org/10.1002/2015JC010863, 2015.

2216 Leber, G. M., Beal, L. M., and Elipot, S.: Wind and Current Forcing Combine to Drive Strong Upwelling in the Agulhas
2217 Current, J. Phys. Oceanogr., 47(1), 123–134, https://doi.org/10.1175/JPO-D-16-0079.1, 2017.

2218 Lee, T. : Decadal weakening of the shallow overturning circulation in the South Indian Ocean, Geophys. Res. Lett.,
2219 31(18), L18305. https://doi.org/10.1029/2004GL020884, 2004.

2220 Leetmaa, A., Quadfasel, D. R., and Wilson, D.: Development of the flow field during the onset of the Somali current,
2221 1979, J. Phys. Oceanogr., 12, 1325–1342, doi:10.1175/1520-0485(1982)012<1325:DOTFFD>2.0.CO;2, 1982.

2222 Lenanton, R., Caputi, N., Kangas, M., and Craine, M.: The ongoing influence of the Leeuwin Current on economically
2223 important fish and invertebrates off temperate Western Australia - has it changed?, J R Soc West Aus, 92, 111 - 128, 2009.

2224 Lévy, M., Shankar, D., André, J., Shenoi, S., Durand, F., and de Boyer Montégut, C.: Basin-wide seasonal evolution of the
2225 Indian Ocean's phytoplankton blooms, J. Geophys. Res. :Oceans, doi:112(C12),10.1029/2007JC004090, 2007.

2226 Lighthill, M. J.: Dynamic response of the Indian Ocean to onset of the Southwest Monsoon, Philosophical Transactions of
2227 the Royal Society of London Series A, Mathematical and Physical Sciences, 265(1159), 45–92,
2228 https://doi.org/10.1098/rsta.1969.0040, 1969.

2229 Locarnini, R. A., Mishonov, A. V., Baranova, O. K., Boyer, T. P., Zweng, M. M., Garcia, H. E., Reagan, J. R., Seidov, D.,
2230 Weathers, K., Paver, C. R. and Smolyar, I.: World Ocean Atlas 2018, Volume 1: Temperature, A. Mishonov Technical
2231 Ed.; NOAA Atlas NESDIS 81, 52, 2018.

2232 Longhurst, A. R., and Wooster, W. S.: Abundance of oil sardine (Sardinella longiceps) and upwelling on the southwest
2233 coast of India, Can. J. Fish. Aquat., 47 , 2407–2419, doi:10.1139/f90-268, 1990.

2234 Longhurst, A.: A major seasonal phytoplankton bloom in the Madagascar Basin, Deep-Sea Res. Part I: Oceanographic
2235 Research Papers, 48(11), 2413–2422, doi: 10.1016/S0967-0637(01)00024-3, 2001.

2236 Lotliker, A. A., Baliarsingh, S. K., Trainer, V. L., Wells, M. L., Wilson, C., Udaya Bhaskar, T. V. S., Samanta, A., and
2237 Shahimol, S. R.: Characterization of oceanic Noctiluca blooms not associated with hypoxia in the Northeastern Arabian
2238 Sea, Harmful Algae, 74, 46–57, https://doi.org/10.1016/j.hal.2018.03.008, 2018.

2239 Lourey, M. J., Dunn, J. R., and Waring, J.: A mixed-layer nutrient climatology of Leeuwin Current and Western
2240 Australian shelf waters: seasonal nutrient dynamics and biomass, J Mar Syst, 59(1-2), 25-51,
2241 doi:10.1016/j.jmarsys.2005.10.001, 2006.

2242 Lourey, M., Thompson, P., McLaughlin, J., Bonham, P., and Feng, M.: Primary production and phytoplankton community
2243 structure during a winter shelf-scale phytoplankton bloom off Western Australia, Mar. Biol, 160, 355–369,
2244 doi:10.1007/s00227-012-2093-4, 2012.

2245 Lowe, R. J., Ivey, G. N., Brinkman, R. M., and Jones, N. L.: Seasonal circulation and temperature variability near the
2246 North West Cape of Australia, J. Geophys. Res. Oceans, 117(C4), doi:10.1029/2011JC007653, 2012.

2247 Lugomela, C., Lyimo, T. J., Bryceson, I., Semesi, A. K., and Bergman, B.: *Trichodesmium* in coastal waters of Tanzania:
2248 diversity, seasonality, nitrogen and carbon fixation, Hydrobiologia, 477, 1–13, doi: 10.1023/A:1021017125376, 2002.

2249 Luis, A. J., and Kawamura, H.: Air-sea interaction, coastal circulation and primary production in the eastern Arabian sea:
2250 A review, J. Oceanogr, 60, 205–218, doi:10.1023/B:JOCE.0000038327.33559.34, 2004.

2251 Luther, M. E., and O'Brien, J. J.: Modelling the variability of the Somali Current, In J. C. J. Nihoul, and B. M. Jamart
2252 (Eds.), Mesoscale/synoptic coherent structures in geophysical turbulence, : proceedings of the 20th International Liège
2253 Colloquium on Ocean Hydrodynamics, Elsevier Oceanography Series, 50,373–386, 1989.

2254 Lutjeharms, J. R. E., and Jorge da Silva, A.: The Delagoa Bight eddy, Deep-Sea Res., 35, 619-634, doi:10.1016/0198-
2255 0149(88)90134-3, 1988.

2256 Lutjeharms, J. R. E., and Roberts, H. R.: The Natal pulse: An extreme transient on the Agulhas Current, J. Geophys. Res.,
2257 93(C1), 631, https://doi.org/10.1029/JC093iC01p00631, 1988.

2258 Lutjeharms J. R. E., and Connell, A. D. : The Natal Pulse and inshore counter currents off the South African east coast, S.
2259 Afr. J. Sci, 85, 533–535, 1989.

2260 Lutjeharms, J.R.E., and Machu, E.: An upwelling cell inshore of the East Madagascar Current. Deep-Sea Res. I, 47, 2405-
2261 2411, doi:10.1016/S0967-0637(00)00026-1, 2000.

2262 Lutjeharms, J. R. E., Valentine, H. R., and van Ballegooyen, R. C.: The hydrography and water masses of the Natal Bight,
2263 South Africa, Cont. Shelf Res. 20, 1907–1939, https://doi.org/10.1016/S0278-4343(00)00053-4, 2000.

2264 Lutjeharms, J. R. E., Boebel, O., van der Vaart, P. C. F., de Ruijter, W. P. M., Rossby, T., and Bryden, H. L.: Evidence
2265 that the natal pulse involves the Agulhas Current to its full depth, Geophys. Res. Lett., 28(18), 3449–3452.,
2266 https://doi.org/10.1029/2000GL012639, 2001.

2267 Lutjeharms, J. R. E., Boebel, O., and Rossby, H. T.: Agulhas cyclones, Deep Sea Res., Part II, 50(1), 13–34,
2268 https://doi.org/10.1016/S0967-0645(02)00378-8, 2003.

2269 Lutjeharms, J. R. E.: The coastal oceans of south-eastern Africa. In: The Sea, Volume 14B, editors: A. R. Robinson and K.
2270 H. Brink, Harvard University Press, Cambridge, MA, pp. 783- 834, 2006.
2271 Lutjeharms, J. R. E.:*The Agulhas Current,* Springer, Berlin, Heidelbert, New York, 2006.

2272 Machu, E., Lutjeharms, J. R. E., Webb, A. M., and Van Aken, H. M.: First hydrographic evidence of the southeast
2273 Madagascar upwelling cell, Geophys. Res. Lett., 29(21), 2009, doi:10.1029/2002GL015381, 2002.

2274 Madden, R. A., and Julian, P. R. : Description of Global-Scale Circulation Cells in the Tropics with a 40–50 Day Period. J
2275 Atmos Sci., 29(6), 1109–1123. https://doi.org/10.1175/1520-0469(1972)029<1109:DOGSCC>2.0.CO;2, 1972.

2276 Madhupratap, M., Kumar, S. P., Bhattathiri, P., Kumar, M. D., Raghukumar, S., Nair, K., and Ramaiah, N.: Mechanism of
2277 the biological response to winter cooling in the northeastern Arabian Sea, Nature, 384(6609), 549–552,
2278 doi:10.1038/384549a0, 1996.

2279 Mahongo, S.B., Francis, J., and Osima, S.E.: Wind Patterns of Coastal Tanzania: Their Variability and Trends. West.
2280 Indian Ocean J. Mar. Sci., 10 (2), 107-120, 2012.

2281 Malan, N., Backeberg, B., Biastoch, A., Durgadoo, J. V., Samuelsen, A., Reason, C., and Hermes, J.: Agulhas Current
2282 Meanders Facilitate Shelf-Slope Exchange on the Eastern Agulhas Bank, J. Geophys. Res. Oceans, 123(7), 4762–4778,
2283 https://doi.org/10.1029/2017JC013602, 2018.

2284 Malauene, B.S., Shillington, F.A., Roberts, M.J., and Moloney, C.L.: Cool, elevated chlorophyll a waters off northern
2285 Mozambique, Deep-Sea Res. II, 100, 68–78, doi: 10.1016/j.dsr2.2013.10d.017, 2014.

2286 Manghnani, V., Morrison, J. M., Hopkins, T. S., and Bo¨hm, E.: Advection of upwelled waters in the form of plumes off
2287 Oman during the Southwest Monsoon, Deep-Sea Res. II, 45, 2027–2052, https://doi.org/10.1016/S0967-0645(98)00062-9,
2288 1998.

2289 Marra, J., Dickey, T. D., Ho, C., Kinkade, C. S., Sigurdson, D. E., Weller, R., and Barber, R.T.: Variability in primary
2290 production as observed from moored observations in the central Arabian Sea in 1995, Deep-Sea Res., 45, 2253-2267,
2291 https://doi.org/10.1016/S0967-0645(98)00070-8, 1998.

2292 McCosker, E., Davies, C.L. & Beckley, L.E.: Oceanographic influence on coastal zooplankton assemblages at three IMOS
2293 National Reference Stations in Western Australia. Mar. Freshw. Res. 71(12), 1672-1685
2294 https://doi.org/10.1071/MF19397, 2020.

2295 McCreary, J. P. Jr., Kundu, P. K., and Molinari, R. L.: A numerical investigation of dynamics, thermodynamics and mixed
2296 layer processes in the Indian Ocean, Prog. Oceanogr. , 31, 181–244, https://doi.org/10.1016/0079-6611(93)90002-U,
2297 1993.

2298 McCreary, J. P., Kohler, K. E., Hood, R. R., and Olson, D. B.: A four-component ecosystem model of biological activity
2299 in the Arabian Sea, Prog. Oceanogr. , 37(3-4), 193–240, https://doi.org/10.1016/S0079-6611(96)00005-5, 1996a.

2300 McCreary, J. P., Han, W., Shankar, D., and Shetye, S. R.: Dynamics of the East India Coastal Current 2. Numerical
2301 solutions, J. Geophys. Res., 101, 13993–14010, doi:10.1029/96jc00560, 1996b.

2302 McCreary, J. P., and Kundu, P. K.: A numerical investigation of the Somali Current during the Southwest Monsoon, J.
2303 Mar. Res, 46, 25–58, https://doi.org/10.1357/002224088785113711, 1988.

2304 McCreary, J.P., Yu, Z., Hood, R.R., Vinayachandran, P.N., Furue, R., Ishida, A., and Richards, K.J.:Dynamics of the
2305 Indian-Ocean oxygen minimum zones, Prog. Oceanogr. 112–113, 15–37, doi:10.1016/j.pocean.2013.03.002, 2013.

2306 McKinnon, A., and Duggan, S.: Summer egg production rates of paracalanid copepods in subtropical waters adjacent to
2307 Australia's North West Cape, Hydrobiologia, 453(1), 121-132, doi:10.1023/A:1013115900841, 2001.

2308 McKinnon, A., and Duggan, S.: Summer copepod production in subtropical waters adjacent to Australia's North West
2309 Cape, Mar. Biol, 143(5), 897-907, doi:10.1007/s00227-003-1153-1, 2003.

2310 McPhaden, M. J. and Nagura, M.: Indian Ocean Dipole interpreted in terms of Recharge Oscillator theory, *Clim. Dyn.*, **42**,
2311 1569– 1586, doi:10.1007/s00382-013-1765-1, 2014.

2312 Menaché, M.: Première campagne océanographique du "Commandant Robert Giraud" dans le canal de Mozambique, 11
2313 Octobre - 28 Novembre 1957. Cah. Océanogr., 15, 4, 224-35, 1963.

2314 Messie, M., Ledesma, J., Kolber, D., Michisaki, R., Foley, D., and Chavez, F. : Potential new production estimates in four
2315 eastern boundary upwelling ecosystems, Prog. Oceanogr. , 83, 151-158, https://doi.org/10.1016/j.pocean.2009.07.018,
2316 2009.

2317 Messie, M., and Chavez, F. : Seasonal regulation of primary production in eastern boundary upwelling systems, *Prog.*
2318 *Oceanogr.* , 134, 1-18, https://doi.org/10.1016/j.pocean.2014.10.011, 2015.

2319 Meyer, A. A., Lutjeharms, J. R. E., de Villiers, S.: The nutrient characteristics of the Natal Bight, South Africa, J. Mar.
2320 Syst., 35, 11–37, https://doi.org/10.1016/S0924-7963(02)00043-X, 2002.

2321 Miller, A.R., and Risebrough, R. W.: Preliminary cruise report ATLANTIS II, Cruise 8: International Indian Ocean
2322 Expedition, 5 July 1963 – 20 December 1963, Woods Hole Oceanographic Institution, Woods Hole, Massachusetts,
2323 USA, 32 pp, doi:10.1575/1912/5872, 1963.

2324 Moffett, J. and Goepfert, T. and Naqvi, S. W. A.: Reduced iron associated with secondary nitrite maxima in the Arabian
2325 Sea. Deep-Sea Res. Part I: Oceanographic Research Papers, 54, 1341-1349, 10.1016/j.dsr.2007.04.004., 2007.

2326 Montecino, V., and Lange, C. B.: The Humboldt Current System: Ecosystem components and processes, fisheries, and
2327 sediment studies, Prog. Oceanogr., 83 , 65–79, doi:10.1016/j.pocean.2009.07.041, 2009.

2328 Moore, T. S., Matear, R. J., Marra, J., and Clementson, L.: Phytoplankton variability off the Western Australian Coast:
2329 Mesoscale eddies and their role in cross-shelf exchange, Deep Sea Res. Part II: Top. Stud. Oceanogr., 54(8), 943-960,
2330 doi:10.1016/j.dsr2.2007.02.006, 2007.

2331 Morrison, J. M., Codispoti, L. A., Gaurin, S., Jones, B., Manghnani, V., and Zheng, Z.: Seasonal variation of hydrographic
2332 and nutrient fields during the US JGOFS Arabian Sea Process Study, *Deep-Sea Res. Part II: Trop. Stud. Oceanogr.*,
2333 *45*(10–11), 2053–2101. https://doi.org/10.1016/S0967-0645(98)00063-0, 1998

2334 Muhling, B. A., Beckley, L. E., and Olivar, M. P.: Ichthyoplankton assemblage structure in two meso-scale Leeuwin
2335 Current eddies, eastern Indian Ocean, Deep Sea Res. Part II: Top. Stud. Oceanogr., 54(8), 1113-1128,
2336 doi:10.1016/j.dsr2.2006.05.045, 2007.

2337 Muhling, B. A., and Beckley, L .E.: Seasonal variation in horizontal and vertical structure of larval fish assemblages off
2338 south-western Australia, with implications for larval transport, J. Plankton Res., 29(11), 967-983,
2339 doi:10.1093/plankt/fbm072, 2007.

2340 Muhling, B. A., Beckley, L. E., Gaughan, D., Jones, C., Miskiewicz, A., and Hesp, S.: Spawning, larval abundance and
2341 growth rate of Sardinops sagax off southwestern Australia: influence of an anomalous eastern boundary current, Mar.
2342 Ecol. Prog. Ser., 364, 157-167, doi:10.3354/meps07480, 2008a.

2343 Muhling, B. A., Beckley, L. E., Koslow, J. A., and Pearce, A. F.: Larval fish assemblages and water mass structure off the
2344 oligotrophic south-western Australian coast, Fish. Oceanogr., 17(1), 16-31, doi:10.1111/j.1365-2419.2007.00452.x,
2345 2008b.

2346 Mukherjee, A., Shankar, D., Fernando, V., Amol, P., Aparna, S. G., Fernandes, R., Michael, G. S., Khalap, S. T.,
2347 Satelkar, N. P., Agarvadekar, Y., Gaonkar, M. G., Tari, A. P., Kankonkar, A. and Vernekar, S.: Observed seasonal and
2348 intraseasonal variability of the East India Coastal Current on the continental slope, J. Earth Syst. Sci., 123, 1197–1232,
2349 doi:10.1007/s12040-014-0471-7, 2014.

2350 Mukherjee, A., Shankar, D., Chatterjee, A., and Vinayachandran, P. N.: Numerical simulation of the observed near-
2351 surface East India Coastal Current on the continental slope, Clim. Dyn., 50, 3949–3980,
2352 doi:https://doi.org/10.1007/s00382-017-3856-x, 2017.

2353 Mukherjee, A. and Kalita, B. K: Signature of La Ni˜na in interannual variations of the East India Coastal Current during
2354 spring, Clim. Dyn., 53, 551–568, doi: 10.1007/s00382-018-4601-9, 2019.

2355 Mukherjee, A., Chatterjee, A., and Francis, P.A.: Role of Andaman and Nicobar Islands in eddy formation along western
2356 boundary of the Bay of Bengal, Nature Sci. Rep., 9, 10152, doi:10.1038/s41598-019-46542-9, 2019.

2357 Mukhopadhyay, S., Shankar, D., Aparna, S. G. , Mukherjee, A.: Observations of the sub-inertial, near-surface East India
2358 Coastal Current, Cont. Shelf Res., 148, 159 – 177, doi: doi.org/10.1016/j.csr.2017.08.020, 2017.

2359 Mukhopadhyay, S., Shankar, D., Aparna, S. G., Mukherjee, A., Fernando, V., Kankonkar, A., Khalap, S., Satelkar, N.,
2360 Gaonkar, M. G., Tari, A. P., Khedekar, R. and Ghatkar, S.: Observed variability of the East India Coastal Current on the
2361 continental slope during 2009–2018, J. Earth Syst. Sci., 129, 77, doi:10.1007/s12040-020-1346-8, 2020.

2362 Mulholland, M. R., and Capone, D. G.: Dinitrogen fixation in the Indian Ocean, Indian Ocean Biogeochem, Process,
2363 Ecol. Var., 167–186, doi: 10.1029/2009GM000850, 2009.

2364 Murgese, D. S., and De Deckker, P.: The distribution of deep-sea benthic foraminifera in core tops from the eastern Indian
2365 Ocean, Mar. Micropaleontol., 56, 25-49, doi:10.1016/j.marmicro.2005.03.005, 2005.

2366 Murthy, A. V. S.: Observations of coastal upwelling around India, In J.Lighthill and R.P.Pearse (Ed.) Monsoon dynamics,
2367 Cambridge University Press, 523-528, 1981.

2368 Murty, B. C.: On the temperature and salinity structure of the Bay of Bengal, Curr. Sci., 27(7), 249-249, 1958.

2369 Murty, C.S. and Varadachari, V.V.R.: Upwelling along the east coast of India, B. Natl. Inst. Sci. India, 38, 80–86, 1968.

2370 Mwaluma, J.: Zooplankton species distribution and abundance during the monsoons off the Kenyan coast, 1992. In: Heip
2371 C.H.R., Hemminga, M.A., and de Bie, M.J.M. (Eds), Monsoons and Coastal Ecosystems in Kenya. Cruise reports
2372 Netherlands Indian Ocean Programme, 5, National Museum of Natural History, Leiden, Netherlands, 113–115, 1995.

2373 Naqvi, S.: Geographical extent of denitrification in the Arabian Sea in relation to some physical processes, Oceanologica
2374 Acta, 14 , 281–290, url: http://drs.nio.org/drs/handle/2264/3222, 1991.

2375 Naqvi, S., Jayakumar, D., Narvekar, P., Naik, H., Sarma, V., D'souza, W., Joseph, S. and George, M.: Increased marine
2376 production of N_2O due to intensifying anoxia on the Indian continental shelf, Nature, 408, 346–349,
2377 https://doi.org/10.1038/35042551, 2000.

2378 Naqvi, S. W. A., Naik, H., and NarvekarP. V.: The Arabian Sea, in: Biogeochemistry of Marine Systems, edited by:
2379 Black, K. and Shimmield, G., Sheffield Academic Press, Sheffield, 156– 206, 2003.

2380 Naqvi, S. W. A, Bange, H. W., Gibb, S. W., Goyet, C., Hatton, A. D. and Upstill-Goddard, R. C.: Biogeochemical ocean-
2381 atmosphere transfers in the Arabian Sea, *Prog. Oceanogr.*, *65*(2-4 SPEC. ISS.), 116–144,
2382 https://doi.org/10.1016/j.pocean.2005.03.005, 2005.

2383 Naqvi, S. W. A., Naik, H., Jayakumar, D. A., Shailaja, M. S. and NarvekarP. V.: Seasonal oxygen deficiency over the
2384 western continental shelf of India, in: Past and Present Water Column Anoxia, edited by: Neretin, L. N., NATO Science
2385 Series, IV. Earth and Environmental Sciences, 64, Springer, Dordrecht. https://doi.org/10.1007/1-4020-4297-3_08, 2006.

2386 Naqvi, S. W. A., Naik,H., Jayakumar, D. A., Pratihary, A., Narvenkar, G., Kurian, S., Agnihotri, R., Shailaja, M. S. and
2387 Narvekar, P. V.: Seasonal anoxia over the western Indian continental shelf, in: Indian Ocean: Biogeochemical Processes
2388 and Ecological Variability, edited by: Wiggert, J. D., Hood, R. R., Naqvi, S. W. A., Brink, K. H., and Smith, S. L.,
2389 *Geophys. Monogr. Ser.*, 185, AGU, Washington, D.C., 333–345, 2009.

2390 Naqvi, S. W. A., Bange, H. W., Farías, L., Monteiro, P. M. S., Scranton, M. I., and Zhang, J.: Marine hypoxia/anoxia as a
2391 source of CH_4 and N_2O, *Biogeosciences*, *7*(7), 2159–2190, https://doi.org/10.5194/bg-7-2159-2010 , 2010.

2392 Naulita, Y., Arhatin, R. E. and Nabil: Upwelling index along the south coast of Java from satellite imagery of wind stress
2393 and sea surface temperature, IOP Conf. Series, Earth Environ. Sci., 429, 012025, doi:10.1088/1755-1315/429/1/012025,
2394 2020.

2395 Nehring, D. ed., : The oceanological conditions in the western part of the Mozambique Channel in February-March 1980 ,
2396 Geodät. geophys. Veröffentl., 4, 163 pp, 1984.

2397 Nehring, D., E. Hagen, A. Jorge da Silva, R. Schemainda, G. Wolf, N. Michelchen, W. Kaiser, L. Postel, F. Gosselck, U.
2398 Brenning, E. Kühner, G. Arlt, H. Siegel, L. Gohs and G. Bublitz, : Results of oceanological studies in the Mozambique
2399 Channel in February – March 1980, Beitr. Meereskd., 56, 51-63, 1987.

2400 Newell, B. S.: The hydrography of the British East African Coastal Waters. London, East African Marine Fisheries
2401 Research Organisation., Fishery Publications, 12, 23p, 1959.

2402 Nguli, M. M.: Temperature, salinity and water mass structure along the Kenyan coast during the 1992 cruises A1 and A2
2403 of R.V. Tyro. In: Heip C.H.R., Hemminga, M.A., and de Bie, M.J.M. (Eds), Monsoons and Coastal Ecosystems in Kenya,
2404 Cruise reports Netherlands Indian Ocean Programme, 5, National Museum of Natural History, Leiden, Netherlands, 71-
2405 80, 1995.

2406 Noyon, M., Morris, T., Walker, D., and Huggett, J.: Plankton distribution within a young cyclonic eddy off south-western
2407 Madagascar, Deep-Sea Res. Part II, 166, 141–150, doi:10.1016/j.dsr2.2018.11.001, 2019.

2408 Nuncio, M., and Kumar, S. P.: Life cycle of eddies along the western boundary of the Bay of Bengal and their
2409 implications, J. Marine. Syst., 94, 9–17, doi:10.1016/j.jmarsys.2011.10.002, 2012.

2410 Nyadjro, E. S., Jensen, T. G., Richman, J. G., and Shriver, J. F.:On the relationship between wind, SST and the
2411 thermocline in the Seychelles-Chagos Thermocline Ridge, IEEE Geoscience and Remote Sensing Letters, 14(12),2315–
2412 2319,_ https://doi.org/10.1109/LGRS.2017.2762961, 2017.

2413 Ockhuis, S., Huggett, J.A., Gouws, G., and Sparks, C.: The 'suitcase hypothesis': Can entrainment of meroplankton by
2414 eddies provide a pathway for gene flow between Madagascar and KwaZulu-Natal, South Africa? Afr. J. Mar. Sci., 39, 4,
2415 435-451, doi:10.2989/1814232X.2017.1399292, 2017.

2416 Ogata, T. and Masumoto, Y.: Interactions between mesoscale eddy variability and Indian Ocean dipole events in the
2417 Southeastern tropical Indian Ocean—case studies for 1994 and 1997/1998, Ocean Dyn., 60, 717–730,
2418 doi:10.1007/s10236-010-0304-4, 2010.

2419 Ogata, T. and Masumoto, Y.:, Interannual modulation and its dynamics of the mesoscale eddy variability in the
2420 southeastern tropical Indian Ocean, J. Geophys. Res., 116, C05005, doi:10.1029/2010JC006490, 2011.

2421 Olsen, E., Padera, M., Funke, M., Pires, P., Wenneck, T., and Zacarias, L.: Cruise Reports Dr Fridtjof Nansen, Survey of
2422 the living marine resources of North Mozambique (SWIOFP/ASCLME 2009 Cruise 1) 6 August–20 August 2009, Report
2423 No. EAF-N/2009/7, Institute of Marine Research, Bergen, Norway, 2009.

2424 Painter, S.C.: The biogeochemistry and oceanography of the East African Coastal Current. Prog. Oceanogr. , 186, 102374,
2425 doi:10.1016/j.pocean.2020.102374, 2020.

2426 Panikkar, N. K., and Jayaraman R.: Biological and oceanographic differences between the Arabian Sea and the Bay of
2427 Bengal as observed from the Indian region, *Proceedings of the Indian Academy of Sciences*, 64 B, 231-
2428 240, https://doi.org/10.1007/BF03052161,1966.

2429 Pankajakshan, T., Pattanaik, J., and Ghosh, A. K.: An atlas of upwelling indices along east and west coast of India, IODC,
2430 NIO of India, 1997.

2431 Parameswaran, U. V., Abdul Jaleel, K. U., Sanjeevan, V. N., Gopal, A., Vijayan, A. K., Gupta, G. V. M., and Sudhakar,
2432 M.: Diversity and distribution of echinoderms in the South Eastern Arabian Sea shelf under the influence of seasonal
2433 hypoxia, *Prog. Oceanogr.*, *165*, 189–204, https://doi.org/10.1016/j.pocean.2018.06.005, 2018.

2434 Parvathi, V., Suresh, I., Lengaigne, M., Ethe, C., Vialard, J., Levy, M., Neetu, S., Aumont, O., Resplandy, L., Naik, H.,
2435 and Naqvi, S.W.A.: Positive Indian Ocean dipole events prevent anoxia off the west coast of India, Biogeosciences, 14
2436 (6), 1541–1559, doi:10.5194/bg-14-1541-2017, 2017.

2437 Paterson, H. L., Feng, M., Waite, A. M., Gomis, D., Beckley L. E., Holliday, D., and Thompson, P. A.: Physical and
2438 chemical signatures of a developing anti-cyclonic eddy in the Leeuwin Current, Eastern Indian Ocean, J. Geophys. Res.,
2439 113, C07049:1-14, doi:10.1029/2007JC004707, 2008.

2440 Pauly, D., and Christensen, V.: Primary production required to sustain global fisheries, *Nature*, 374**,** 255–257,
2441 https://doi.org/10.1038/374255a0, 1995.

2442 Pearce, A. F., and Pattiaratchi, C.: The Capes Current: a summer countercurrent flowing past Cape Leeuwin and Cape
2443 Naturaliste, Western Australia, Cont Shelf Res., 19(3), 401-420, doi:10.1016/S0278-4343(98)00089-2, 1999.

2444 Pearce, A. F.: Eastern boundary currents of the southern hemisphere., J. R. Soc. West, Aus., 74, 35-45, 1991.

2445 Pearce, A. F., Lynch, M., and Hanson, C. E.: The Hillarys Transect (1): seasonal and cross-shelf variability of physical
2446 and chemical water properties off Perth, Western Australia, 1996–98. Cont Shelf Res., 26(15), 1689-1729,
2447 doi:10.1016/j.csr.2006.05.008, 2006.

2448 Phillips, B. F., and Pearce, A. F.: Spiny lobster recruitment off Western Australia, Bull. Mar. Sci., 61(1), 21-41, 1997.

2449 Piontkovski, S. A., and Al-Oufi, H. S.: The Omani shelf hypoxia and the warming Arabian Sea Int. J. Environ. Sci., *72*(2),
2450 256-264, doi:10.1080/00207233.2015.1012361, 2015.

2451 Pivan, X., Krug, M., and Herbette, S.: Observations of the vertical and temporal evolution of a Natal Pulse along the
2452 Eastern Agulhas Bank, J. Geophys. Res. Oceans, 121, 7108– 7122, doi:10.1002/2015JC011582, 2016.

2453 Prakash, S., and Ramesh, R.: Is the Arabian Sea getting more productive?, Curr. Sci., *92*(5), 667–671, 2007.

2454 Prakash, S., Ramesh, R., Sheshshayee, M., Dwivedi, R., and Raman, M.: Quantification of new production during a winter
2455 Noctiluca scintillans bloom in the Arabian Sea, Geophys. Res. Lett., 35(8), doi:10.1029/2008GL033819, 2008.

2456 Prakash, S., Roy, R., and Lotliker, A.: Revisiting the Noctiluca scintillans paradox in northern Arabian Sea, Curr. Sci.,
2457 113(7), 1429, doi:10.18520/cs/v113/i07/1429-1434, 2017.

2458 Prasanna Kumar, S., M. Madhupratap, M. Dileep Kumar, P. M. Muraleedharan, S. N. de Souza, M. Gauns, and Sarma V.
2459 V. S. S.: High biological productivity in the central Arabian Sea during summer monsoon driven by Ekman pumping and
2460 lateral advection, Curr. Sci., 81, 1633 – 1638, 2001.

2461 Prasanna Kumar, S., Nuncio, M., Ramaiah, N., Sardesai, S., Narvekar, J., Fernandes, V., and Paul, J. T. : Eddy-
2462 mediated biological productivity in the Bay of Bengal during fall and spring intermonsoons, Deep Sea Res., Part I, 54,
2463 1619–1640, doi:10.1016/j.dsr.2007.06.002, 2007.

2464 Praveen, V., Ajayamohan, R. S., Valsala, V., and Sandeep, S.: Intensification of upwelling along Oman coast in a
2465 warming scenario, Geophys.Res. Lett.*, 43*(14), 7581-7589, https://doi.org/10.1002/2016GL069638, 2016.

2466 Pripp. T., Gammelsrød, T., and Krakstad, J. O.: Physical influence on biological production along the western shelf of
2467 Madagascar. Deep-Sea Res. II, 100, 174–183, doi:10.1016/j.dsr2.2013.10.025, 2014.

2468 Qu, T., Meyers, G. and Godfrey, J. S.: Ocean dynamics in the region between Australia and Indonesia and its influence on
2469 the variation of sea surface temperature in a global general circulation model, J. Geophys. Res., 99, 18,433-18,445,
2470 https://doi.org/10.1029/94JC00858, 1994.

2471 Qu, T. and Meyers, G.: Seasonal characteristics of circulation in the southeastern tropical Indian Ocean, J. Phys.
2472 Oceanogr., 35, 255-267, doi:10.1175/JPO-2682.1, 2005a.

2473 Qu, T. and Meyers, G.: Seasonal variation of barrier layer in the southeastern tropical Indian Ocean, J. Geophys. Res.,
2474 110, C11003, doi:10.1029/2004JC002816, 2005b.

2475 Quadfasel, D., and Schott, F.: Water mass distribution at intermediate layers off the Somali coast during the onset of the
2476 southwest monsoon 1979, J. Phys. Oceanogr., 12, 1358–1372, https://doi.org/10.1175/1520-
2477 0485(1982)012<1358:WMDAIL>2.0.CO;2, 1982.

2478 Quadfasel, D. and Cresswell, G. R.: A note on the seasonal variability of the South Java Current, J. Geophys. Res., 97,
2479 3685–3688, doi:10.1029/91JC03056, 1992.

2480 Quartly, G.D., and Srokosz, M.A.: Eddies in the southern Mozambique Channel. Deep-Sea Res. II, 51, 69–83,
2481 doi:10.1016/j.dsr2.2003.03.001, 2004.

2482 Raes, E. J., Waite, A. M., McInnes, A. S., Olsen, H., Nguyen, H. M., Hardman-Mountford, N., and Thompson, P. A.:
2483 Changes in latitude and dominant diazotrophic community alter N2 fixation, Mar. Ecol. Prog. Ser., 516, 85-102,
2484 doi:10.3354/meps11009, 2014.

2485 Raes, E. J., Thompson, P. A., McInnes, A. S., Nguyen, H. M., Hardman-Mountford, N., and Waite, A. M.: Sources of new
2486 nitrogen in the Indian Ocean, Global Biogeochem. Cycles, 29(8), 1283-1297, doi:10.1002/2015GB005194, 2015.

2487 Raes, E. J., Bodrossy, L., van de Kamp, J., Bissett, A., and Waite, A. M.: Marine bacterial richness increases towards
2488 higher latitudes in the eastern Indian Ocean, Limnol. Oceanogr. Letters, 3(1), 10-19, doi:10.1002/lol2.10058, 2018.

2489 Rahmstorf, S.: Thermohaline circulation: The current climate, Nature, 421(6924), 699–699,
2490 https://doi.org/10.1038/421699a, 2003.

2491 Raj, R.P., Peter, B.N., and Pushpadas, D.: Oceanic and atmospheric influences on the variability of phytoplankton bloom
2492 in the Southwestern Indian Ocean, J. Mar. Syst., 82, 217–229, doi:10.1016/j.jmarsys.2010.05.009, 2010.

2493 Ramamirtham, C. P., and Rao, D. S.: On upwelling along the west coast of India, J. mar. biol. Ass. India, 15 , 306–317,
2494 1973.

2495 Ramanantsoa, J.D., Krug, M, Penvend, P., Rouault, M., and Gula J.: Coastal upwelling south of Madagascar: Temporal
2496 and spatial variability, J. Mar. Syst., 178, 29-37, doi:10.1016/j.jmarsys.2017.10.005, 2018a.

2497 Ramanantsoa, J. D., Penven, P., Krug, M., Gula, J., and Rouault, M.: Uncovering a new current: The Southwest
2498 MAdagascar Coastal Current. Geophys. Res. Lett., 45, https://doi.org/10.1002/2017GL075900, 2018b.

2499 Rao, R. R., and Sivakumar, R.: On the possible mechanisms of the evolution of a mini-warm pool during the pre-summer
2500 monsoon season and the genesis of onset vortex in the South-Eastern Arabian Sea, Q. J. R. Meteorol. Soc., 125 , 787–809,
2501 doi:10.1002/qj.49712555503, 1999.

2502 Rao, R. R., Girish Kumar, M. S., Ravichandran, M., Rao, A. R., Gopalakrishna, V. V., and Thadathil, P.: Interannual
2503 variability of Kelvin wave propagation in the wave guides of the equatorial Indian Ocean, the coastal Bay of Bengal and
2504 the southeastern Arabian Sea during 1993–2006, Deep-Sea Res., Part-I., 57,1–13, doi:10.1016/j.dsr.2009.10.008, 2009.

2505 Rao, T. V. N., Rao, D. P., Rao, B. P., and Raju, V. S. R.: Upwelling and Sinking along Visakhapatnam coast, Indian J.
2506 Mar. Sci., 15:84–87, 1986.

2507 Rath, S., Vinayachandran, P. N., Behara, A., and Neema, C. P. : Dynamics of summer monsoon current around Sri Lanka,
2508 Ocean Dynamics, 69(10), 1133–1154, https://doi.org/10.1007/s10236-019-01295-x, 2019.

2509 Rennie, S. J., Pattiaratchi, C. P., and McCauley, R. D.: Eddy formation through the interaction between the Leeuwin
2510 Current, Leeuwin Undercurrent and topography, Deep Sea Res. Part II: Top. Stud. Oceanogr., 54(8), 818-836,
2511 doi:10.1016/j.dsr2.2007.02.005, 2007.

2512 Resplandy, L., Vialard, J., Lévy, M., Aumont, O., and Dandonneau, Y.: Seasonal and intraseasonal biogeochemical
2513 variability in the thermocline ridge of the southern tropical Indian Ocean, J. Geophys. Res. , 114(C7), C07024.
2514 https://doi.org/10.1029/2008JC005246, 2009.

2515 Resplandy, L., Lévy, M., Madec, G., Pous, S., Aumont, O., and Kumar, D. : Contribution of mesoscale processes to
2516 nutrient budgets in the Arabian Sea, J. Geophys. Res. , 116(C11), C11007. https://doi.org/10.1029/2011JC007006, 2011.

2517 Ridderinkhof H., and de Ruiter, W.: Moored current observations in the Mozambique Channel, Deep-Sea Res. II, 50,
2518 1933–1955, doi:10.1016/S0967-0645(03)00041-9, 2003.

2519 Risien, C.M., and C. B.: A Global Climatology of Surface Wind and Wind Stress Fields from Eight Years of QuikSCAT
2520 Scatterometer Data, J. Phys. Oceanogr., 38, 2379-2413, https://doi.org/10.1175/2008JPO3881.1, 2008.

2521 Rixen, T., Goyet, C., and Ittekkot, V.: Diatoms and their influence on the biologically mediated uptake of atmospheric
2522 CO2 in the Arabian Sea upwelling system, Biogeosciences, 3, 1–13, https://doi.org/10.5194/bg-3-1-2006, 2006.

2523 Rixen, T., Cowie, G., Gaye, B., Goes, J. I., Gomes, H., Hood, R. R., Lachkar, Z., Schmidt, H., Segschneider, J. and Singh,
2524 A.: Reviews and syntheses: Present, past, and future of the oxygen minimum zone in the northern Indian Ocean,
2525 Biogeosciences, 17, 1–30, doi:10.5194/bg-17-1-2020, 2020.

2526 Roberts, M. J. : Chokka squid (Loligo vulgaris reynaudii) abundance linked to changes in South Africa's Agulhas Bank
2527 ecosystem during spawning and the early life cycle, ICES J. Mar. Sci., 62(1), 33–55,
2528 https://doi.org/10.1016/j.icesjms.2004.10.002, 2005.

2529 Roberts, M. J., and van den Berg, M. : Currents along the Tsitsikamma Coast South Africa and potential transport of
2530 squid paralarvae and ichthyoplankton, Afr. J. Mar. Sci., 27(2), 375–388, doi:10.2989/18142320509504096, 2005.

2531 Roberts, M. J., Ribbink, A. J., Morris, T., Duncan, F., Barlow, R., Kaehler, S., Huggett, J., Kyewalyanga, M., Harding, R.,
2532 and van den Berg, M.: 2007 Western Indian Ocean Cruise and Data Report: Alg. 160. African Coelacanth Ecosystem
2533 Programme, Grahamstown, 142 pp, doi:10.13140/RG.2.2.28920.88324, 2008.

2534 Roberts, M. J. , van der Lingen, C. D., Whittle, C., and van den Berg, M.: Shelf currents, lee-trapped and transient eddies
2535 on the inshore boundary of the Agulhas Current, South Africa: their relevance to the KwaZulu-Natal sardine run, Afr. J.
2536 Mar. Sci., 32(2), 423–447, doi:10.2989/1814232x.2010.512655, 2010.

2537 Roberts, M.J., Ternon, J-F., and Morris, T.: Interaction of dipole eddies with the western continental slope of the
2538 Mozambique Channel, Deep-Sea Res. II, 100, 54–67, doi:10.1016/j.dsr2.2013.10.016, 2014.

2539 Roberts, M.: The Western Indian Ocean Upwelling Research Initiative (WIOURI): A Flagship IIOE2 Project. CLIVAR
2540 Exchanges, 19, 26-30 , http://www.researchgate.net/publication/283855749, 2015.

2541 Roberts M, Nieuwenhys C.: Observations and mechanisms of upwelling in the northern KwaZulu-Natal Bight, Afr. J.
2542 Mar. Sci., 38: sup1, S43-S63, doi: 10.2989/1814232X.2016.1194319, 2016.

2543 Roberts, M., Nieuwenhuys, C., and Guastella, L.: Circulation of shelf waters in the KwaZulu-Natal Bight, South Africa,
2544 Afr. J. Mar. Sci., 38, S7-S21, 10.2989/1814232X.2016.1175383, 2016.

2545 Robinson, A.R. (Ed.) Eddies in Marine Science. Springer-Verlag, Berlin, 1983.

2546 Robinson, J., Guillotreau, P., Jiménez-Toribio, R., Lantz, F., Nadzon, L., Dorizo, J., Gerry, C., and Marsac, F. : Impacts of
2547 climate variability on the tuna economy of Seychelles, Climate Research, 43(3), 149–162.
2548 https://doi.org/10.3354/cr00890, 2010.

2549 Rochford, D. J.: Seasonal interchange of high and low salinity surface waters off south-west Australia, CSIRO, Division
2550 of Fisheries and Oceanography Technical Paper No. 29, 1969

2551 Roel, B. A., Hewitson, J., Kerstan, S., and Hampton, I.: The role of the Agulhas Bank in the life cycle of pelagic fish, S.
2552 Afr. J. Sci 90, 185–96, 1994.

2553 Rossi, V., Feng, M., Pattiaratchi, C., Roughan, M., and Waite, A. M.: Linking synoptic forcing and local mesoscale
2554 processes with biological dynamics off Ningaloo Reef, J. Geophys. Res. Oceans, 118(3), 1211-1225,
2555 doi:10.1002/jgrc.20110, 2013a.

2556 Rossi, V., Feng, M., Pattiaratchi, C., Roughan, M., and Waite, A. M.: On the factors influencing the development of
2557 sporadic upwelling in the Leeuwin Current system, J. Geophys. Res. Oceans, 118(7), 3608-3621, doi:10.1002/jgrc.20242,
2558 2013b.

2559 Rouault, M. J., Penven, P.: New perspectives on Natal Pulses from satellite observations, J. Geophys. Res.,116, C07013,
2560 doi:10.1029/2010JC006866, 2011.W

2561 Rousseaux, C. S., Lowe, R., Feng, M., Waite, A. M., and Thompson, P. A.: The role of the Leeuwin Current and mixed
2562 layer depth on the autumn phytoplankton bloom off Ningaloo Reef, Western Australia, Cont Shelf Res., 32, 22-35,
2563 doi:10.1016/j.csr.2011.10.010, 2012.

2564 Roxy, M. K., Modi, A., Murtugudde, R., Valsala, V., Panickal, S., Prasanna Kumar, S., and Lévy, M.: A reduction in
2565 marine primary productivity driven by rapid warming over the tropical Indian Ocean, Geophys.Res. Lett*, 43*(2), 826-833,
2566 https://doi.org/10.1002/2015GL066979, 2016.

2567 Ruijter, W.D., Leeuwen,P and Lutjeharms, J.: Generation and Evolution of Natal Pulses: Solitary Meanders in the
2568 Agulhas Current, J. Phys. Oceanography, 29, 3043-3055, doi:https://doi.org/10.1175/1520-
2569 0485%281999%29029%3C3043%3AGAEONP%3E2.0.CO%3B2, 1999.

2570 Sabarros, P.S., Ménard, F., Lévénez, J.-J., Tew-Kai, E., and Ternon, J.-F.: Mesoscale eddies influence distribution and
2571 aggregation patterns of micronekton in the Mozambique Channel, Mar. Ecol. Prog. Ser. ,395, 101–107,
2572 doi:10.3354/meps08087, 2009.

2573 Sætre, R., and de Paula e Silva, .: The marine fish resources of Mozambique. Reports on surveys with the R/V Dr Fridtjof
2574 Nansen, Serviço de Investigações Pesqueiras, Maputo, Institute of Marine Research, Bergen, Norway, 179 pp, 1979.

2575 Saetre, R. and Jorge Da Silva, A.: Water masses and circulation of the Mozambique Channel. Revista de Investigacao
2576 Pesqueira, No. 3, Instituto de Desenvolvimento Pesqueiro, Maputo, 83 pp., 1982.

2577 Saji, N. H., Goswami, B. N., Vinayachandran, P. N., and Yamagata, T.: A dipole mode in the tropical Indian Ocean,
2578 Nature., 401, 360–363, doi:10.1038/43854, 1999.

2579 Sanilkumar, K. V., Kuruvilla, T. V., Jogendranath, D. and Rao, R. R: Observations of the Western Boundary Current of
2580 the Bay of Bengal from a hydrographic survey during March 1993, Deep–Sea Res. :Part I, 44, 135–145, doi:
2581 10.1016/S0967–0637(96)00036-2, 1997.

2582 Sarma, G. S.: Seasonal variation of some hydrographic properties of the shelf waters off the west coast of India, Bull. Nat.
2583 Inst. Sci. India, 38263–276, 263–276, 1968.

2584 Sarma, G. S.: Upwelling off the southwest coast of India, Indian J. Mar. Sci., 7 , 209–218,
2585 http://nopr.niscair.res.in/handle/123456789/39557, 1978.

2586 Sarma, V. V. S. S.: Net plankton community production in the Arabian Sea based on O2 mass balance model, Global
2587 biogeochem. cycles, 18(4), https://doi.org/10.1029/2003GB002198, 2004

2588 Sarma, V. V. S. S. Sridevi, B., Maneesha, K., Sridevi, T., Naidu, S. A., Prasad, V. R., Venkataraman, V., Achrya, T.,
2589 Bharati, M. D., Subbaiah, Ch.V., Kiran, B.S., Reddy, N. C. P., Sarma, V. V., Sadhuram, Y., Murty, T. V. R: Impact of
2590 atmospheric and physical forcings on biogeochemical cycling of dissolved oxygen and nutrients in the coastal Bay of
2591 Bengal, J. Oceanogr., 69(2), 229-243, Doi: 10.1007/s10872-012-0168-y, 2013.

2592 Sarma, V. V. S. S. and Udaya Bhaskar, T. V .S. : Ventilation of oxygen to oxygen minimum zone due to anticyclonic
2593 eddies in the Bay of Bengal, J. Geophys. Res. Biogeosci., 123, 2145-2153, doi: 10.1029/2018JG004447, 2018.

2594 Sarma, V. V. S. S., Desai, D. V., Patil, J. S, Khandeparker, L., Aparna, S. G., Shankar, D., Selrina D'Souza,
2595 Dalabehera, H. B., Mukherjee, J., Sudharani, P., and Anil, A. C.: Ecosystem response in temperature fronts in the
2596 northeastern Arabian Sea, Progress in Oceanography, 165, 317-331, https://doi.org/10.1016/j.pocean.2018.02.004, 2018.

2597 Sastry, A. A. R., and Myrland, P.: Distribution of temperature, salinity and density in the Arabian Sea along the South
2598 Malabar Coast (South India) during the post-monsoon season, Indian J. Fish., 6 , 223–255, 1959.

2599 Saunders, M. I., Thompson, P. A., Jeffs, A. G., Säwström, C., Sachlikidis, N., Beckley, L. E., and Waite, A. M.: Fussy
2600 feeders: phyllosoma larvae of the western rocklobster (Panulirus cygnus) demonstrate prey preference, PLoS One, 7(5),
2601 doi:10.1371/journal.pone.0036580, 2012.

2602 Saville-Kent, W.: The naturalist in Australia, 302 pp.: CRC Press, Boca Raton, Fla, doi:10.5962/bhl.title.18339, 1897.

2603 Säwström, C., Beckley, L. E., Saunders, M. I., Thompson, P. A., and Waite, A. M.: The zooplankton prey field for rock
2604 lobster phyllosoma larvae in relation to oceanographic features of the south-eastern Indian Ocean, J. Plankton Res., 36(4),
2605 1003-1016, doi:10.1093/plankt/fbu019, 2014.

2606 Saxena, H., Sahoo, D., Khan, M. A., Kumar, S., Sudheer, A. K. and Singh, A.:Dinitrogen fixation rates in the Bay of
2607 Bengal during summer monsoon, Environ. Res. Commun., 2, 051007, doi: 10.1088/2515-7620/ab89fa, 2020.

2608 Schmidt, T. M., DeLong, E. F., and Pace, N. R.: Analysis of a marine picoplankton community by 16S rRNA gene
2609 cloning and sequencing, J. Bacteriol., 173(14), 4371-4378, doi:10.1128/jb.173.14.4371-4378.1991, 1991.

2610 Schott, F.: Monsoon response of the Somali Current and associated upwelling. Prog. Oceanogr. , 12, 3, 357–381,
2611 doi:10.1016/0079-6611(83)90014-9, 1983.

2612 Schott, F., and McCreary, J. P.: The monsoon circulation of the Indian Ocean, *Prog. Oceanogr.*, 51 (1) ,1 –123,
2613 https://doi.org/10.1016/S0079-6611(01)00083-0, 2001.

2614 Schott, F. A., Xie, S. P., and McCreary, J. P.: Indian Ocean circulation and climate variability. Reviews of Geophysics, 47,
2615 1, 1–46, doi:10.1029/2007RG000245, 2009.

2616 Sen Gupta, R., Moraes, C., George, M. D., Kureishy, T. W., Noronha, R. J., and Fondekar, S. P.: Chemistry and
2617 hydrography of the Andaman Sea, Indian J. Mar. Sci. , 10,228-233, Doi: 10.1016/0198-0149(84)90035-9, 1981.

2618 SenGupta, R. and Naqvi, S.W.A.: Chemical Oceanography of the Indian Ocean, North of equator, Deep-Sea Res., 31,
2619 671-706, https://doi.org/10.1016/0198-0149(84)90035-9, 1984.

2620 Sewell, R. B. S.: The temperature and salinity of the surface-waters of the Bay of Bengal and Andaman Sea, with
2621 reference to Laccadive Sea, in Geographic and oceanographic research in Indian waters V, Mem. Asiatic Soc. of Bay of
2622 Bengal, 207-356, 1929.

2623 Shah, P., Sajeev, R., and Gopika, N.: Study of upwelling along the west coast of India - A climatological approach, J.
2624 Coast. Res., 31 , 1151–1158, doi:10.2112/JCOASTRES-D-13-00094.1, 2015.

2625 Shalapyonok, A., Olson, R. J., and Shalapyonok, L. S.: Arabian Sea phytoplankton during southwest and
2626 northeast Monsoons 1995: composition, size structure and biomass from individual cell properties measured by

2627 flow cytometry, Deep Sea Res. II Top. Stud. Oceanogr. 48, 1231–1261, https://doi.org/10.1016/S0967-0645(00)00137-5,
2628 2001.

2629 Shankar, D., Mccreary, J. P., Han, W., and Shetye, S. R. Dynamics of the East India Coastal Current 1. Analytic solutions
2630 forced by interior Ekman pumping and local alongshore winds, J. Geophys. Res., 101, 13975–13991,
2631 doi:10.1029/96jc00559, 1996.

2632 Shankar, D., and Shetye, S. R.: On the dynamics of the Lakshadweep High and Low in the southeastern Arabian Sea, J.
2633 Geophys. Res, 102 , 12551–12562, doi:10.1029/97JC00465, 1997.

2634 Shankar, D., Vinayachandran, P. N., and Unnikrishnan, A. S.: The monsoon currents in the north Indian Ocean, Prog.
2635 Oceanog., 52, doi:10.1016/s0079-6611(02)00024-1, 63–120, 2002.

2636 Shankar, D., Remya, R., Anil, A., and Vijith, V.: Role of physical processes in determining the nature of fisheries in the
2637 eastern Arabian Sea, Prog. Oceanogr., 172 , 124–158, doi:10.1016/j.pocean.2018.11.006, 2019.

2638 Shenoi, S. S. C., P. K. Saji and A. M. Almeida: Near-surface circulation and kinetic energy in the tropical Indian Ocean
2639 derived from Lagdrangian drifters; J. Mar. Res. 57 885–907, doi:doi.org/ 10.1357/002224099321514088, 1999.

2640 Shenoi, S. S. C. , Shankar, D, and Shetye, S. R.: Differences in heat budgets of the near-surface Arabian Sea and Bay of
2641 Bengal: Implications for the summer monsoon, J. Geophys. Res., 107(C6), 3052. https://doi.org/10.1029/2000JC000679,
2642 2002.

2643 Shenoi, S. C., Shankar, D., Gopalakrishna, V. V., and Durand, F.: Role of ocean in the genesis and annihilation of the core
2644 of the warm pool in the southeastern Arabian Sea, Mausam, 56 , 147–160, 2005.

2645 Shenoy, D.M., Sujith, K.B., Gauns, M.U., Patil, S., Sarkar, A., Naik, H., Narvekar, P.V., and Naqvi, S.W.A.: Production
2646 of dimethylsulphide during the seasonal anoxia off Goa, Biogeochemistry, 110(1-3):47-55, doi:10.1007/s10533-012-9720-
2647 5, 2012.

2648 Shetye, S. R., Chandra Shenoi, S. S., Antony, M. K., and Kumar, V. K.: Monthly-mean wind stress along the coast of the
2649 north Indian Ocean, Proceedings of the Indian Academy of Sciences - Earth and Planetary Sciences, 94 , 129–137,
2650 doi:10.1007/BF02871945, 1985.

2651 Shetye, S. R., Gouveia, A. D., Shenoi, S. S. C., Sundar, D., Michael, G. S., Almeida, A. M., and Santanam, K.:
2652 Hydrography and circulation off the west coast of India during the southwest monsoon 1987, J. Mar. Res., 48 , 359–378,
2653 doi:10.1357/002224090784988809, 1990.

2654 Shetye, S. R., Shenoi, S. S. C., Gouveia, A. D., Michael, G. S., Sundar, D., and Nampoothiri, G.: Wind-driven coastal
2655 upwelling along the western boundary of the Bay of Bengal during the southwest monsoon, Cont. Shelf Res., 11, 1397-
2656 1408, Doi: 10.1016/0278-4343(91)90042-5, 1991.

2657 Shetye, S.R., Gouveia, A.D., Shenoi, S.S.C., Sundar, D., Michael, G.S., and Nampoothiri, G.: The western boundary
2658 current of the seasonal subtropical gyre in the Bay of Bengal, J. Geophys. Res., 98, 945–954,
2659 doi:10.1029/92jc02070,1993.

2660 Shetye, S.R., Gouveia, A.D., Shankar, D., Shenoi, S.S.C., Vinayachandran, P.N., Sundar, D., Michael, G.S., and
2661 Nampoothiri, G.: Hydrography and circulation in the western Bay of Bengal during the northeast monsoon, J. Geophys.
2662 Res., 101, 14011–14025, doi:10.1029/95jc03307, 1996.

2663 Shetye, S. R., and Gouveia, A. D.: Coastal circulation in the North Indian Ocean: Coastal segment (14, S-W). In:
2664 Robinson, A.R., Brink, K.H. (Eds.), The Global Coastal Ocean: Regional Studies and Syntheses, The Sea, vol. 11. John
2665 Wiley and Sons, New York, pp. 523–555 (Chapter 18), 1998.

2666 Shi, W., Morrison, J. M., Bo¨hm, E., and Manghnani, V.: The Oman upwelling zone during 1993, 1994 and 1995, Deep-
2667 Sea Res. II, 47, 1227–1247, http://dx.doi.org/10.1016/S0967-0645(99)00142-3, 2000.

2668 Sikka, D.R.: Some aspects of the large scale fluctuations of summer monsoon rainfall over India in relation to fluctuations
2669 in the planetary and regional scale circulation parameters, *Proc. Indian Acad. Sci. (Earth Planet Sci.),* 89**,** 179–195 ,
2670 https://doi.org/10.1007/BF02913749, 1980.

2671 Singh, A., Gandhi, N., Ramesh, R. and Prakash, S.: Role of cyclonic eddy in enhancing primary and new production in the
2672 Bay of Bengal, J. Sea Res., 97, 5-13, Doi: 10.1016/j.seares.2014.12.002, 2015.

2673 Singh, A., Gandhi, N., and Ramesh, R.: Surplus supply of bioavailable nitrogen through N_2 fixation to primary producers
2674 in the eastern Arabian Sea during autumn, Cont. Shelf. Res., 181, 103–110, doi:10.1016/j.csr.2019.05.012, 2019.

2675 Smith, R. L., and Bottero, J. S.: On upwelling in the Arabian Sea. In M. Angel (Ed.), A voyage of discovery, 291–304.
2676 New York: Pergamon Press., 1977.

2677 Smith, S.L., and Codispoti, L.: Southwest Monsoon of 1979: Chemical and biological response of Somali coastal waters,
2678 Science, 209, 597-600, doi: 10.1126/science.209.4456.597, 1980.

2679 Smith, R. L., Huyer, A., Godfrey, J. S., and Church, J. A.: The Leeuwin Current off western Australia, 1986–1987, J.
2680 Phys. Oceanogr., 21(2), 323-345, https://doi.org/10.1175/1520-0485(1991)021<0323:TLCOWA>2.0.CO;2, 1991.

2681 Smitha, B. R., Sanjeevan, V. N., Vimalkumar, K. G., and Revichandran, C.: On the Upwelling off the southern tip and
2682 along the west coast of India, J. Coast. Res., 95–102, doi:10.2112/06-0779.1, 2008.

2683 Sprintall, J., Chong, J., Syamsudin, F., Morawitz, W., Hautala, S., Bray, N., and Wijffels, S.: Dynamics of the South Java
2684 Current in the Indo-Australian basin, Geophys. Res. Lett., 26, 2493–2496, doi:10.1029/1999GL002320, 1999.

2685 Sreeush, M. G., Valsala, V., Pentakota, S., Prasad, K. V. S. R., and Murtugudde, R.: Biological production in the Indian
2686 Ocean upwelling zones – Part 1: refined estimation via the use of a variable compensation depth in ocean carbon models,
2687 Biogeosciences, 15, 1895-1918, doi:10.5194/bg-15-1895-2018, 2018.

2688 Srokosz, M. A., and Quartly, G. D.: The Madagascar Bloom: A serendipitous study, J. Geophys. Res. Oceans, 118, 14–25,
2689 doi:10.1029/2012JC008339, 2013.

2690 Strzelecki, J., and Koslow, J.: Mesoplankton, In Strategic Research Fund for the Marine Environment Final Report (Vol.
2691 2), 88-102, CSIRO Australia, 2006.

2692 Strzelecki, J., Koslow, J. A., and Waite, A.: Comparison of mesozooplankton communities from a pair of warm- and cold-
2693 core eddies off the coast of Western Australia, Deep Sea Res. Part II: Top. Stud. Oceanogr., 54(8), 1103-1112,
2694 doi:10.1016/j.dsr2.2007.02.004, 2007.

2695 Sudheesh, V., Gupta, G.V.M., Sudharma, K., Naik, H., Shenoy, D., Sudhakar, M., and Naqvi, S.: Upwelling intensity
2696 modulates N_2O concentrations over the western Indian shelf, J. Geophys. Res. Oceans, 121, 8551–8565,
2697 doi:10.1002/2016JC012166, 2016.

2698 Sudheesh, V.: Influence of Upwelling on Seasonal Hypoxia/Anoxia and Greenhouse Gases along the Southwestern
2699 Continental Shelf of India, Ph.D Thesis, Cochin University of Science and Technology, Cochin,
2700 http://hdl.handle.net/10603/256272 , 2018.

2701 Sudheesh, V., Gupta, G. V. M., and Naqvi, S. W. A.: Massive Methane Loss During Seasonal Hypoxia/Anoxia in the
2702 Nearshore Waters of Southeastern Arabian Sea, *Front. Mar. Sci.*, *7*. https://doi.org/10.3389/fmars.2020.00324, 2020.

2703 Suginohara, N.: Coastal upwelling: Onshore-offshore circulation, equatorward coastal jet and poleward undercurrent over
2704 a continental shelf-slope, J. Phys. Oceanogr., 12, 272–284,1982.

2705 Suresh, I., Vialard, J., Lengaigne, M., Han, W., McCreary, J., Durand, F., & Muraleedharan, P. M.: Origins of wind-
2706 driven intraseasonal sea level variations in the North Indian Ocean coastal waveguide, Geophys. Res.
2707 Lett., 40, 5740– 5744. https://doi.org/10.1002/2013GL058312, 2013.

2708 Susanto, R. D., Gordon, A. L., and Zheng, Q.: Upwelling along the coasts of Java and Sumatra and its relation to ENSO,
2709 Geophys. Res. Lett., 28, 1599-1602, doi:10.1029/2000GL011844, 2001.

2710 Susanto, R. D., and Marra, J.: Effect of the 1997/98 El Nino on chlorophyll a variability along the southern coasts of Java
2711 and Sumatra, Oceanography, 18(4), 124-127, doi:10.5670/oceanog.2005.13, 2005.

2712 Sutton, A. L., and Beckley, L. E.: Influence of the Leeuwin Current on the epipelagic euphausiid assemblages of the
2713 south-east Indian Ocean, Hydrobiologia, 779(1), 193-207, doi:10.1007/s10750-016-2814-7, 2016.

2714 Sverdrup, H. U.: On the evaporation from the oceans, J. Mar. Res. 1, 3-14, 1937.

2715 Swallow, J. C., and Bruce, J. C.: Current measurements off the Somali coast during the southwest monsoon of 1964,
2716 Deep-Sea Res., 13, 861–888, https://doi.org/10.1016/0011-7471(76)90908-6, 1966.

2717 Swart, V. P., Largier, J. L.: Thermal structure of Agulhas Bank water, South Afr. J. Mar. Sci., 5:1, 243-252, doi:
2718 10.2989/025776187784522153, 1987.

2719 Takahashi, T., Sutherland, S. C.,Chipman, D. W.,Goddard, J. G., Ho, C., Newberger, T., Sweeney, C., and Munro, D. R.:
2720 Climatological distributions of pH, pCO_2, total CO_2, alkalinity, and $CaCO_3$ saturation in the global surface ocean, and
2721 temporal changes at selected locations, Mar. Chem.,164:95-125, https://doi.org/10.1016/j.marchem.2014.06.004, 2014.

2722 Taylor, J., and Pearce, A.: Ningaloo Reef currents: Implications for coral spawn dispersal, zooplankton and whale shark
2723 abundance, J. R. Soc. West Aus, 82(2), 57-65, 1999.

2724 Ternon, J.-F., Bach, P., Barlow, R., Huggett, J., Jaquemet, S., Marsac, F., Menard, F., Penven, P., Potier, M., and Roberts,
2725 M.: The Mozambique Channel: from physics to upper trophic levels, Deep-Sea Res. II 100, 1–9,
2726 doi:10.1016/j.dsr2.2013.10.012, 2014.

2727 Tew-Kai, E., and Marsac, F.: Patterns of variability of sea surface chlorophyll in the Mozambique Channel: A quantitative
2728 approach, J. Mar. Syst., 77, 77–88, doi:10.1016/j.jmarsys.2008.11.007, 2009.

2729 Tew Kai, E., and Marsac, F.: Influence of mesoscale eddies on spatial structuring of top predators' communities in the
2730 Mozambique Channel, Prog. Oceanogr 86, 214–223, doi:10.1016/j.pocean.2010.04.010, 2010.

2731 Thompson, R. O.R.Y., and Veronis, G.: Poleward boundary current off Western Australia, Mar. Freshw. Res., 34(1), 173-
2732 185, doi:10.1071/MF9830173, 1983 .

2733 Thompson, R. O.R.Y.: Observations of the Leeuwin Current off Western Australia, J. Phys. Oceanogr., 14(3), 623-628,
2734 doi:10.1175/1520-0485(1984)014<0623:ootlco>2.0.co;2, 1984.

2735 Thompson, R.O.R.Y.: Continental-shelf-scale model of the Leeuwin Current, J. Mar. Res., 45(4), 813-827,
2736 doi:10.1357/002224087788327190, 1987.

2737 Thompson, P., Wild-Allen, K., Lourey, M., Rousseaux, C., Waite, A., Feng, M., and Beckley, L. E.: Nutrients in an
2738 oligotrophic boundary current: evidence of a new role for the Leeuwin Current, Prog. Oceanogr., 91(4), 345-359,
2739 doi:10.1016/j.pocean.2011.02.011, 2011.

2740 Thushara,V. and Vinayachandran, P. N. : Formation of summer phytoplankton bloom in the northwestern Bay of Bengal
2741 in a coupled physical-ecosystem model, J. Geophys. Res. Oceans, 121 (12), 8535-8550, Doi: 10.1002/2016JC011987,
2742 2016.

2743 Thushara, V., Vinayachandran, P. N., Matthews, A. J., Webber, B. G. M., and Queste, B. Y. : Vertical distribution of
2744 chlorophyll in dynamically distinct regions of the southern Bay of Bengal, Biogeosciences, 16(7), 1447–1468,
2745 https://doi.org/10.5194/bg-16-1447-2019, 2019.

2746 Thushara V., and Vinayachandran, P. N. : Unprecedented Surface Chlorophyll Blooms in the Southeastern Arabian Sea
2747 During an Extreme Negative Indian Ocean Dipole, Geophys. Res. Lett. https://doi.org/10.1029/2019GL085026, 2020.

2748 Tomczak, M., and Godfrey, J.S.: Regional Oceanography: An Introduction. Pergamon Press, Oxford, 1994.

2749 Tranter, D.J. and Newell, B. S.: Enrichment experiments in the Indian Ocean, Deep-Sea Res. Oceanogr. Abstr., 10(1-2), 1-
2750 9, doi:10.1016/0011-7471(63)90173-6, 1962.

2751 Tranter, D. J. and Kerr, J.D. : Seasonal variations in the Indian Ocean along 110°E. V. Zooplankton biomass, Mar.
2752 Freshw. Res. **20**, 77-84, 1969.

2753 Tranter, D.J. and Kerr, J.D. : Further studies of plankton ecosystems in the eastern Indian Ocean. III. Numerical
2754 abundance and biomass, Mar. Freshw. Res., **28**, 557-583, 1977.

2755 Tripathi, N., Sahu, L. K., Singh, A., Yadav, R., and Karati, K. K.: High levels of isoprene in the marine boundary layer of
2756 Arabian Sea during spring inter-monsoon: Role of phytoplankton bloom, ACS Earth and Space Chemistry,
2757 doi:10.1021/acsearthspacechem.9b00325, 2020a.

2758 Tripathi, N., Sahu, L. K., Singh, A., Yadav, R., Patel, A., Patel, K., andMeenu, P.: Elevated levels of biogenic non-
2759 methane hydrocarbons in the marine boundary layer of the Arabian Sea during the inter-monsoon, J. Geophys. Res.
2760 Atmos., https://doi.org/10.1029/2020JD032869, 2020b.

2761 Tsugawa, M., and Hasumi, H.: Generation and growth mechanism of the Natal pulse. J. Phys. Oceanogr., 40, 1597–1612,
2762 doi:10.1175/2010JPO4347.1, 2010.

2763 Turpie J. K, Beckley, L. E., Katua, S. M.: Biogeography and the selection of priority areas for the conservation of South
2764 African coastal fishes, Biol. Conserv. 92, 59–72, https://doi.org/10.1016/S0006-3207(99)00063-4, 2000.

2765 Twomey, L. J., Waite, A. M., Pez, V., and Pattiaratchi, C. B.: Variability in nitrogen uptake and fixation in the
2766 oligotrophic waters off the south west coast of Australia, Deep Sea Res. Part II: Top. Stud. Oceanogr., 54(8), 925-942.
2767 doi:10.1016/j.dsr2.2006.10.001, 2007

2768 Valsala, V. and Maksyutov, S.: A short surface pathway of the subsurface Indonesian throughflow water from the Java
2769 coast associated with upwelling, Ekman transport, and subduction, Int. J. Oceanogr., 540783, 1-15,
2770 doi:10.1155/2010/540783, 2010.

2771 Van Leeuwen, P. J., de Ruijter, W. P. N., and Lutjeharms, J. R. E.: Natal pulses and the formation of Agulhas Rings, J.
2772 Geophys. Res., 105, 6425-6436, https://doi.org/10.1029/1999JC900196, 2000.

2773 Varadachari, V. V. R.: On the process of upwelling and sinking on the east coast of India, Os. Univ. Press, Inst. of
2774 Oceanogr. Sci., Wormley, England, Prof. Mahadevan Shastiabdapurti commemoration Vol:1–27, 1961.

2775 Varela, R., Álvarez, I., Santos, F., deCastro, M., and Gómez-Gesteira, M.: Has upwelling strengthened along worldwide
2776 coasts over 1982-2010?, Sci. Rep, 5, 10016, doi:10.1038/srep10016, 2015.

2777 Varela, R., Santos, F., Gómez-Gesteira, M., Álvarez, I., Costoya, X., and Días, J. M.: Influence of coastal upwelling on
2778 SST trends along the south coast of Java, PLoS ONE, 11(9), e0162122, doi:10.1371/journal.pone.0162122, 2016.

2779 Veldhuis, M. J., Kraay, G. W., Van Bleijswijk, J. D., and Baars, M. A.: Seasonal and spatial variability in phytoplankton
2780 biomass, productivity and growth in the northwestern Indian Ocean: The southwest and northeast monsoon, 1992–1993.
2781 Deep-Sea Res. Part I: Oceanographic Research Papers, 44(3), 425–449, https://doi.org/10.1016/S0967-0637(96)00116-1,
2782 1997.

2783 Vialard, J., Foltz, G. R., McPhaden, M. J., Duvel, J. P., and C. de Boyer Monte´gut: Strong Indian Ocean sea surface
2784 temperature signals associated with the Madden-Julian Oscillation in late 2007 and early 2008, Geophys. Res. Lett., 35,
2785 L19608, doi:10.1029/ 2008GL035238, 2008.

2786 Vialard, J., Shenoi, S. S. C., McCreary, J. P., Shankar, D., Durand, F., Fernando, V., and Shetye, S. R.: Intraseasonal
2787 response of the northern Indian Ocean coastal waveguide to the Madden-Julian Oscillation, Geophys. Res. Lett., 36,
2788 doi:10.1029/2009GL038450, 2009a.

2789 Vialard, J., Duvel, J. P., McPhaden, M. J., Bouruet-Aubertot, P., Ward, B., Key, E., Bourras, D., Weller, R., Minnett, P.,
2790 Weill, A., Cassou, C., Eymard, L., Fristedt, T., Basdevant, C., Dandonneau, Y., Duteil, O., Izumo, T., de Boyer Montégut,
2791 C., Masson, S., … Kennan, S. : Cirene: Air—Sea Interactions in the Seychelles—Chagos Thermocline Ridge Region,
2792 Bull. Amer. Meteor Soc., 90(1), 45–62, https://doi.org/10.1175/2008BAMS2499.1, 2009b.

2793 Vic, C., Capet, X., Roullet, G., and Carton, X.: Western boundary upwelling dynamics off Oman. Ocean Dynamics, 67(5),
2794 585–595, https:// doi.org/10.1007/s10236-017-1044-5, 2017.

2795 Vidya, P. J., S. Das, M. and Murali, R. : Contrasting Chl-*a* responses to the tropical cyclones Thane and Phailin in the
2796 Bay of Bengal, J. Mar. Syst., doi: 10.1016/j.jmarsys.2016.10.001, 2017.

2797 Vinayachandran, P. N., and Shetye, S. R.: The warm pool in the Indian Ocean, Proceedings of the Indian Academy of
2798 Sciences - Earth and Planetary Sciences, 100 , 165–175. doi:10.1007/BF02839431, 1991.

2799 Vinayachandran, P. N., Shetye, S. R., Sengupta, D., and Gadgil, S.: Forcing mechanisms of the Bay of Bengal circulation,
2800 Curr. Sci., 71, 753–763, 1996.

2801 Vinayachandran, P. N., and Yamagata, T.: Monsoon Response of the Sea around Sri Lanka: Generation of Thermal
2802 Domesand Anticyclonic Vortices, J. Phys. Oceanogr., 28(10), 1946–1960. https://doi.org/10.1175/1520-
2803 0485(1998)028<1946:MROTSA>2.0.CO;2, 1998.

2804 Vinayachandran, P. N., Masumoto, Y., Mikawa, T., and Yamagata, T. : Intrusion of the Southwest Monsoon Current into
2805 the Bay of Bengal J. Geophys. Res. : Oceans, 104(C5), 11077–11085, https://doi.org/10.1029/1999JC900035, 1999.

2806 Vinayachandran, P. N., Murty, V. S. N., Ramesh Babu, V.: Observations of barrier layer formation in the Bay of Bengal
2807 during summer monsoon, J. Geophys. Res.-Oceans, doi: 10.1029/2001JC000831, 2002.

2808 Vinaychandran, P.N. and Mathew, S.: Phytoplankton bloom in the Bay of Bengal during the northeast monsoon and its
2809 intensification by cyclones, Geophy. Res. Lett., doi: 10.1029/2002GL016717, 2003.

2810 Vinayachandran P. N., Chauhan, P., Mohan, M., and Nayak, S. : Biological response of the sea around Sri Lanka to
2811 summer monsoon, Geophys. Res. Lett., 31, doi:10.1029 /2003GL018533, 2004.

2812 Vinayachandran, P. N., McCreary Jr., J.P, Hood, .R. R and. Kohler, K.E.: A numerical investigation of the phytoplankton
2813 bloom in the Bay of Bengal during Northeast Monsoon, J. Geophys. Res., 110 (C12001), doi:10.1029/2005JC002966,
2814 2005.

2815 Vinayachandran, P. N., Shankar, D., Kurian, J., Durand, F., and Shenoi, S. S. C.: Arabian Sea Mini warm pool and the
2816 monsoon onset vortex, Curr. Sci., 93(2), 203-214, 2007.

2817 Vinayachandran, P. N., and Saji, N. H.: Mechanisms of South Indian Ocean intraseasonal cooling, Geophys. Res. Lett.,
2818 35(23), L23607, https://doi.org/10.1029/2008GL035733, 2008.

2819 Vinayachandran, P. N. : Impact of Physical Processes on Chlorophyll Distribution in the Bay of Bengal, 71– 86,
2820 AGU, Washington, D. C., doi:10.1029/2008GM000705, 2009.

2821 Vinayachandran, P. N., Matthews, A. J., Kumar, K. V., Sanchez-Franks, A., Thushara, V., George, J., Vijith, V., Webber,
2822 B. G. M., Queste, B. Y., Roy, R., Sarkar, A., Baranowski, D. B., Bhat, G. S., Klingaman, N. P., Peatman, S. C., Parida, C.,
2823 Heywood, K. J., Hall, R., King, B., … Joshi, M: BoBBLE: Ocean–Atmosphere Interaction and Its Impact on the South
2824 Asian Monsoon, Bull. Am. Meteorol. Soc., 99(8), 1569–1587. https://doi.org/10.1175/BAMS-D-16-0230.1, 2018.

2825 Vinayachandran, P. N , Umasankar Das, Shankar, D., Jahfer,A., Behara, A., Balakrishnan Nair, T.M. , and Bhat, G.S.:
2826 Maintenance of the southern Bay of Bengal cold pool, Deep-Sea Res. Part -II, https://doi.org/10.1016/j.dsr2.2019.07.012,
2827 2020.

2828 Vos de, A., Pattiaratchi, C. B., and Wijeratne, E. M. S.: Surface circulation and upwelling patterns around Sri Lanka,
2829 Biogeosciences, 11, 5909–5930, https://doi.org/10.5194/bg-11-5909-2014, 2014.

2830 Waite, A., Muhling, B. A., Holl, C. M., Beckley, L. E., Montoya, J. P., Strzelecki, J., Thompson, P. A. and Pesant, S. C.:
2831 Food web structure in two counter-rotating eddies based on δ15N and δ13C isotopic analyses, Deep-Sea Res. Part 2 Top.
2832 Stud. Oceanogr., 54(8), 1055-1075. doi:10.1016/j.dsr2.2006.12.010, 2007a.

2833 Waite, A., Thompson, P. A., Pesant, S. C., Feng, M., Beckley, L. E., Domingues, C. M., Gaughan, D., Hanson, C., Holl,
2834 C. M., Koslow, T., Meuleners, M., Montoya, J. P., Moore, T., Muhling, B. A., Paterson, H., Rennie, S., Strzelecki, J. and
2835 Twomey, L.: The Leeuwin Current and its eddies: An introductory overview, Deep Sea Res. Part II Top. Stud. Oceanogr.,
2836 54(8), 789-796, doi:10.1016/j.dsr2.2006.12.008, 2007b.

2837 Waite, A. M., Rossi, V., Roughan, M., Tilbrook, B., Thompson, P. A., Feng, M., Wyatt, A. S. J., and Raes, E. J.:
2838 Formation and maintenance of high-nitrate, low pH layers in the eastern Indian Ocean and the role of nitrogen fixation,
2839 Biogeosciences, 10(8), 5691–5702, doi:10.5194/bg-10-5691-2013, 2013.

Waite, A. M., Beckley, L. E., Guidi, L., Landrum, J. P., Holliday, D., Montoya, J., Paterson, H., Feng, M., Thompson, P. A., and Raes, E. J.: Cross-shelf transport, oxygen depletion, and nitrate release within a forming mesoscale eddy in the eastern Indian Ocean, Limnol. Oceanogr., 61(1), 103-121, doi:10.1002/lno.10218, 2016.

Waite, A. M., Raes, E., Beckley, L. E., Thompson, P. A., Griffin, D., Saunders, M., Säwström, C., O'Rorke, R., Wang, M., Landrum, J. P. , and Jeffs, A.: Production and ecosystem structure in cold-core vs. warm-core eddies: Implications for the zooplankton isoscape and rock lobster larvae, Limnol. Oceanogr., 64(6), 2405-2423, doi:10.1002/lno.11192, 2019.

Walker, N. D., : Satellite observations of the Agulhas Current and episodic upwelling south of Africa. Deep-Sea Res., 33A, 1083–1106, doi:10.1016/0198-0149(86)90032-4, 1986.

Wallen, I.E.: The International Indian Ocean Expedition: A Status Report, Journal of the Washington Academy of Sciences, 54, 3, March 1964, pp. 45-53, https://www.jstor.org/stable/24535159, 1964.

Wang, Y., and McPhaden, M. J.: Seasonal cycle of cross-equatorial flow in the central Indian Ocean. J. Geophys. Res. : Oceans, 122(5), 3817–3827, https://doi.org/10.1002/2016JC012537, 2017.

Warren, B. A.: Medieval Arab references to the seasonally reversing currents of the north Indian Ocean, Deep-Sea Res., 13, 167–171, https://doi.org/10.1016/0011-7471(66)91097-7, 1966.

Warren, B. A.: The shallow oxygen minimum of the South Indian Ocean, Deep Sea Res. Part I Oceanogr. Res. Pap., 28(8), 859-864, doi:10.1016/S0198-0149(81)80005-2, 1981.

Weaver, A. J., and Middleton, J. H.: On the dynamics of the Leeuwin Current, J. Phys. Oceanogr., 19(5), 626-648, doi:10.1175/1520-0485(1989)019<0626:otdotl>2.0.co;2, 1989.

Webber, B. G. M., Matthews, A. J., Vinayachandran, P. N., Neema, C. P., Sanchez-Franks, A., Vijith, V., Amol, P., and Baranowski, D. B. : The Dynamics of the Southwest Monsoon Current in 2016 from High-Resolution In Situ Observations and Models, J. Phys. Oceanogr., 48(10), 2259–2282, https://doi.org/10.1175/JPO-D-17-0215.1, 2018.

Webster, P.J., Moore, A.M., Loschnigg, J.P., and Leben, R.R.: Coupled ocean-atmosphere dynamics in the Indian Ocean during 1997-98, Nature., 401:356–360, doi:10.1038/43848,1999.

Wei, X., Liao, X., Zhan, H. and Liu, H.: Estimates of potential new production in the Java-Sumatra upwelling system, Chin. J. Oceanol. Limnol., 30, 1063-1067, doi:10.1007/s00343-012-1281-x, 2012.

Weimerskirch, H., Le Corre, M., Jaquemet, S., Potier, M., and Marsac, F.: Foraging strategy of a top predator in tropical waters: great frigate birds in the Mozambique Channel, Mar. Ecol. Prog. Ser., 275, 297–308, doi:10.3354/meps275297, 2004.

Weller, E., Holliday, D., Feng, M., Beckley, L., and Thompson, P.: A continental shelf scale examination of the Leeuwin Current off Western Australia during the austral autumn–winter, Cont Shelf Res., 31(17), 1858-1868, doi:10.1016/j.csr.2011.08.008, 2011.

Wiggert, J., Hood, R., Banse, K., and Kindle, J.: Monsoon-driven biogeochemical processes in the Arabian Sea, Prog. Oceanogr., 65(2–4), 176–213, doi:10.1016/j.pocean.2005.03.008, 2005.

Wiggert, J. D., Murtugudde, R. G. and Christian, J. R.: Annual ecosystem variability in the tropical Indian Ocean: results of a coupled bio-physical ocean general circulation model, Deep-Sea Res. II 53, 644–676, 2006.

2875 Wiggert, J. D., and Murtugudde, R. G.: The sensitivity of the Southwest Monsoon phytoplankton bloom to variations in
2876 aeolian iron deposition over the Arabian Sea, J. Geophys. Res. 112. http://dx.doi.org/10.1029/2006JC003514, 2007.

2877 Wilson, S., Carleton, J., and Meekan, M.: Spatial and temporal patterns in the distribution and abundance of
2878 macrozooplankton on the southern North West Shelf, Western Australia, Estuar. Coast. Shelf Sci., 56(5-6), 897-908,
2879 doi:10.1016/S0272-7714(02)00285-8, 2003.

2880 Wirth, A., Willebrand, J., and Schott, F.: Variability of the Great Whirl from observations and models, Deep-Sea
2881 Res. Pt. II, 49,1279–1295, https://doi.org/10.1016/S0967-0645(01)00165-5, 2002.

2882 Woo, M., Pattiaratchi, C., and Schroeder, W.: Dynamics of the Ningaloo Current off Point Cloates, Western Australia,
2883 Mar. Freshw. Res., 57(3), 291-301, doi:10.1071/mf05106, 2006a.

2884 Woo, M., Pattiaratchi, C., and Schroeder, W.: Summer surface circulation along the Gascoyne continental shelf, Western
2885 Australia, Cont Shelf Res., 26(1), 132-152, doi:10.1016/j.csr.2005.07.007, 2006b.

2886 Woo, M., and Pattiaratchi, C.: Hydrography and water masses off the western Australian coast, Deep Sea Res. Part I
2887 Oceanogr. Res. Pap., 55(9), 1090-1104, doi:10.1016/j.dsr.2008.05.005, 2008.

2888 Wright, J. J., Konwar, K. M., and Hallam, S. J.: Microbial ecology of expanding oxygen minimum zones,Nature
2889 Publishing Group, 10(6), 381–394, https://doi.org/10.1038/nrmicro2778, 2012.

2890 Wyrtki, K.: The upwelling in the region between Java and Australia during the South-East monsoon, Aust. J. Mar.
2891 Freshw. Res., 13, 217-225, doi:10.1071/MF9620217, 1962.

2892 Wyrtki, K. Physical oceanography of the Indian Ocean. Pp. 18–36 in B. Zeitzschel, ed. ,The biology of the Indian Ocean.
2893 Springer-Verlag, New York, 1973.

2894 Xie, S.-P., Annamalai, H., Schott, F. A., and McCreary Jr. J.P.: Structure and mechanism of South Indian Ocean climate
2895 variability, *J.Clim.*, 15, 864–878, https://doi.org/10.1175/1520-0442(2002)015<0864:SAMOSI>2.0.CO;2, 2002.

2896 Xu, J., Lowe, R. J., Ivey, G. N., Pattiaratchi, C., Jones, N. L., and Brinkman, R.: Dynamics of the Wei summer shelf
2897 circulation and transient upwelling off Ningaloo Reef, Western Australia, J. Geophys. Res. Oceans, 118(3), 1099-1125,
2898 doi:10.1002/jgrc.20098, 2013.

2899 Xue, L., Wang, H., Jiang, L.-Q., Cai, W.-J., Wei, Q., Song, H.,Kuswardani, R. T. D., Pranowo, W. S., Beck, B., Liu, L.
2900 and Yu, W.: Aragonite saturation state in a monsoonal upwelling system off Java, Indonesia, J. Mar. Sys., 153, 10–17,
2901 doi:10.1016/j.jmarsys.2015.08.003, 2016.

2902 Yamagata, T., Behera, S. K., Luo, J.-J., Masson, S., Jury, M. R., & Rao, S. A. : Coupled Ocean-Atmosphere Variability in
2903 the Tropical Indian Ocean, Geophysical Monograph Series, 147, 189–211, https://doi.org/10.1029/147GM12, 2004.

2904 Yokoi, T., Tozuka, T., and Yamagata, T.: Seasonal Variations of the Seychelles Dome Simulated in the CMIP3 Models, J.
2905 Phys. Oceanogr., 39(2), 449–457, https://doi.org/10.1175/2008JPO3914.1, 2008.

2906 Yu, W., Hood, R., D'Adamo, N., McPhaden, M. et.al., :Eastern Indian Ocean upwelling Research Initiative (EIOURI),
2907 The EIOURI Science Plan, ESSO - Indian National Centre for Ocean Information Services (INCOIS), Hyderabad, India,
2908 49pp, 2016.

2909 Zavala-Garay, J., Theiss, J., Moulton, M., Walsh C., van Woesik R., Mayorga-Adame, C.G., García-Reyes, M., Mukaka,

D.S., Whilden K., and Shaghude, Y.W.: On the dynamics of the Zanzibar Channel, J. Geophys. Res. Oceans, 120, 6091–6113, doi:10.1002/2015JC010879, 2015.

Figures

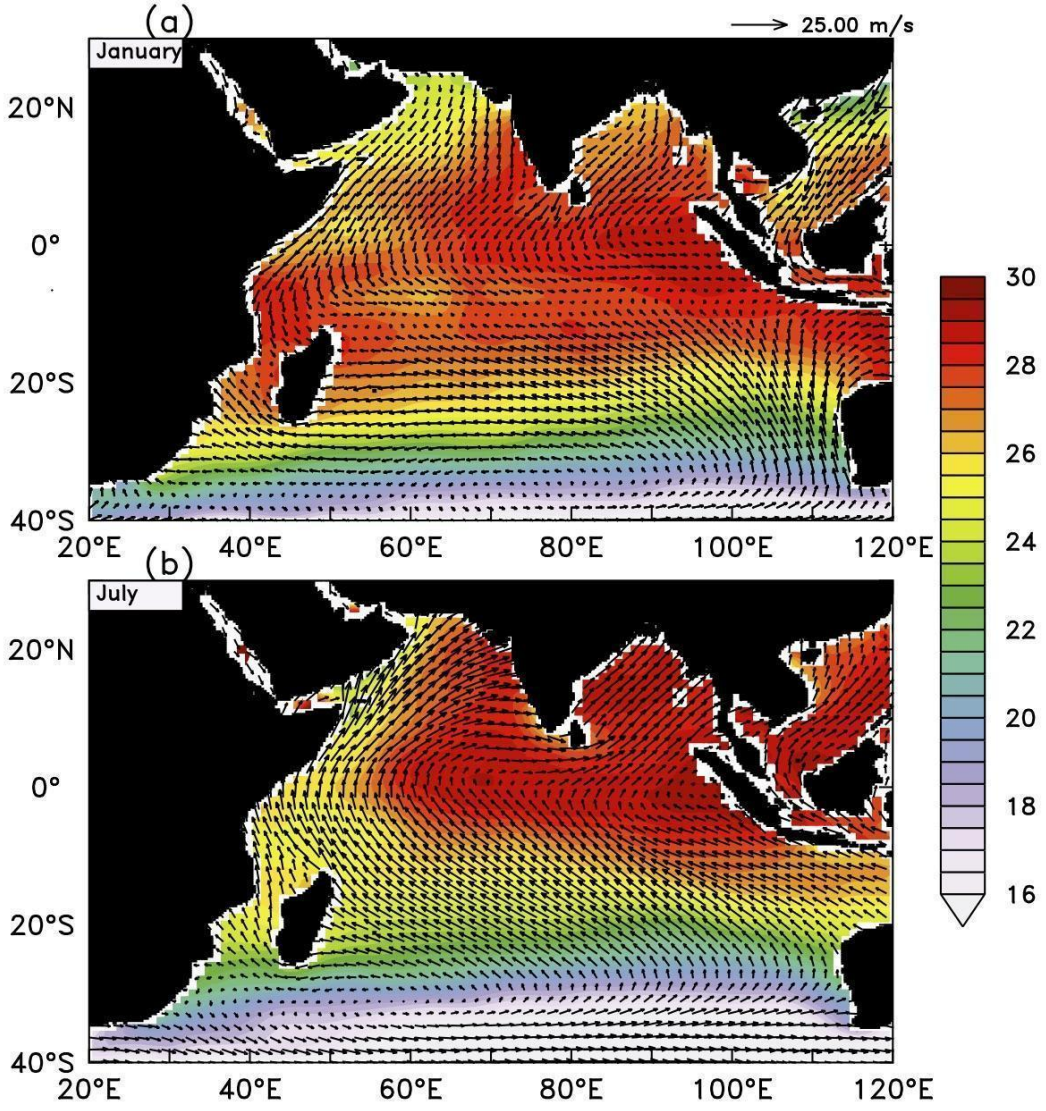

Figure 1A: Climatological (Locarnini, 2018) SST averaged from surface to 50 m depth (shaded) and winds (vectors m s $^{-1}$), data from QuikSCAT (http://apdrc.soest.hawaii.edu.) for the months of (a) January and (b) July. The scale for SST is given to the right of each panel and the scale vector for wind speed is given at the top of each panel.

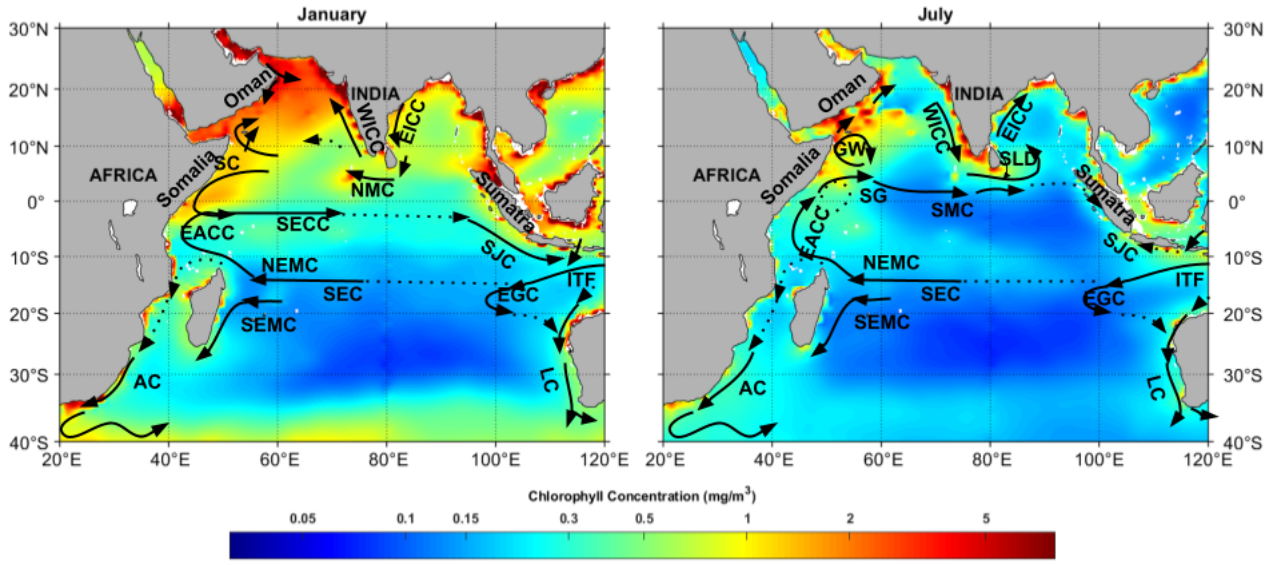

Figure 1B: A schematic representation of the major currents systems (modified after Schott et al., 2009) in the Indian Ocean for January (left panel) and July(right panel) are overlayed on chlorophyll (shaded, mg/m^3) climatology. Abbreviations are: West India Coastal Current (WICC), East India Coastal Current (EICC), Sri Lanka Dome (SLD), South Equatorial Current (SEC), South Equatorial Counter Current (SECC), Northeast and Southeast Madagascar Current (NEMC and SEMC), East African Coastal Current (EACC), Somali Current (SC), Southern Gyre (SG) and Great Whirl (GW) Northeast Monsoon Current(NMC), South Java Current (SJC), Indonesian Through Flow(ITF), East Gyral Current (EGC), and Leeuwin Current (LC), Northeast monsoon currenct (NMC) for and Southwest monsoon (SMC). Chlorophyl data is monthly climatology from SeaWiFs (ref:http://nomads.gfdl.noaa.gov).

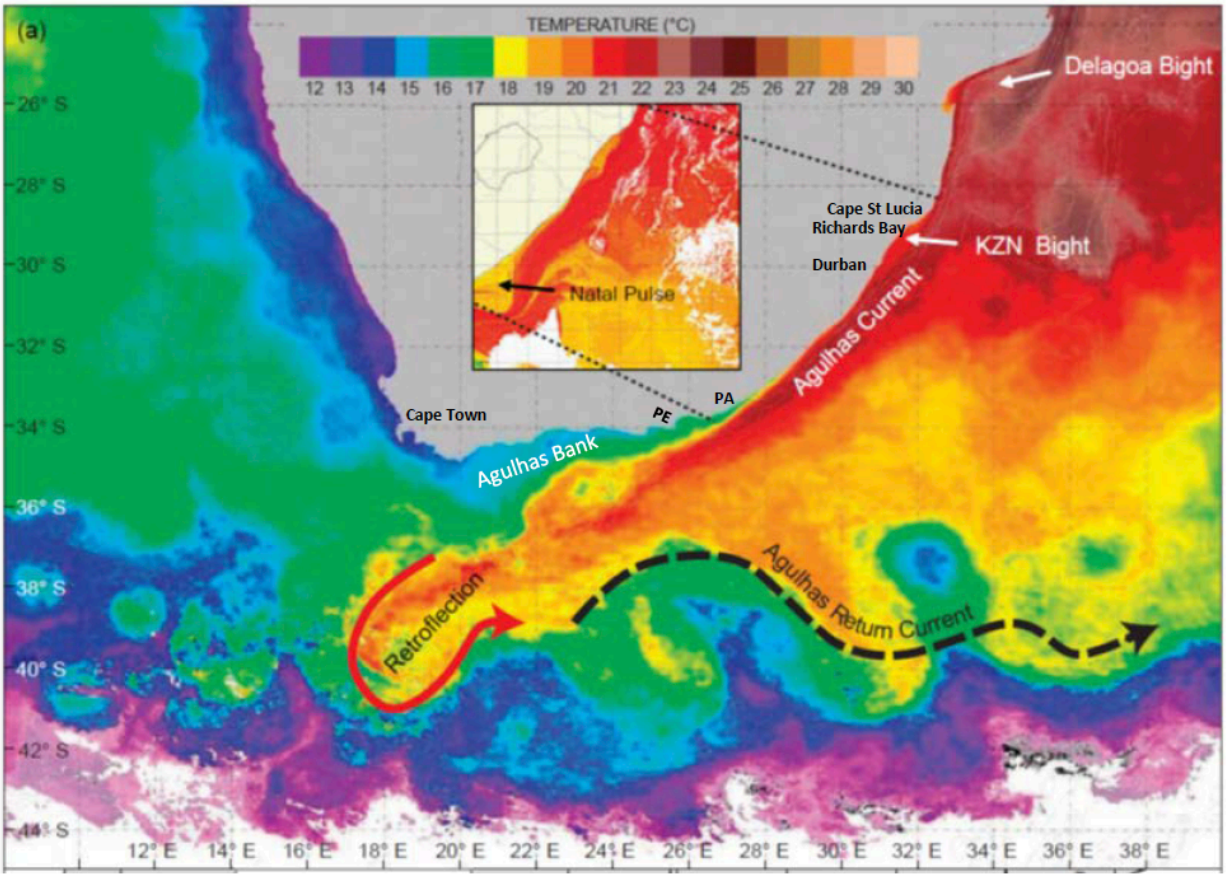

Figure 2: SST image highlighting the Agulhas Current flowing along the east coast of South Africa. PE = Port Elizabeth, PA = Port Alfred. Insert highlights a south-westward propagating Natal pulse (a singular meander in the trajectory) which has a cold core. The shelf on the east coast is narrow with a steep continental slope. Exceptions are the KZN Bight and the Agulhas Bank.

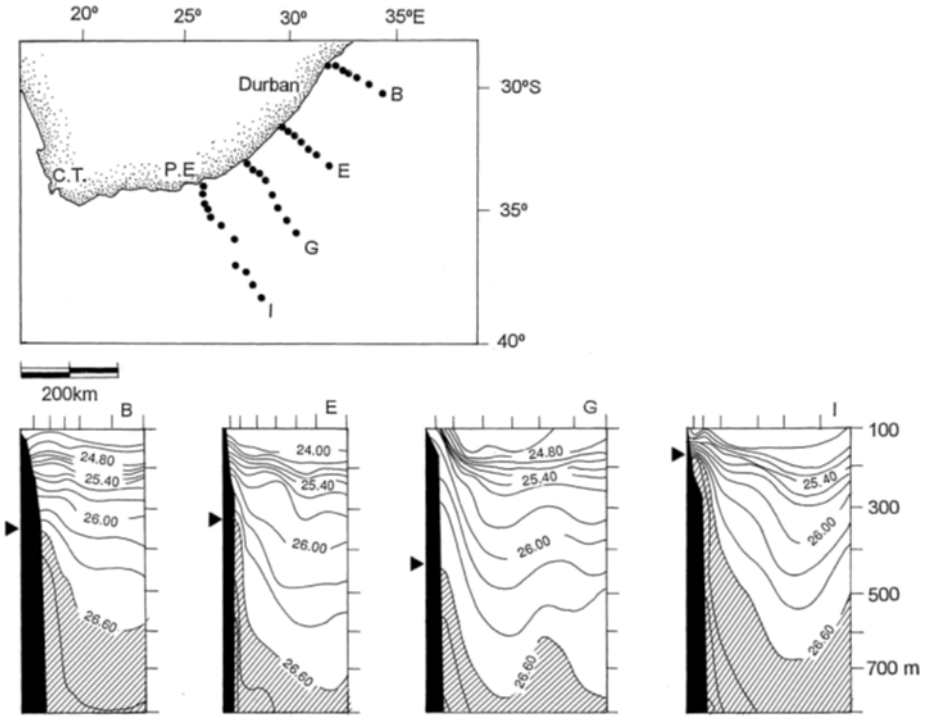

Figure 3: Sections across the Agulhas Current, showing sigma-t values obtained during March 1969 (after Harris and Van Foreest, 1978). All show water with a density greater than 26.60 upwelled along the inshore edge of the Agulhas Current. C.T and P.E represents Cape Town and Prot Elizabeth, respectively.

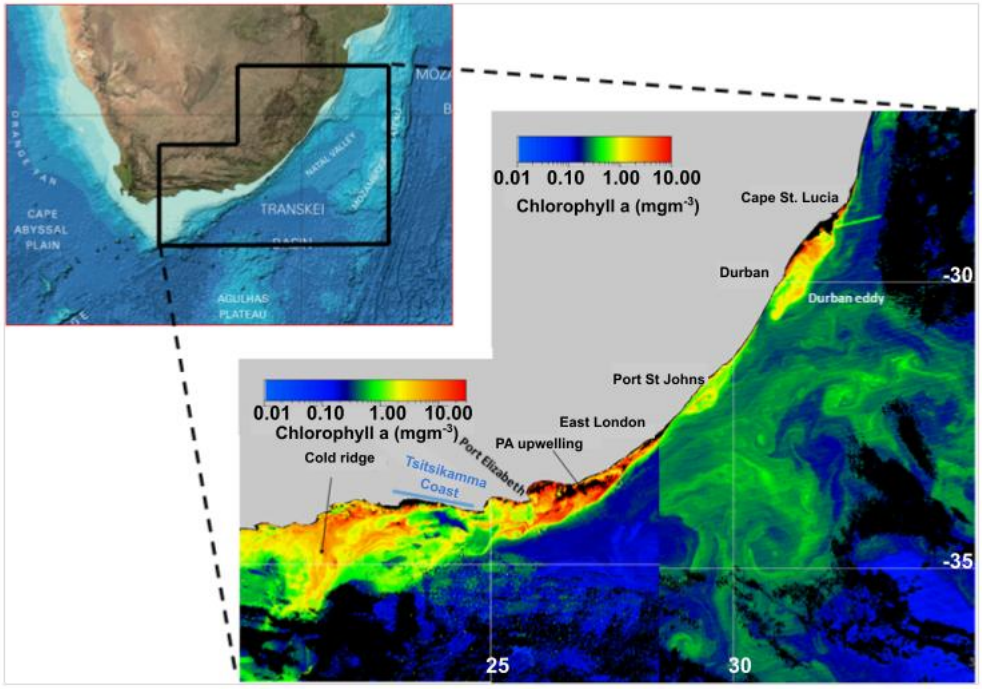

Figure 4: A composite chlorophyll satellite image chosen to highlight the main productivity features commonly found on the inshore edge of the Agulhas Current. Note the different chlorophyll scales applicable to the LHS and RHS parts of the composite. Highlighted are the cold ridge on the central Agulhas Bank (AB), Port Alfred upwelling extending onto the eastern AB, the Durban (break-away) eddy with a similar feature passing Port St Johns where a semi-permanent smaller cyclonic feature often exists.

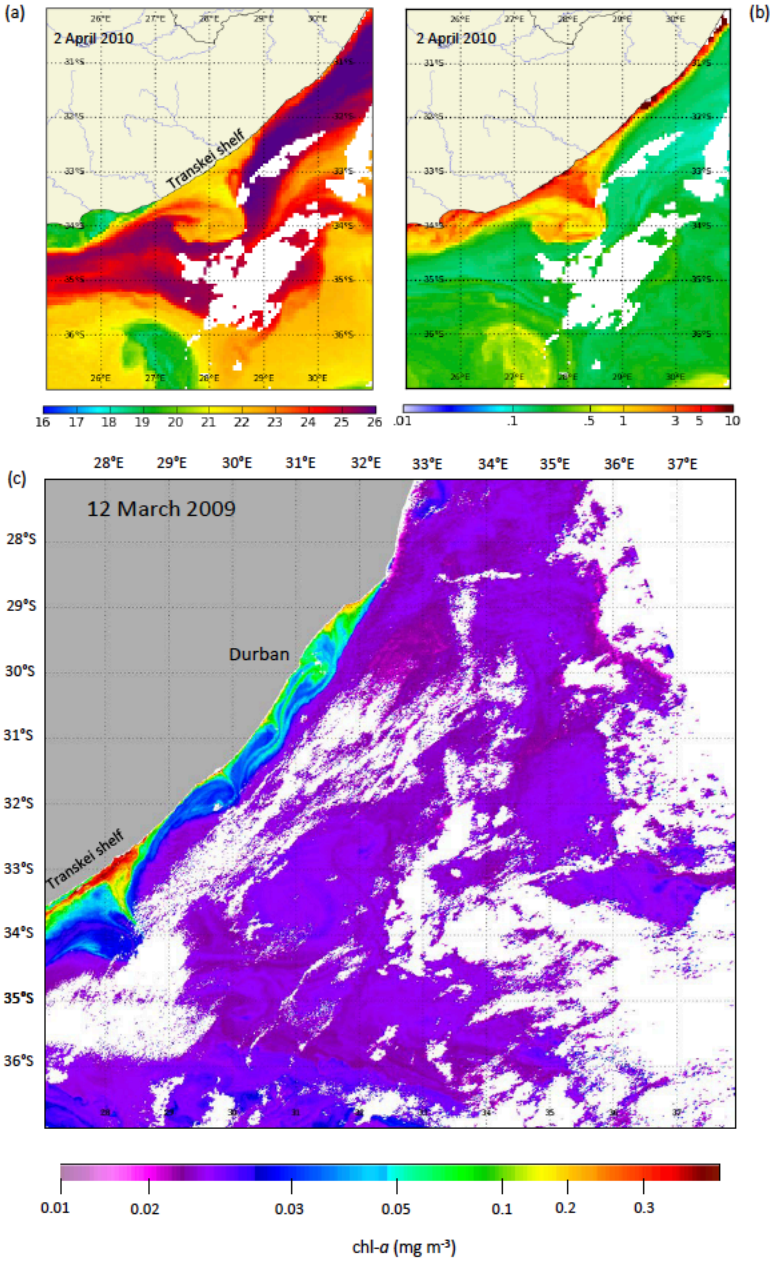

Figure 5: Satellite SST (LHS) and chlorophyll-a (RHS) images of a Natal pulse on 2 April 2010 off the narrow Transkei shelf. Note the high levels of chl-a on the eastern side of the cyclone (meander) which protrude of the shelf.

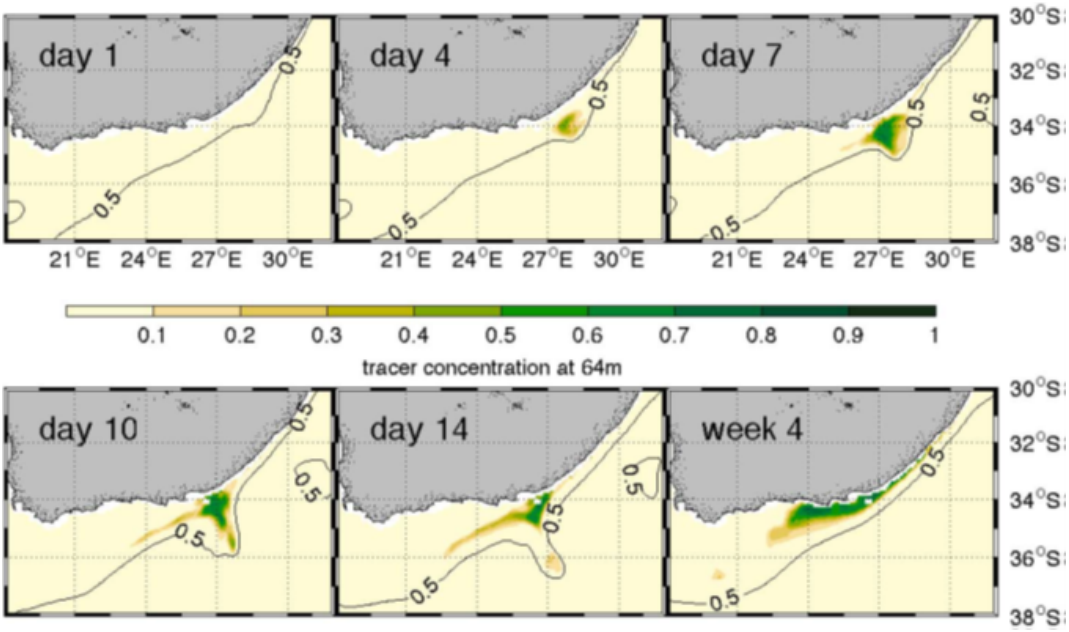

Figure 6: Tracer concentration at 64 m in a AGU-HYCOM to reveal shelf edge upwelling. Tracers were initialized in the Agulhas Current below 400 m over a 6-week period during a meander event in 2001 and used as a proxy for upwelling. The 0.5-m sea level contour is highlighted to show the inshore edge of the current as the meander propagates along the coast (after Malan et al., 2018).

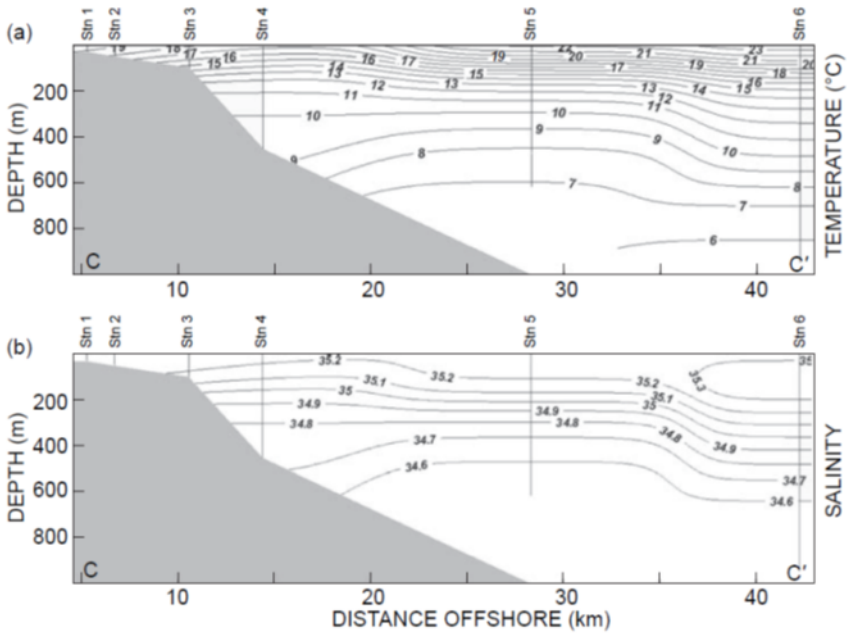

Figure 7: Vertical sections of CTD data collected along a trans-shelf transect off Port St Johns to a depth of 1 000 m near Port St Johns on 4 May 2005 (see Roberts et al., 2010). Both temperature (a) and salinity (b) show slope upwelling with a surface temperature of 16 °C near Station 4 in the centre of the Port St Johns–Waterfall Bluff cyclonic eddy. Graphic after Roberts et al. (2010).

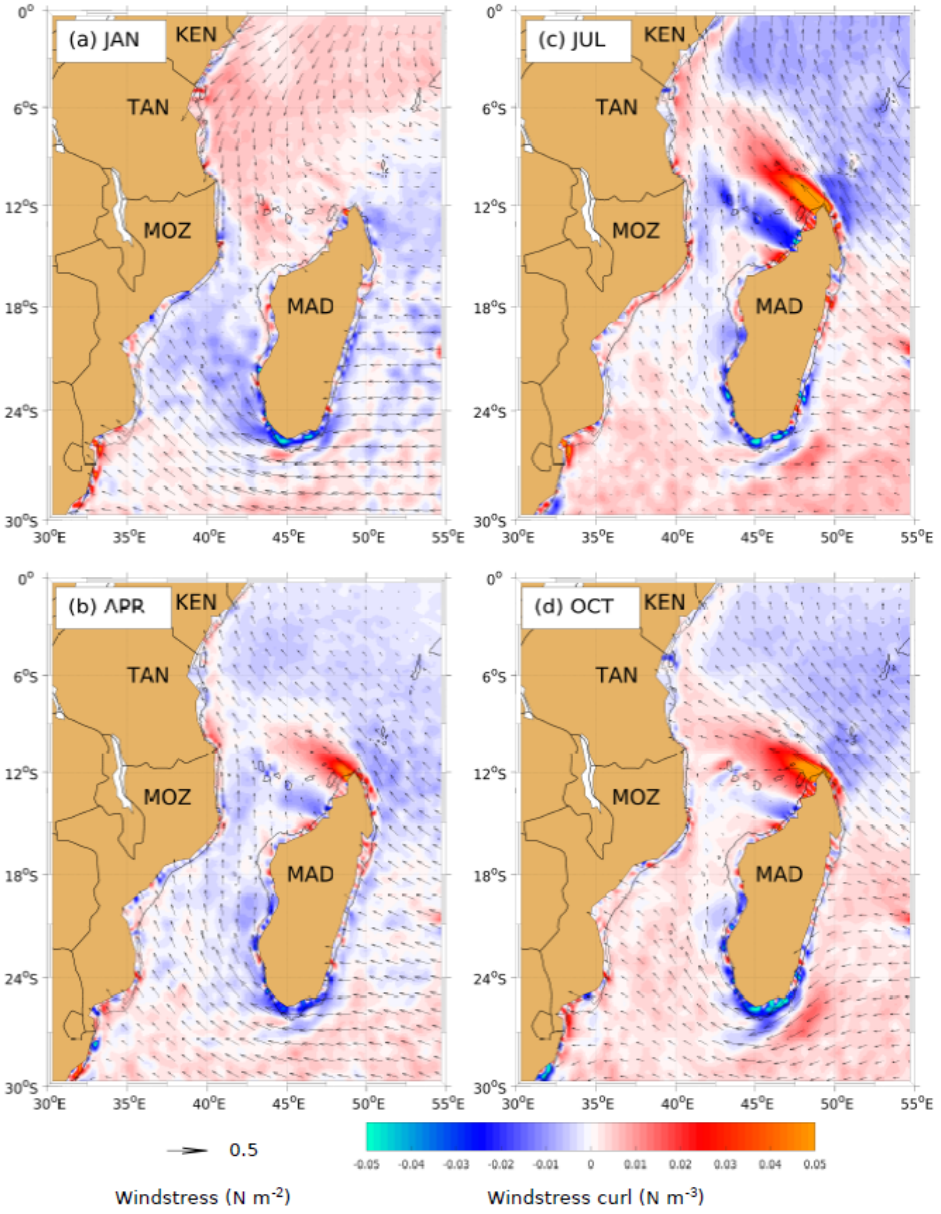

3015

3016 **Figure 8: Climatological monthly means of wind stress (vectors) and wind stress curl (shading) during different seasons. Austral**
3017 **summer (a, JAN), fall (b, APR), winter (c, JUL) and spring (d, OCT). Negative (blue) and positive (red) wind stress curl depict**
3018 **favourable upwelling and downwelling areas respectively. The data was extracted from Scatterometer Climatology of Ocean**
3019 **Winds (SCOW), described by Risien and Chelton (2008), mapped globally with a spatial grid resolution of 1/4◦ × 1/4◦, estimated**
3020 **from 10 years' period, ranging between September 1999 and August 2009, measured by NASA Quick Scatterometer (QuikSCAT).**

3021

3022

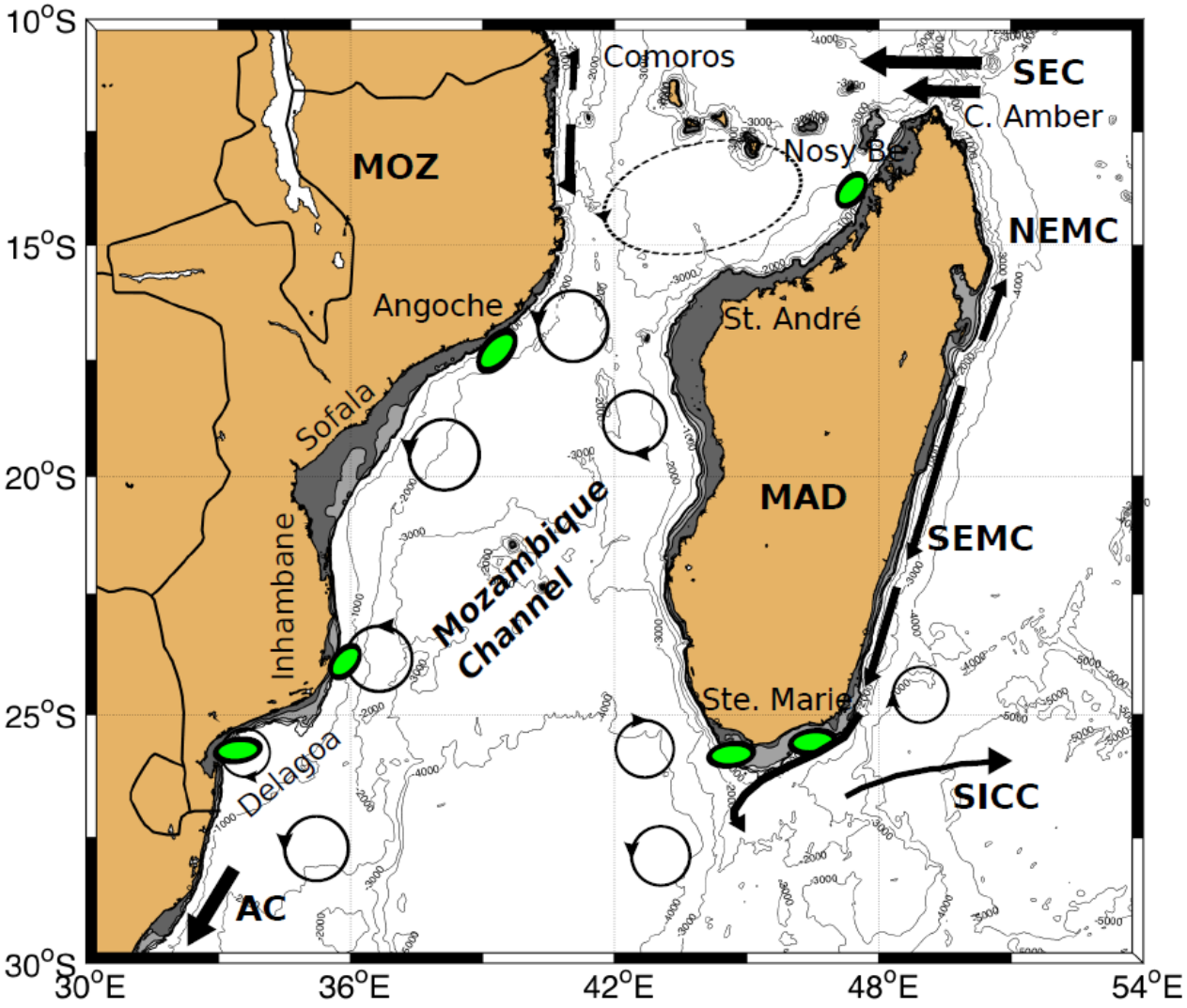

Figure 9: Bathymetry and major circulatory features in the Mozambique Channel and around Madagascar. Currents include the South Equatorial Current (SEC), Northeast and Southeast Madagascar Current (NEMC and SEMC), South Indian Countercurrent (SICC) and the Agulhas Current (AC). Shaded areas show the extent of the continental shelf to a depth of 200 m. Green ellipses denote upwelling areas.

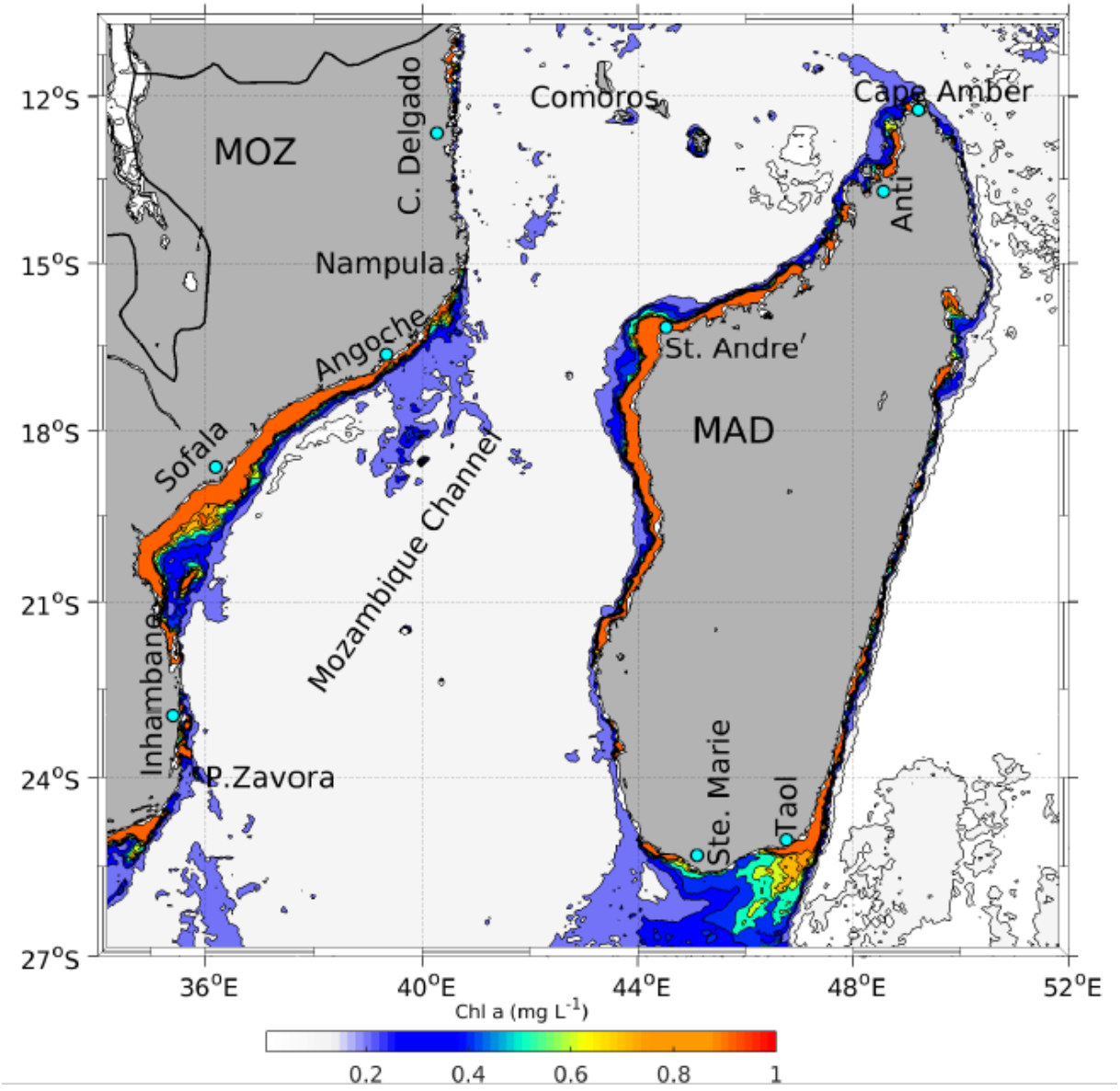

Figure 10: Monthly mean chlorophyll-a concentration for February 2003, derived from Moderate Resolution Imaging Spectroradiometer (MODIS) Aqua satellite (https://oceancolor.gsfc.nasa.gov/data/aqua/). Intermediate values beyond the continental shelf-edge highlight areas of elevated productivity off the Mozambique and Madagascar coasts that are primarily upwelling-driven. Abbreviations: Ponta Zavora, Cabo Delgado, Taolagnaro, Antsiranana.

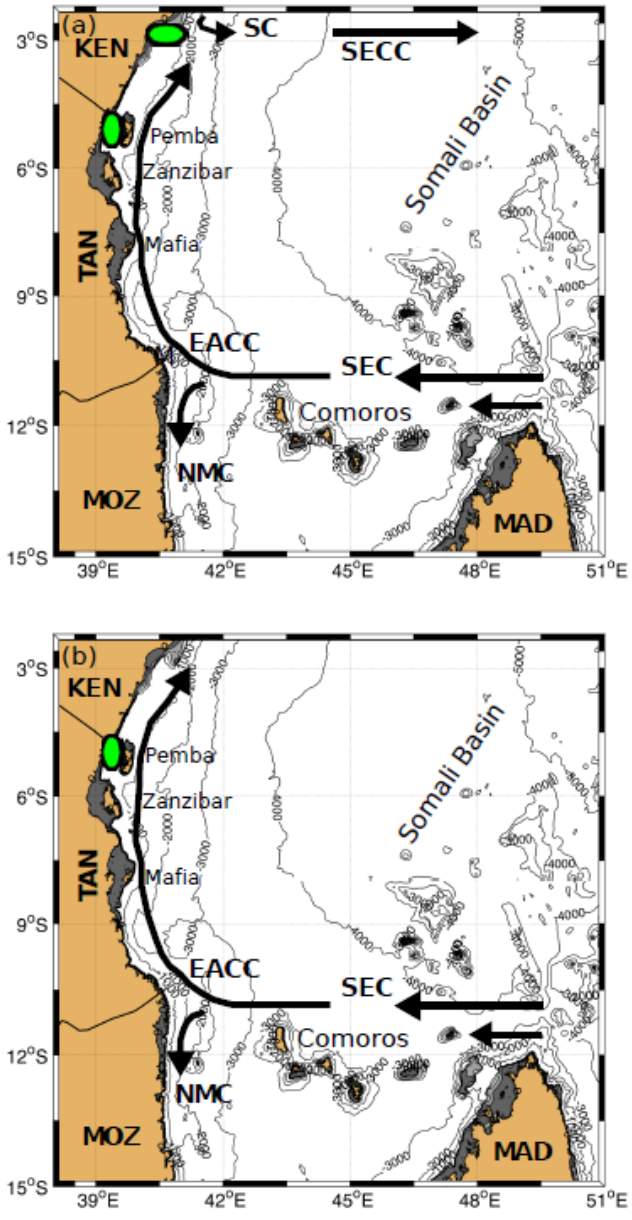

Figure 11: Circulation patterns during (a) the NEM and (b) the SWM, showing the Somali Current (SC), South Equatorial Counter Current (SECC), East African Coastal Current (EACC), South Equatorial Current (SEC) and Northeast Madagascar Current (NMC). Green ellipses denote upwelling areas. Dark grey shading denotes depths within the 200 m isobath, and light grey shading denotes depths from 200 to 500 m. Labels on land indicate Kenya (MEN), Tanzania (TAN), Mozambique (MOZ) and Madagascar (MAS).

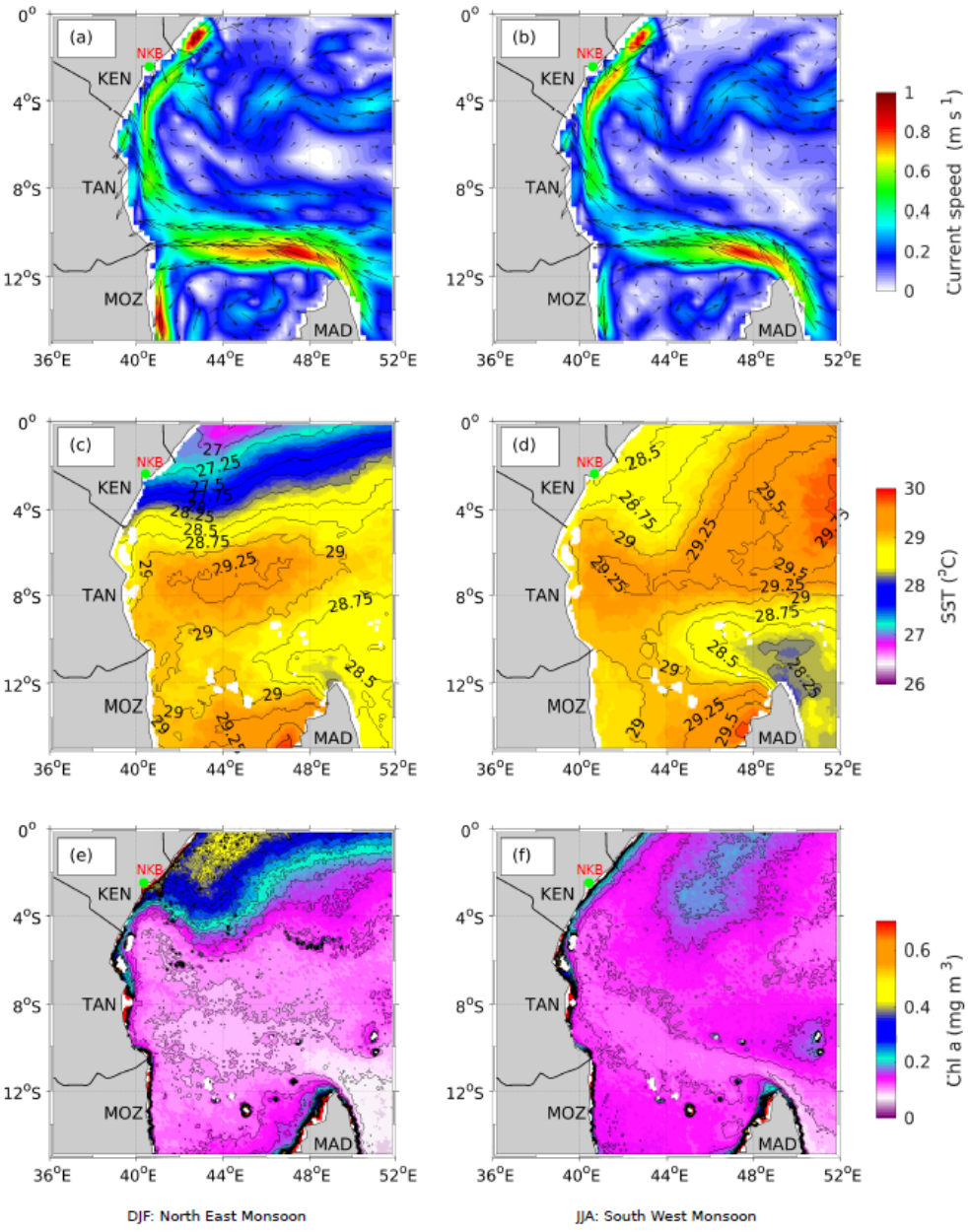

Figure 12: Average surface currents (m s^{-1}) during (a) the NEM (DJF) and (b) the SWM (JJA) derived from daily altimetry (Copernicus Marine Environmental Monitoring Services, CMEMS) over the period 2001-2010 (25-km resolution); average SST (°C) during (c) the NEM and (d) the SWM derived from NOAA AVHRR Pathfinder Version 5 data over the period 1981-2012 (4-km resolution); and surface chlorophyll-*a* (mg m^{-3}) during (e) the NEM and (f) the SWM derived from global SeaWiFS data over the period September 1997 - December 2010 (4-km resolution).

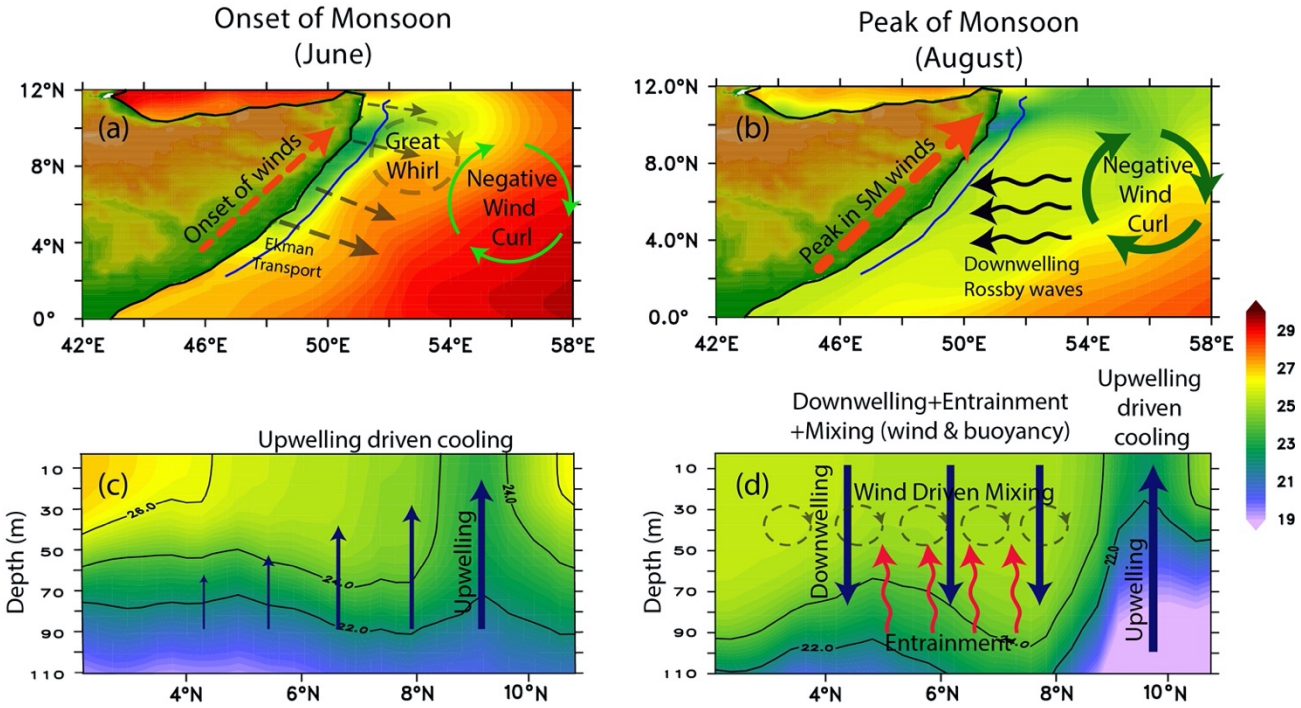

Figure 13: Climatological SST (°C, Panel a and b) and vertical section of temperature (°C, Panel c and d) along the vertical section aligned roughly around 1000 m isobath (blue contour along the Somali coast in the top panels) for the month of June (left panels) and August (right panels). The climatology is computed from model (Modular Ocean Model, Version 5.1) interannual simulations for 1993-2018 (reproduced from Chatterjee et al., 2019; Lakshmi et al., 2020). As the monsoon onset during early June, southwesterly winds blow along the coast of Somalia (red dashed arrow) leading to offshore Ekman transport (which is stronger in the south than the northern part; see Panel a black dashed arrows) driven coastal upwelling (upward blue arrows; Panel c). Though the offshore transport is strongest in the south, the maximum upwelling (upsloping of thermocline) is seen along the front of the Great Whirl north of ~8°N (Panel c). Notably, offshore wind stress curl turns negative south of the Findlater Jet axis favorable for open ocean downwelling. As the monsoon peaks, this negative wind stress curl radiates downwelling Rossby waves (Panel b) which propagate westward and upon reaching the Somali coast deepen the thermocline there against the upwelling favorable winds (downward blue arrows; Panel d). Further, stronger winds during peak monsoon enhance wind driven mixing which further deepen the thermocline in most parts of the Somalia coast. By late summer, the upwelling remains confined to the front of the Great Whirl in the northern part of the Somalia coast.

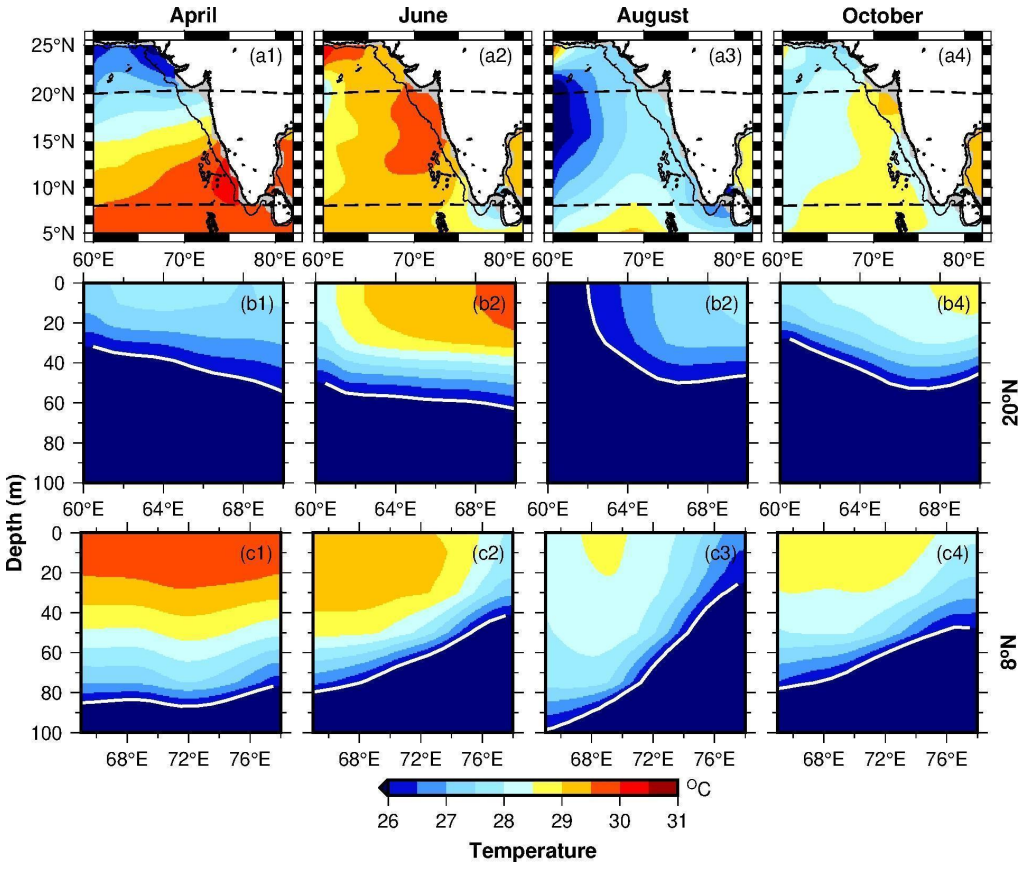

Figure 14: Monthly climatology of temperature from April to October. The data are from *North Indian Ocean Atlas* (Chatterjee et al. 2012). (a1-a4) Sea surface temperature from the eastern Arabian Sea. The black contour represents the 1000 m water-column depth, and the horizontal dashed lines are the 20°N and 8°N. (b1-b4) Vertical section of temperature at 20°N. (c1-c4) Vertical section of temperature at 8°N. The white contour is 26°C. The figure highlights how the upwelling evolves from pre-monsoon to post-monsoon season along the west coast of India. The upwelling sets earlier in the south and progresses slowly towards north. The upward tilt of the isopycnals, though weak, is evident at 20°N towards the end of the summer monsoon.

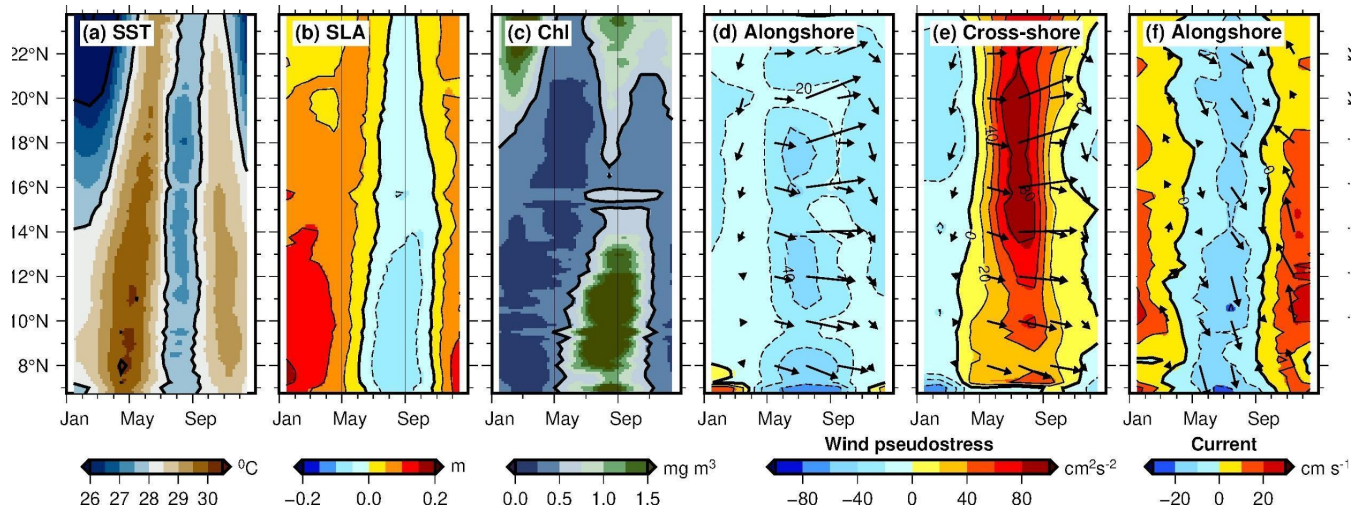

Figure 15: Climatology of (a) sea surface temperature from Terra MODIS, (b) sea-level anomaly from Aviso SSALTO/DUACS, (c) chlorophyll-*a* from SeaWIFS, (d) alongshore and (e) cross-shore wind pseudostress from QuikSCAT, and (f) alongshore current from OSCAR. The data were picked and the vectors were rotated based on the 1000 m contour (see Figure 15). Panels (a) and (c) are redrawn based on (Shankar et al., 2019).

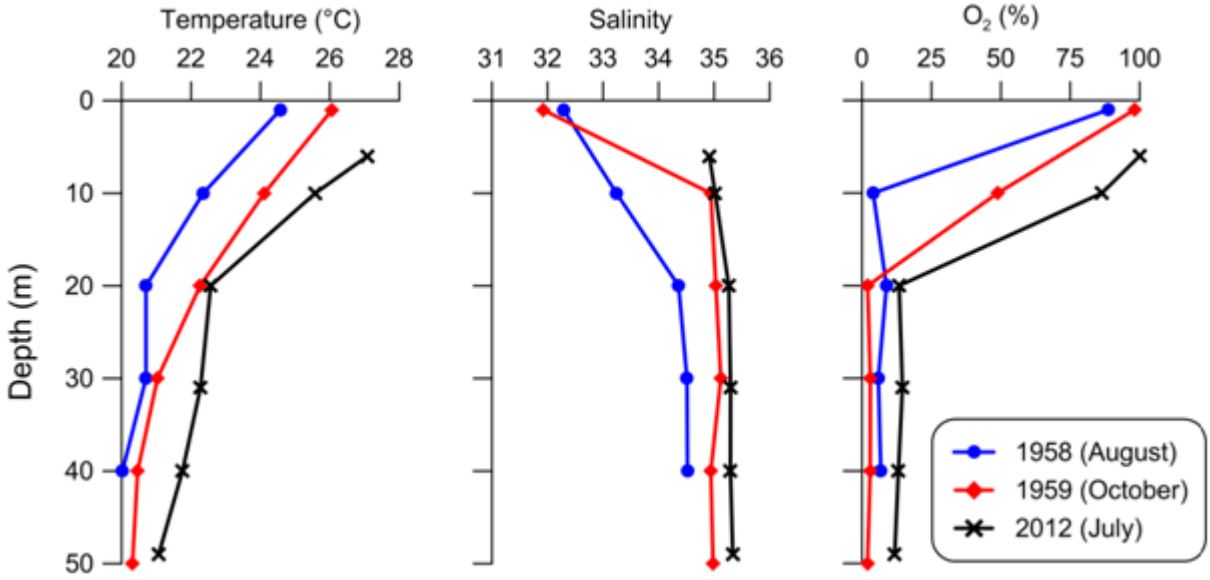

Figure 16: Comparison of historical profiles of temperature, salinity and dissolved oxygen corresponding to peak upwelling months over the inner shelf off Kochi, southwest coast of India (From Gupta et al., 2016).

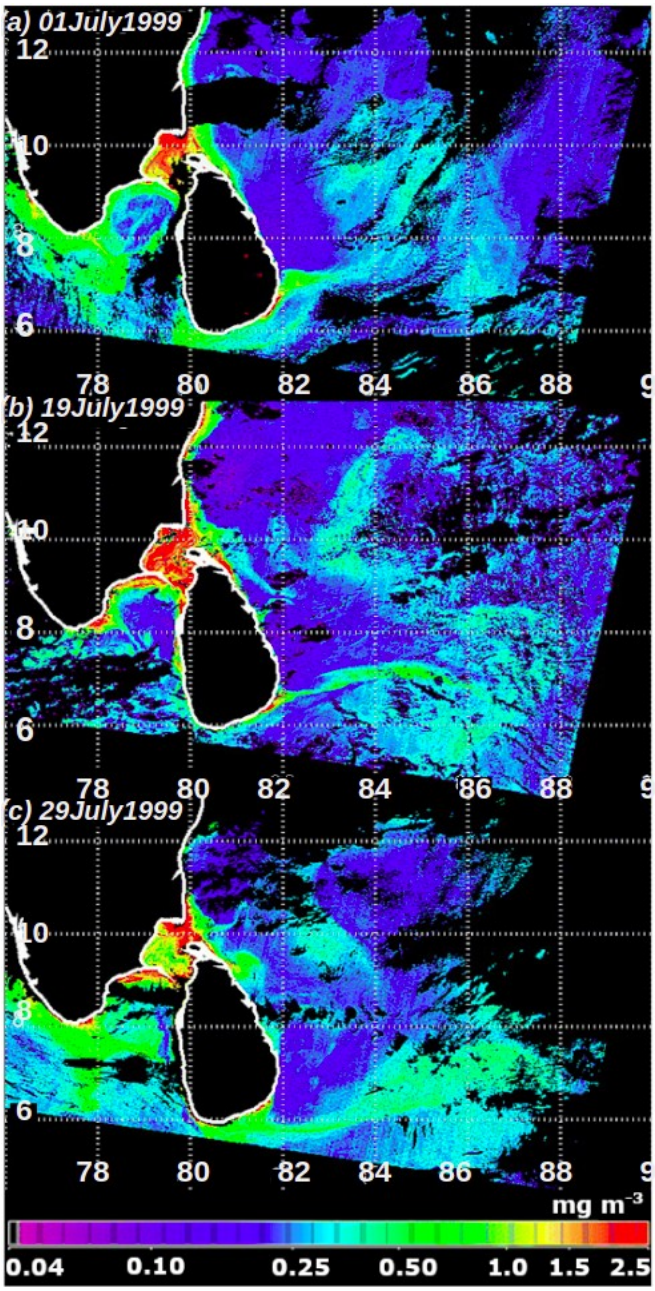

Figure 17: Chlorophyll a (mg m-3) images around Sri Lanka for (a) 1 July 1999, (b) 19 July 1999 and (c) 29 July 1999 obtained from OCM on board IRS-P4 Oceansat (From Vinayachandran et al., 2004).

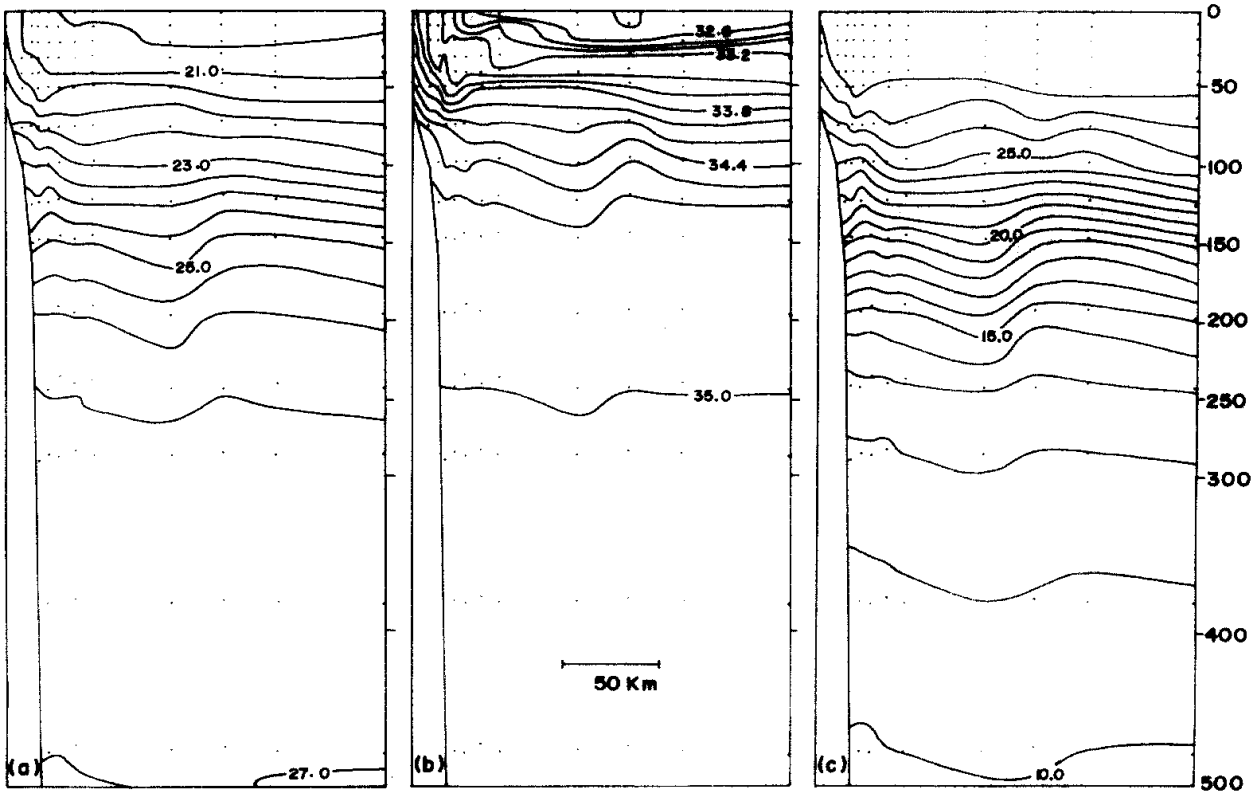

Figure 18: Hydrography along a section (normal to the coast) which lies approximately midway (~15 N) of the east cost of India. (a) potential density (g cm^{-3}); (b) salinity (ppt); (c) temperature (°C). The scale shown in (b) also applies to (a) and (c). (From Shetye et al., 1991).

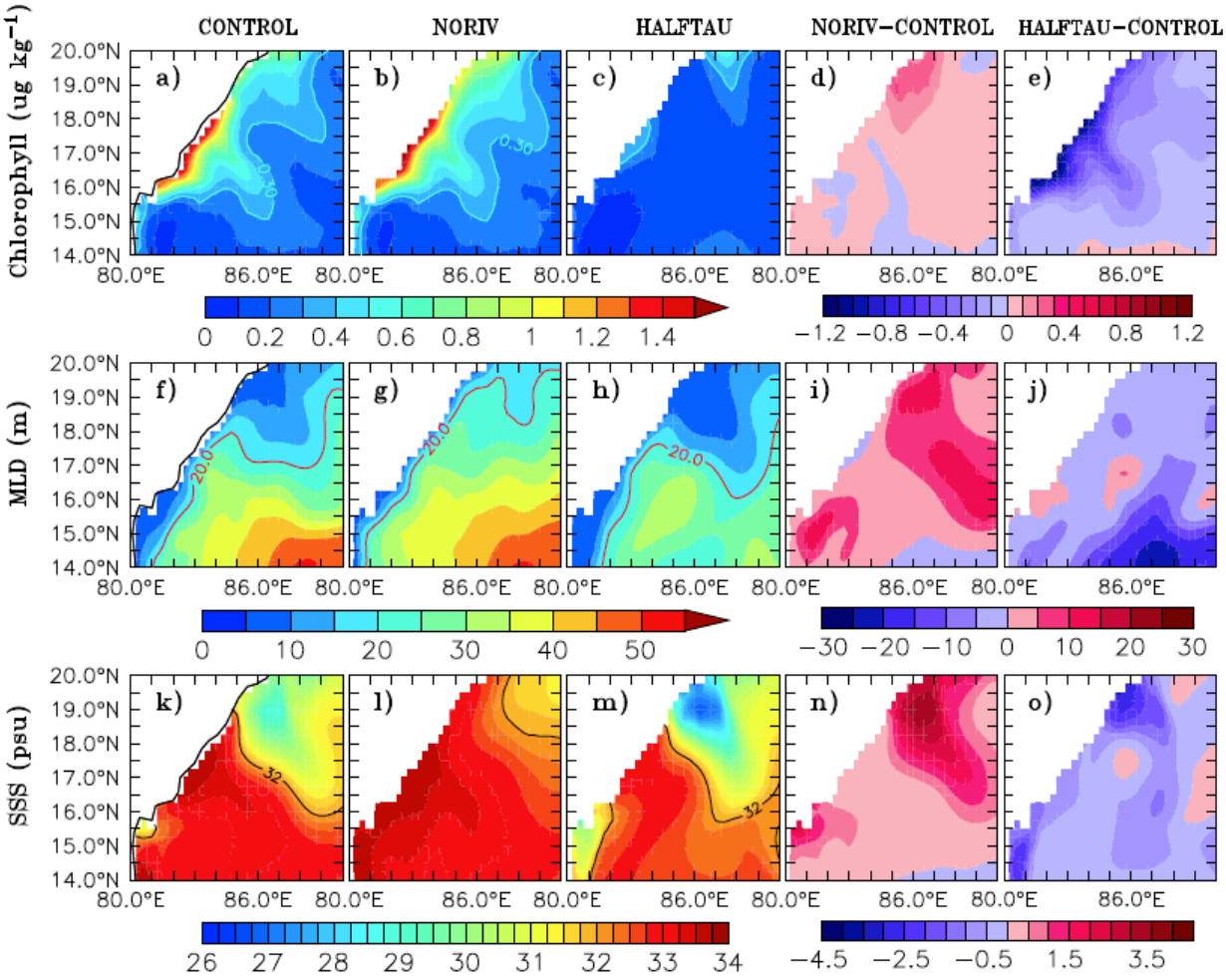

Figure 19: Forcing mechanisms of upwelling induced chlorophyll distribution in the northwestern Bay of Bengal. Comparison of model simulated surface (a–e) chlorophyll, (f–j) MLD, and (k–o) SSS from CONTROL, NORIV, and HALFTAU experiments averaged for the month of August. Contours shown are for chlorophyll, MLD, and salinity of 0.3 ug kg21, 20 m and 32 psu, respectively. Shown are model simulations from a control run which included all the forcings (CONTROL), without river runoff (NORIV) and with the magnitude of wind stress reduced by 50% (HALFTAU) (From Thushara and Vinayachandran, 2016)

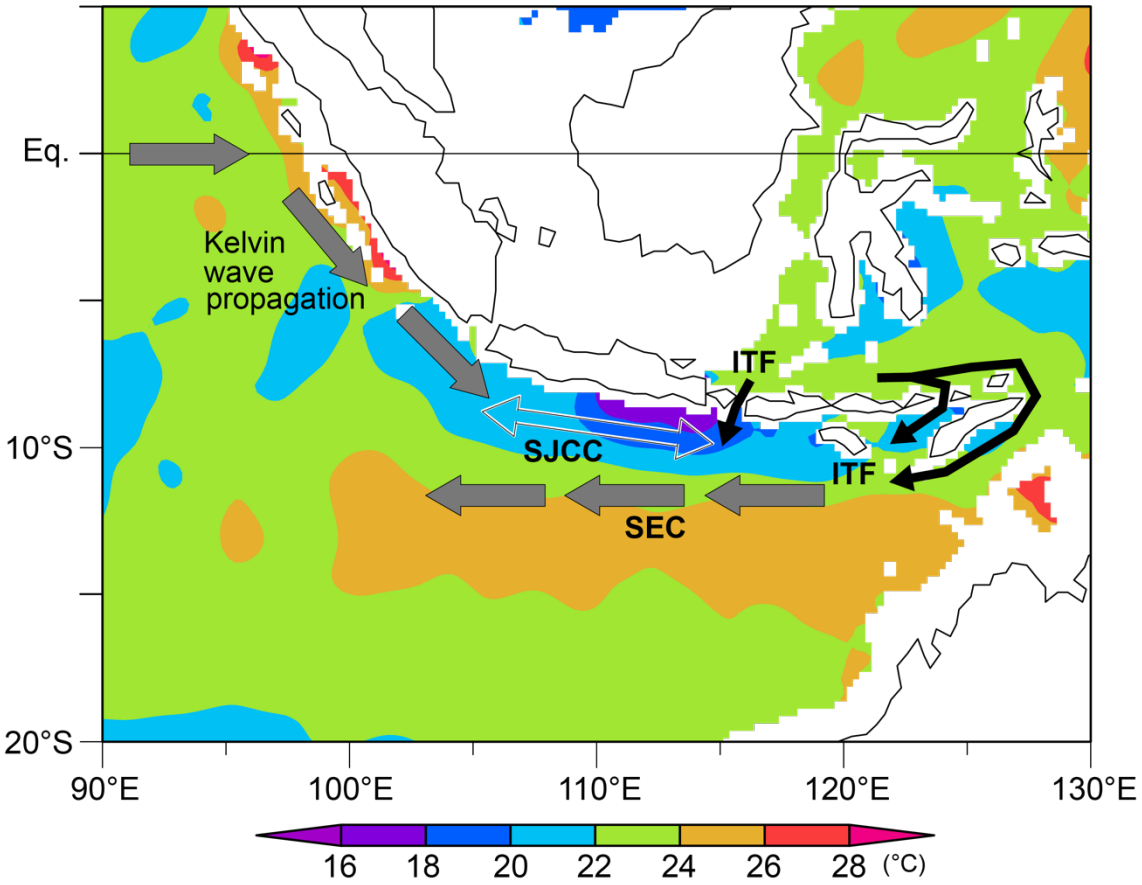

Figure 20. Map of the Sumatra-Java upwelling region and surrounding area. Background color shade shows July-August-September mean climatological temperature at 100 m depth from World Ocean Atlas 2018 (Locarnini et al., 2018). Grey, black, and line arrows schematically indicate representative surface currents near the upwelling system (SEC: South Equatorial Current; SJCC: South Java Coastal Current; ITF: Indonesian throughflow) and a route of Kelvin wave propagation from the equatorial region down to the Sumatra and Java coasts.

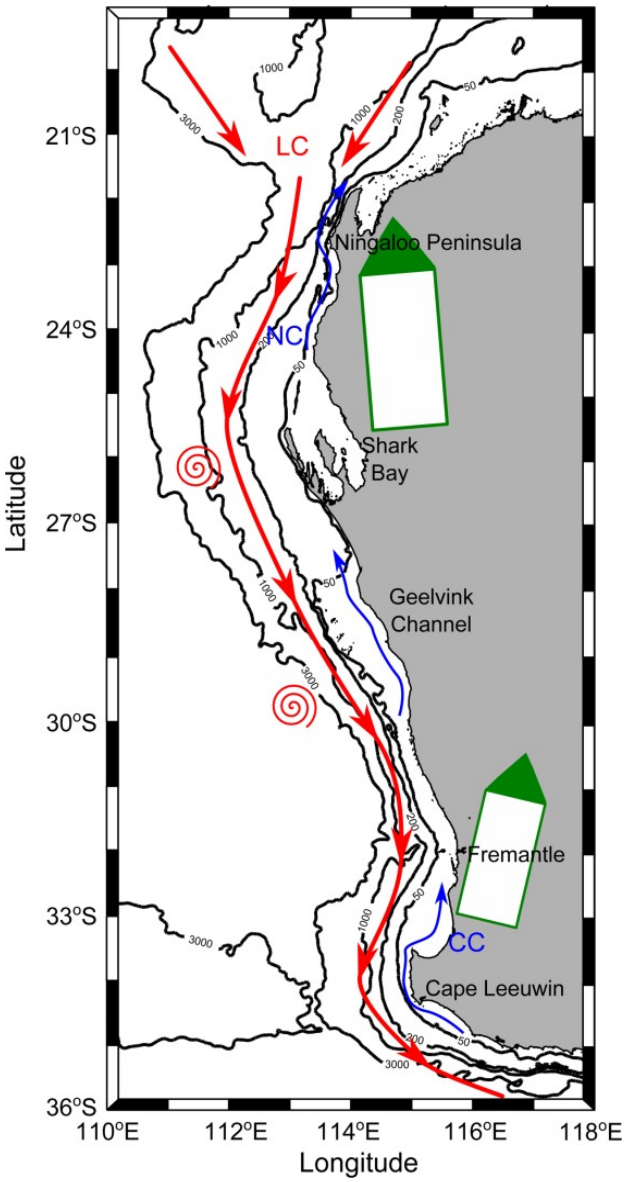

Figure 21. Map of the Western Australian coast with thin black contours showing the 50, 200, 1000 and 3000m isobaths. Green arrows represent mean surface winds, red arrows indicate the Leeuwin Current, red schematic vortices indicates meso-scale eddies and blue arrows indicate the Capes and Ningaloo Currents (from Rossi et al., 2013b)

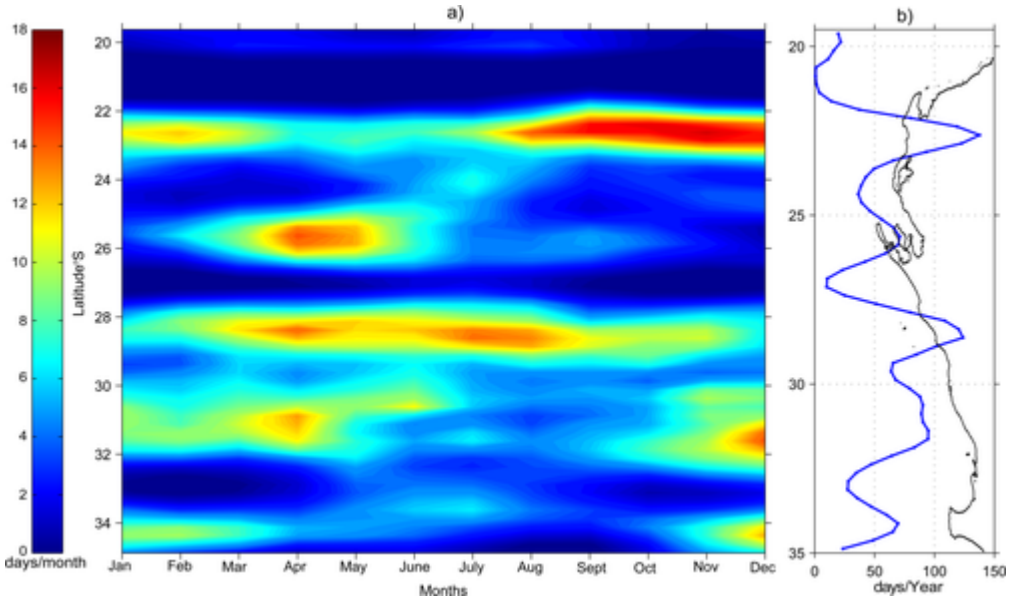

3135

3136 **Figure 22. Climatological analysis of sporadic upwelling events. a) Hovmöller (latitude versus time) diagram of the mean**
3137 **number of "upwelling days" (CUI > 15 m/day during 3 days or more) per month and b) mean number of "upwelling days" per**
3138 **year, recorded from 1995-2010 (from Rossi et al. 2013b).**

3139

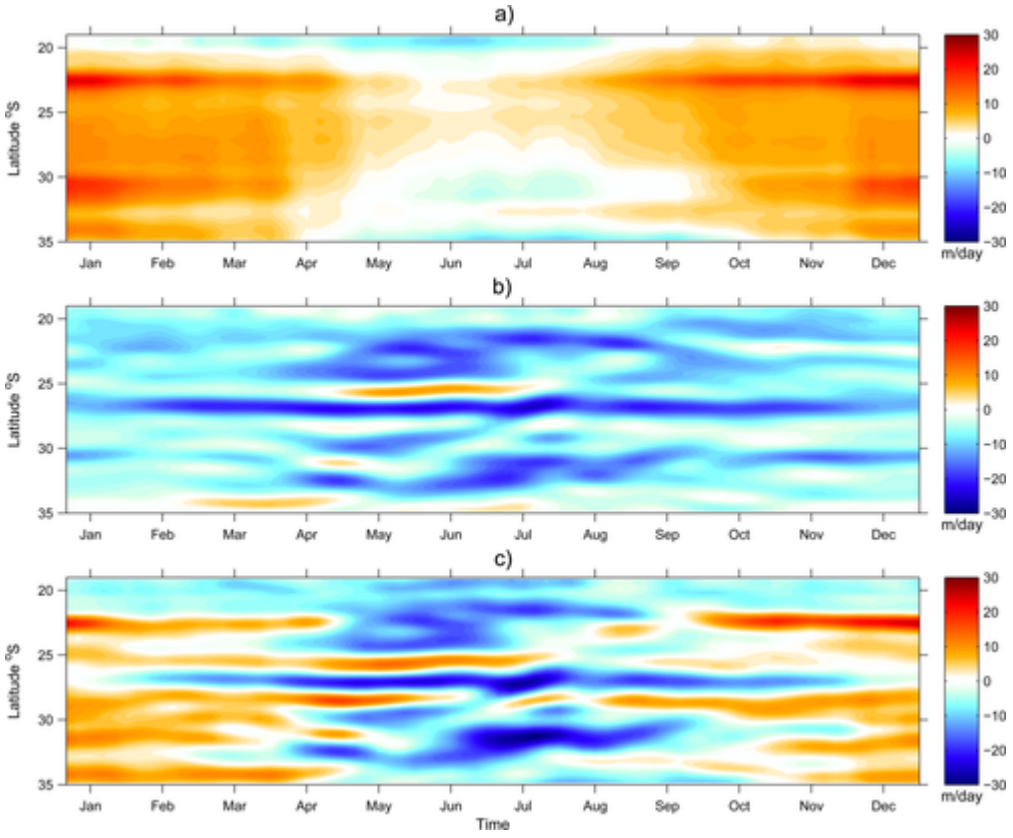

Figure 23: Hovmöller diagrams (latitude versus time) of a) the Ekman upwelling index (m/day, equivalent to vertical velocities), b) the geostrophic upwelling index (m/day, equivalent to vertical velocities), and c) composite upwelling index (in m/day of vertical velocities, a combination of the two previous components). Red colours represent a balance of forces favouring upwelling events (from Rossi et al., 2013b).

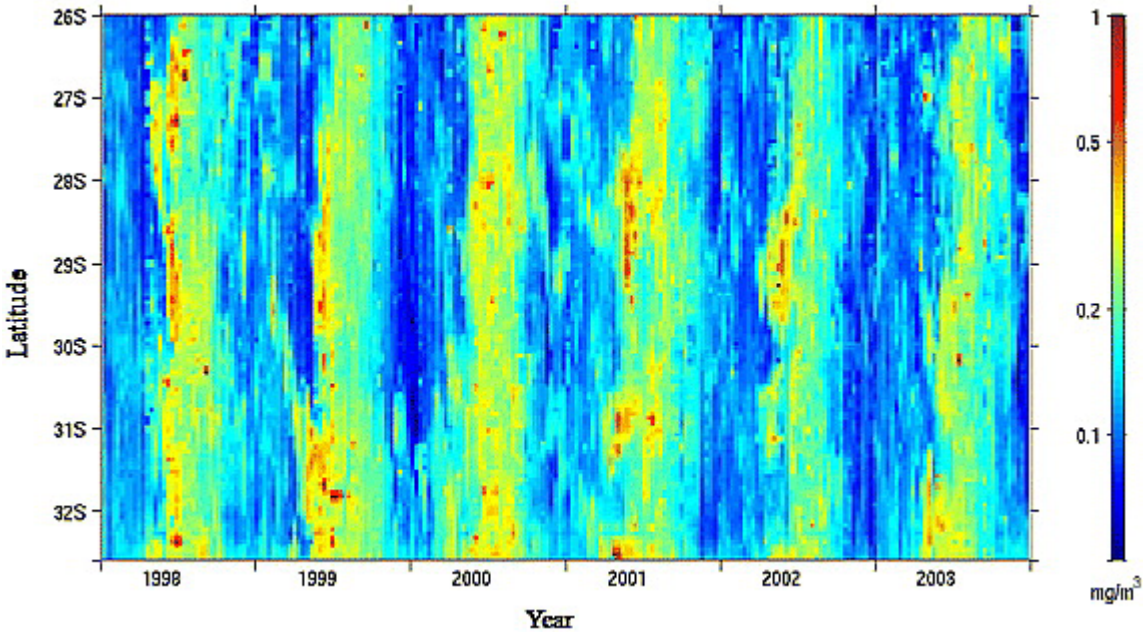

Figure 24. Annual distribution of chlorophyll estimated from SeaWiFS ocean colour data along the shelf break off the west coast of Australia from 26°- 32°S , 1998-2003 (from Koslow et al., 2008).

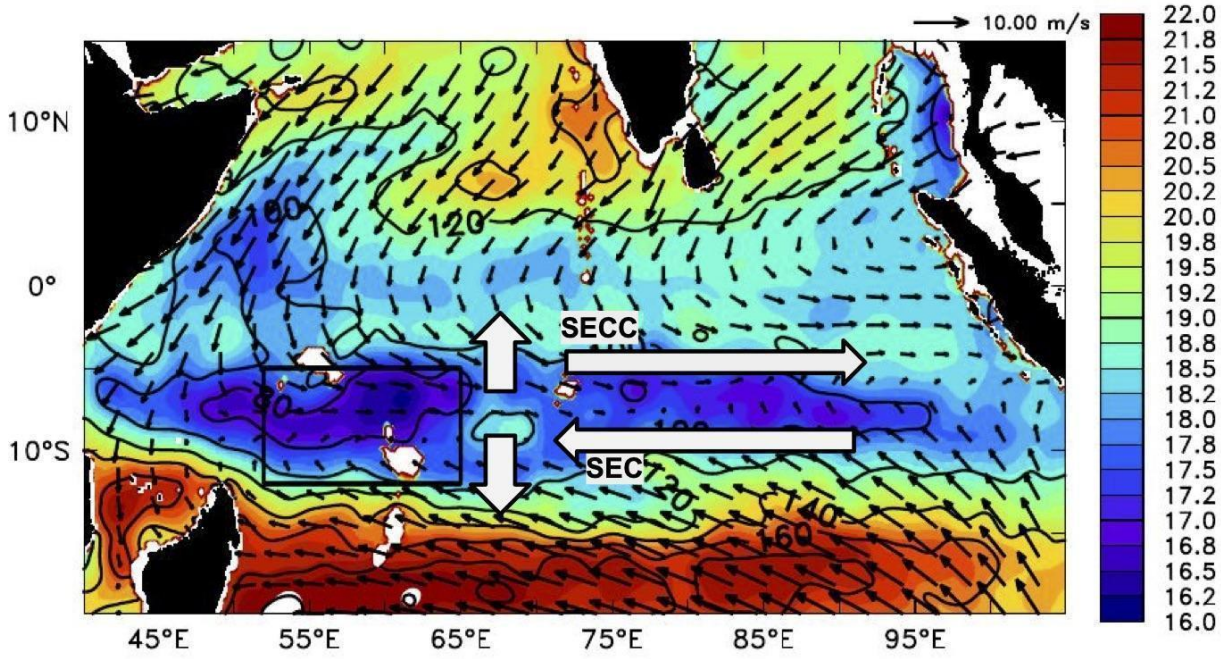

Figure 25: Climatological (Locarnini, 2018) temperature (shading with scale shown to the right) averaged over 0-300m for the months of January and February (shaded) overlayed with wind vectors (m/s) from QuikSCAT Climatology (2000-2008) and thermocline (depth of 20 degree C isotherm, m) depth as the black contour lines. Reference vector for winds is given at the top right corner. The black box marked represents the Seychelles-Chagos Thermocline Ridge (SCTR) . The surface flow indicated by upward and downward white arrows promotes upwelling leading to the formation of the SCTR. The white arrows aligned left is the South equatorial current (SEC) and right is the South equatorial counter currents (SECC). Redrawn after Vialard et al. (2009)

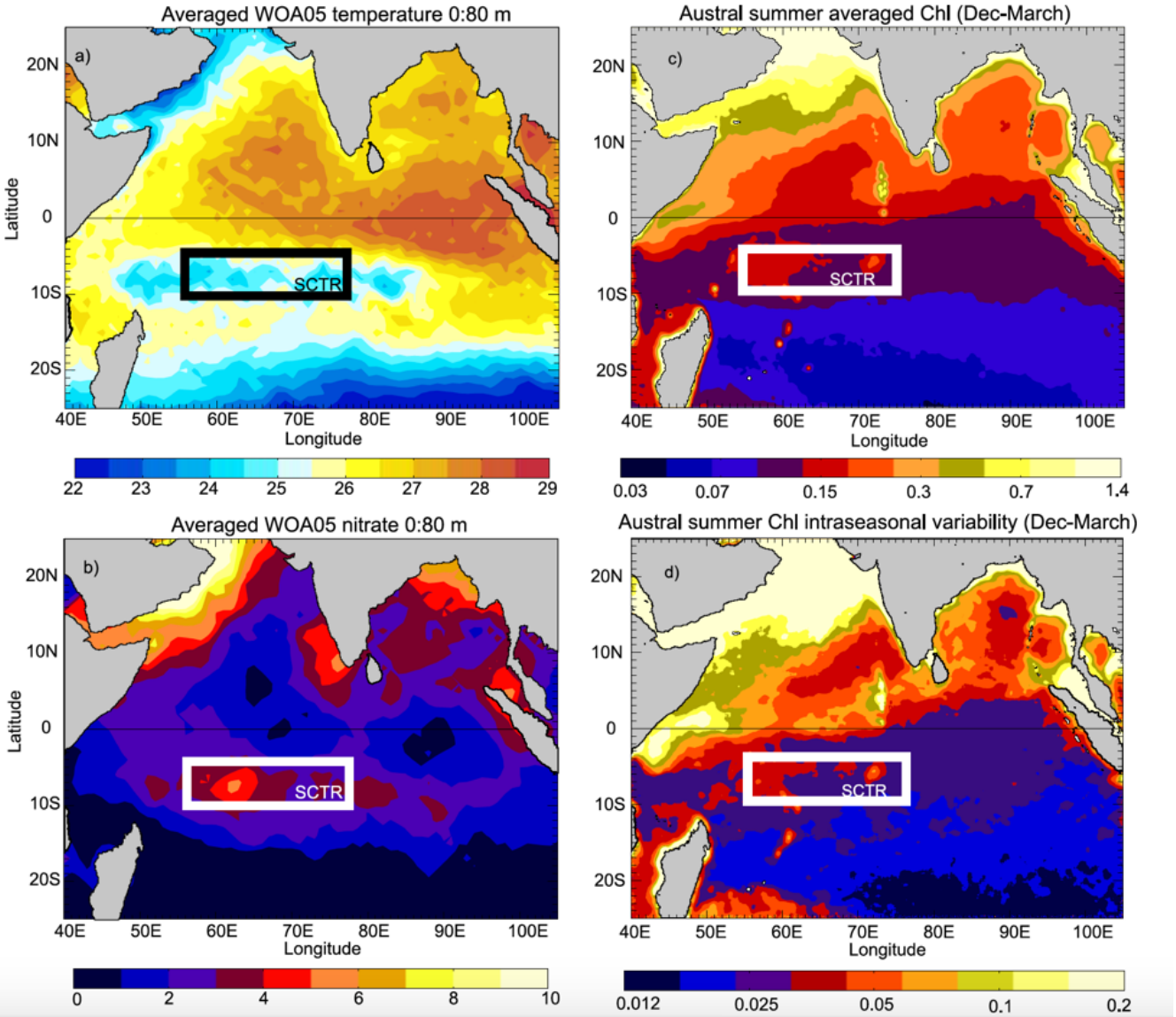

Figure 26: Annual World Ocean Atlas (2005) (a) temperature and (b) nitrate concentration (in mmol N m^{-3}) averaged between the surface and 80 m in the Indian Ocean. (c) SeaWiFS seasonal mean during austral summer (December–March) (mg m^{-3}). (d) Intraseasonal variability of SeaWiFS Chl during austral summer estimated by the averaged RMS of (Chl-Chl*) between December and March of years 1998–2007. (from Resplandy et al. (2009).

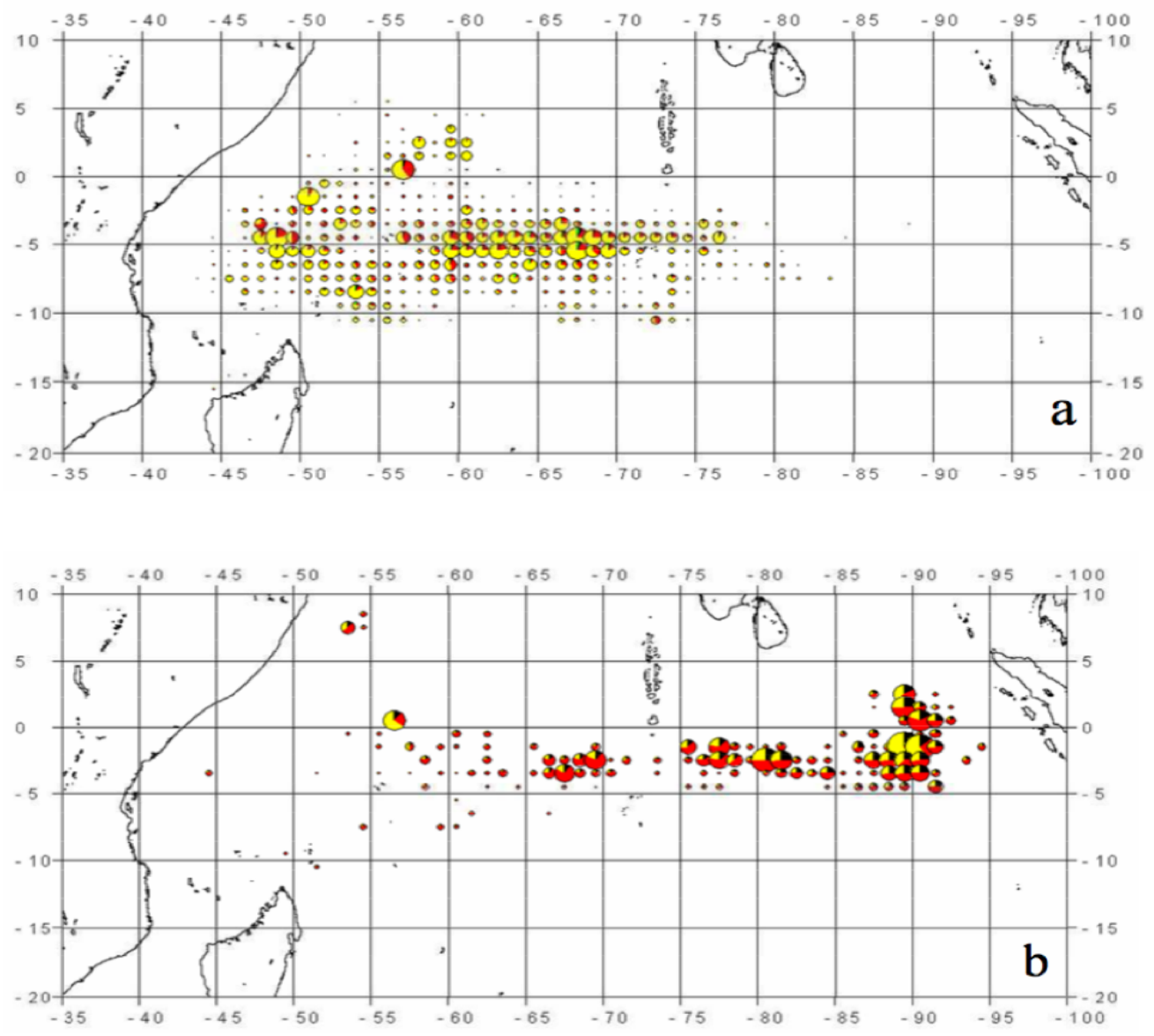

Figure 27: Tuna catch in the Indian Ocean during the 1997/1998 IOD event (bottom panel) compared to catch in normal years (top panel). From Robinson et al. (2010), Copyright Inter-Research 2010.

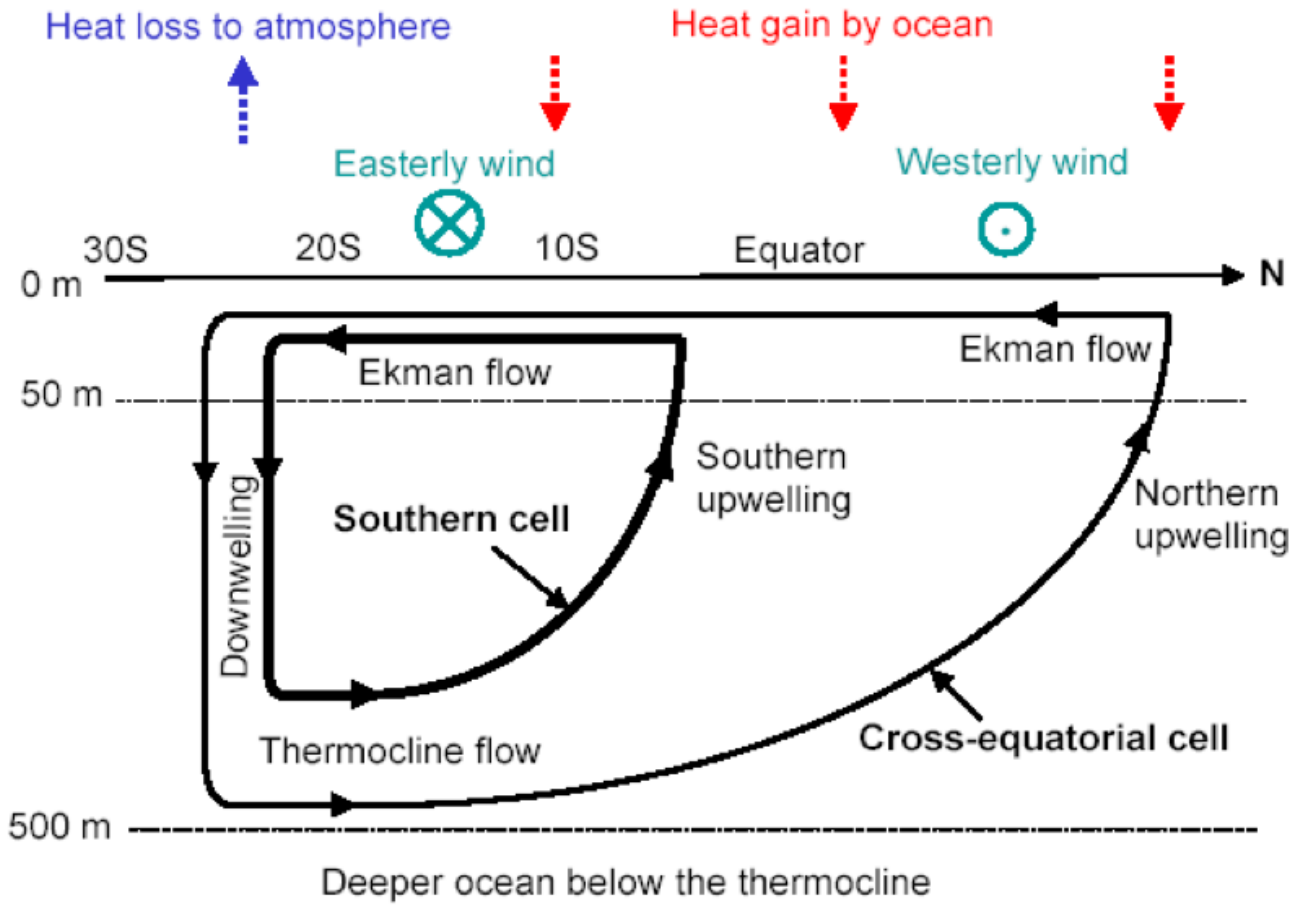

Figure 28: Conceptual illustration of the time-mean meridional overturning circulation of the upper Indian Ocean that consists of a southern and a cross-equatorial cell. The time-mean zonal wind and surface heat flux are also shown schematically. This flow is believed to partially supply the cross-equatorial thermocline flow. From Lee (2004)